5-2016

Multi-signal Accelerated Degradation Testing of Rolling Ball Bearings Through Radial Overload

Anna Marie Mazzolini
University of Tennessee - Knoxville, amazzoli@vols.utk.edu

To the Graduate Council:

I am submitting herewith a thesis written by Anna Marie Mazzolini entitled "Multi-signal Accelerated Degradation Testing of Rolling Ball Bearings Through Radial Overload." I have examined the final electronic copy of this thesis for form and content and recommend that it be accepted in partial fulfillment of the requirements for the degree of Master of Science, with a major in Nuclear Engineering.

Jamie B. Coble, Major Professor

We have read this thesis and recommend its acceptance:

J. Wesley Hines, Guillermo I. Maldonado

Accepted for the Council:
Carolyn R. Hodges

Vice Provost and Dean of the Graduate School

(Original signatures are on file with official student records.)

Multi-signal Accelerated Degradation Testing of Rolling Ball Bearings Through Radial Overload

A Thesis Presented for the
Master of Science
Degree
The University of Tennessee, Knoxville

Anna Marie Mazzolini
May 2016

ACKNOWLEDGEMENTS

I would like to thank my advisor and committee chair, Dr. Jamie Coble, of the Nuclear Engineering department at the University of Tennessee. Her guidance has been instrumental in the completion of this research. I'd like to thank Analysis and Measurement Services (AMS) for their assistance with the bearing testbed design, as well as Cody Walker for his assistance in assembling, modifying, and running the bearing testbed. I would also like to thank the University of Tennessee Mechanical Engineering Department machine shop for their help with the machining of parts for the testbed. Finally, I would also like to thank the other members of my graduate committee, Dr. J. Wesley Hines and Dr. Ivan Maldonado.

Lastly I would like to thank my family and my loving boyfriend, Dylan, for their unwavering support.

ABSTRACT

Bearings are essential components in rotating machinery found in abundance in nuclear power plants. Bearing failure in nuclear power plants can lead to increased operations and maintenance costs and even plant trips. When developing maintenance procedures, it is ideal to minimize costs and equipment downtime while maximizing safety. Reactive, or run-to-failure, maintenance minimizes maintenance costs at the expense of operation costs and safety. Preventative, or time-based, maintenance maximizes safety and minimizes operation costs at the expense of equipment downtime and maintenance costs. Predictive, or condition-based, maintenance attempts to optimize overall costs while maintaining system safety and reducing downtown.

Predictive maintenance uses online equipment condition assessment and remaining useful life (RUL) predictions to schedule inspection and maintenance actions. The development of methods for early and accurate RUL predictions for bearings has the potential to transform maintenance planning in the nuclear power industry, reducing operation and maintenance costs while maintaining or improving overall system safety, reliability, and economics.

In order to develop robust RUL models, examples of run-to-failure data are needed. Using data collected during accelerated degradation tests has the advantages of being easily controlled and of providing ample data over relatively a short test period. A testbed has been designed and constructed that incites bearing failure through the application of a radial load. Several parameters are monitored continuously and online, including motor current, shaft rotational speed, acoustics and bearing vibration and temperature. Bearing maintenance in nuclear power plants to date has relied on vibration data analysis performed at defined inspection intervals. By including several process signals in the testbed design, recommendations are made for online monitoring of bearings in nuclear

power plants that would augment, or perhaps replace, the current maintenance scheme with gains in safety, economics, and system reliability.

TABLE OF CONTENTS

LIST OF TABLES

LIST OF FIGURES

CHAPTER ONE: INTRODUCTION

1.1 Problem

Nuclear power plants rely on the function of a wide variety of systems and equipment including pumps, motors, and fans - many of which rely on bearings. Bearings are integral components in all rotating machinery, and their failure can lead to unplanned downtime and maintenance or even catastrophic system failure. In fact, bearing failure is a leading cause of failure in rotating machinery [1]. In particular, bearings cause 40-50% of motor failures [2]. Bearing faults in a nuclear power plant can result in reactor trips or scrams, plant transients and safety system activation, as well as high operation and maintenance costs [3]. In fact, in 1997 a bearing fault in a reactor cooling pump caused a plant trip, leading to unplanned cold shutdown [4]. Thus maintenance of bearings should be prioritized to improve safety and reliability of nuclear energy production.

The failure of bearings is often wildly unpredictable, even when using statistical population data. This creates a need for component-specific monitoring. In nuclear power plants, where safety is prioritized and outcomes of bearing failure can be detrimental, periodic vibration monitoring of rotating machinery is routine [3]. The vibration monitoring of rotating equipment in nuclear power plants doesn't use continuous data from existing process sensors [5], but rather is performed at defined intervals through inspection round and walk-up testing. Using additional signals continuously could provide information between inspections that would augment the current maintenance routine and further prevent issues resulting from bearing faults. This type of continuous online monitoring could reduce plant downtime, improve maintenance planning, and thus lower operating and maintenance costs. It will also be increasingly valuable for use with newer generation plants. Many of these designs have longer fuel cycles, which will result in fewer planned outages and fewer opportunities to do traditional bearing vibration analysis. There are also designs for plants meant to

be deployed in remote locations, which will have reduced operations and maintenance staff, creating a heightened need for efficient and safe maintenance planning.

The purpose of this work is to construct an accelerated degradation bearing testbed with the capability to fail rolling ball bearings through overload while collecting data from various sensors. These data are analyzed to ensure consistent and repeatable faults are introduced. Post-mortem visual analysis is performed to confirm bearing failure and identify the cause of failure where possible. Initial data analysis is also conducted to demonstrate the usefulness of the sensor data for fault detection and prognostics.

Successful development of online, autonomous condition monitoring and prognostics of bearings will support the safe, reliable, and economic operation of nuclear power plants and other industrial facilities. Incorporating a variety of continuously measured online indicators will augment, and possibly replace, current periodic maintenance with more robust autonomous maintenance that supports reduced inspections along with lower operating and maintenance costs.

1.2 Organization of paper

This thesis presents work completed to design, construct, and operate an accelerated degradation bearing testbed, as well as to evaluate usefulness of data gathered for bearing monitoring and prognostics. Chapter 2 presents a literature review, which covers bearings and their failure mechanisms as well as the history and state of the art in bearing monitoring, diagnostics, and prognostics. Chapter 3 details the experiment, beginning with the procedure used to degrade and fail bearings and collect data, followed by the analysis done and a discussion of the results in Chapter 4. Recommendations for future research, including suggestions to improve this experiment, as well as recommendations for data collection are given in Chapter 5. Final conclusions are given in Chapter 6.

CHAPTER TWO: BACKGROUND AND LITERATURE REVIEW

This research hinges on being able to successfully fail bearings and collect process signal data that are relevant for failure prediction and lifetime estimation. A literature review was conducted in order to understand the mechanics of failure in rolling ball bearings and the data analysis techniques that have already been applied to bearing monitoring and prognostics.

2.1 Understanding rolling ball bearings

At their most basic, bearings are designed to reduce friction between two parts that move against each other. Generally, bearings do this by reducing the contact surface area between moving parts. While there are many types of bearings designed for myriad applications, the following discussion will focus on ball bearings, which are the type of interest in this research because of their ubiquity in industrial applications and, specifically, nuclear power plants.

2.1.1 Dynamics of a rolling ball bearing

As shown in Figure 2.1, a typical rolling ball bearing consists of an inner and outer race, separated by spherical rolling elements that sit in the groves of the two races and allow for smooth movement. A cage holds the rolling elements in place. A bearing housing typically holds one of the races stationary while the other race rotates [6]. In the case of the testing done here, the bearing housing holds the outer race while the inner race rotates with the shaft coupled to the motor. Ball bearings are designed to withstand a certain degree of radial load, as well as a small amount of axial thrust load.

With applied radial load on a ball bearing, only some of the balls are loaded at any given time. This causes the bearing stiffness to vary over time, which creates periodic internal vibrations, known as varying compliance vibrations [6]. These vibrations, which are a function of rotating speed, bearing geometry, and operating load, are an inherent feature of rolling element bearings and occur

even in perfect bearings [7]. The presence of a defect will cause the vibration level to increase significantly [8].

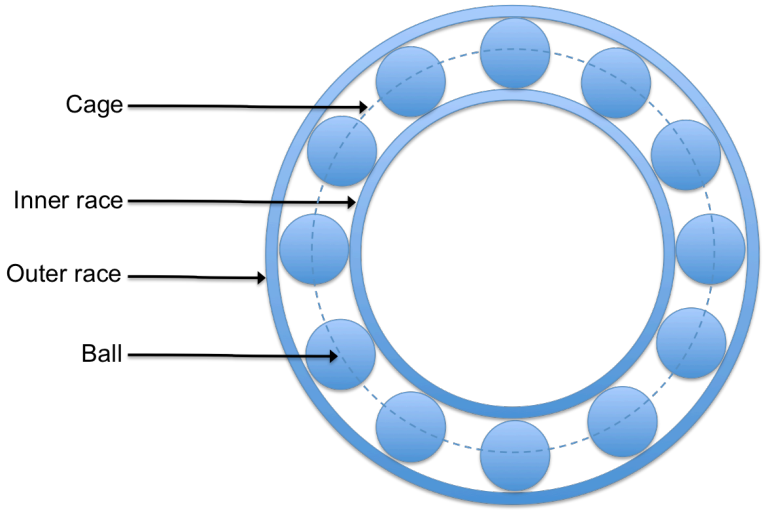

Figure 2.1. Elements of a rolling ball bearing.

2.1.2 Failure of rolling ball bearings

Defects in a bearing can arise from manufacturing faults [9], improper lubrication [10], improper installation, or fatigue [2]. Over time, the defect will grow, eventually leading to failure of the bearing. A defect in any of the bearing elements will result in a specific characteristic vibration frequency [11]. These characteristic frequencies are given by the following equations:

$$\text{Cage fault frequency: } F_{CF} = \frac{1}{2} F_R \left(1 - \frac{D_B cos\theta}{D_P}\right) \tag{2-1}$$

$$\text{Outer race fault frequency: } F_{ORF} = \frac{N_B}{2} F_R \left(1 - \frac{D_B cos\theta}{D_P}\right) \tag{2-2}$$

$$\text{Inner race fault frequency: } F_{IRF} = \frac{N_B}{2} F_R \left(1 + \frac{D_B cos\theta}{D_P}\right) \tag{2-3}$$

$$\text{Ball fault frequency: } F_{BF} = \frac{D_P}{2D_B} F_R \left(1 - \frac{D_B^2 \cos^2\theta}{D_P^2}\right), \tag{2-4}$$

where F_R is the rotation frequency, or shaft frequency; D_B is the diameter of the rolling ball element; D_P is the pitch diameter; θ is the angle of contact between the ball and race; and N_B is the number of balls, shown in Figure 2.2. The contact

angle θ is related to how much axial load the bearings can support. Deep groove ball bearings such as the ones used in this work typically have contact angle of 0° and are designed to support mainly radial load and a small degree of axial load [12]. In general, as the contact angle increases, the amount of axial load that can be supported increases.

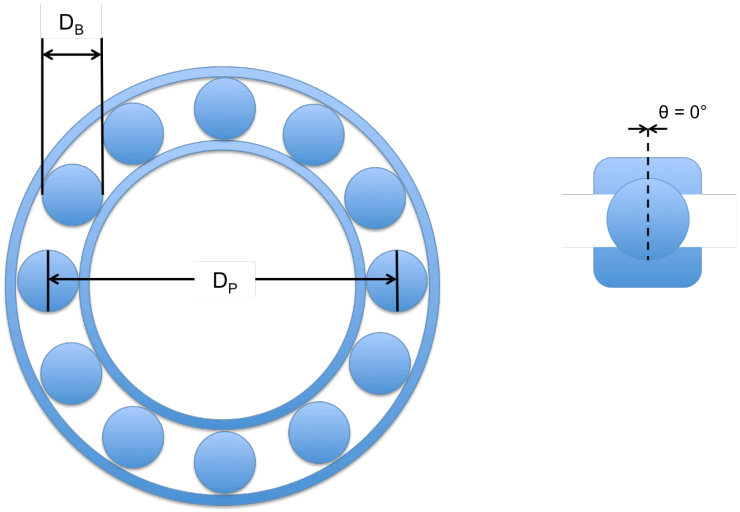

Figure 2.2. Dimensions of a ball bearing.

Radial overload can cause bearing faults in two ways: through static overload or dynamic overload. Overload is defined as any load that would result in the bearing life being decreased to less than one million rotations.

Static overload occurs when the bearing is not in motion and a load is applied such that the materials of the bearing experience plastic deformation, typically in the form of brinelling. Brinelling is where the rolling balls of the bearing press against and make indentations in the race, shown in Figure 2.3. When the bearing then begins moving after such an overload has occurred, the balls will roll across the race defects, causing the defects to grow in size until failure occurs [13]. Brinelling is distinct from false brinelling, which manifests in the

same way as indentations on the race but occurs due to vibration rather than excessive load causing the balls to damage the raceway.

Figure 2.3. Brinelling of a ball bearing [14].

Dynamic overload occurs while the bearing is spinning. Faults that typically occur under dynamic load including smearing, shown in Figure 2.4, where metal from one surface is worn away and deposited on another surface, or spalling, shown in Figure 2.5, where the bearing steel is weakened to the point of cracking [15]. The cracks eventually move towards the surface, where surface cracking or flaking occurs.

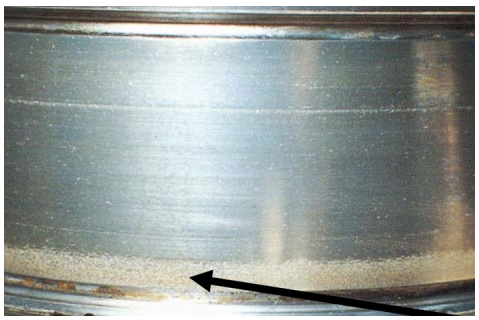

Figure 2.4. Smearing on a bearing [16].

Figure 2.5. Spalling of a bearing [16].

2.2 Accelerated degradation bearing testing

Reliable failure data and process data are necessary for the development of prognostics and diagnostic tools. These data can be collected using accelerated degradation bearing testbeds in a lab environment. Such a testbed would be designed to fail bearings at a rate quicker than typically seen in real life application. Process data are collected as the bearings run. This differs from accelerated life testing where only time to failure data are collected for a group of components in order to estimate component reliability. Data collected from an accelerated degradation testbed can then be used to develop models and methods for condition monitoring, diagnostics, and prognostics. To maximize their utility, these methods and models should be adaptable for use with bearings under normal conditions seen in industry. They can then be incorporated into a maintenance plan.

Bearing failure in an accelerating testing scenario can be incited a variety of ways. The most common ways to cause bearing failure for purposes of testing include mechanical introduction of a defects, application of current, and application of external load.

2.2.1 Introduction of defect directly

One way to reliably create bearing failure is to directly introduce defects on the bearings before running them on a testbed [17, 18]. The defects will eventually

grow until they cause failure. Defects can be created by drilling holes into the bearing race or marring the surface of the bearing race. An advantage to drilling or marring the bearing manually is that the location of the initial fault can be controlled, leading to more focused and specific failure data. This approach, however, must be performed offline and can lead to variations in the testing conditions between the bearing before the introduction of the defect and after [19].

2.2.2 Fluting

Fluting refers to the phenomenon where voltage is discharged across a bearing while it is running, creating race defects [19, 20]. Specifically, pits are produced (Figure 2.6). High vibration and noise result as the defect grows [15]. This is a particular problem in motors controlled by variable frequency drives [21], but may not be much of a concern elsewhere. However, the introduction of defects through purposeful fluting is a viable way to create defects in bearings without having to take the system offline [22].

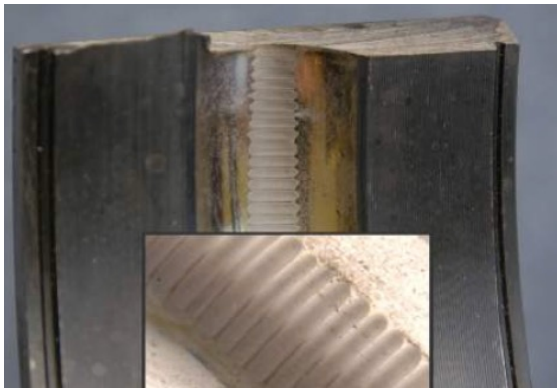

Figure 2.6. Fluting of a bearing [23].

2.2.3 Application of radial force

All bearings are designed to withstand a certain level of radial force. One means of accelerating typical wear in a bearing is to subject it to a higher load than the

capacity of the bearing [20, 24, 25]. Application of force has the advantage that bearings are run from a completely new state until failure. Failing bearings in this way provides more useful data because data from experiments that introduce defects either through fluting or manual damage cannot accurately show defect propagation in the early stages [1]. This can be done in a variety of ways in a lab setting. The following research will focus on failure data that was generated by means of radial overload with a large spring, as described in Chapter 3.

2.3 Important process signals in rolling ball bearing analysis

Bearing monitoring traditionally involves the analysis of vibration, acoustic, temperature, or motor current signals. Another popular monitoring method is oil analysis, which will not be explored here. Oil analysis works best for bearings with a built-in oil supply system and is not used for grease lubricated bearings [26], such as the bearings tested in this research.

2.3.1 Vibration

In general, as faults occur and defects grow, vibrations in a bearing tend to increase. Because of the easily calculable characteristic fault frequencies, vibration analysis is the most commonly used method for fault detection and diagnostics in bearings [9]. Not only can these characteristic frequencies signal a fault in general, they can be used to determine what component of the bearing has failed because each has its own frequency associated with it. This sort of analysis, however, relies on the *a priori* knowledge of the characteristic fault frequencies [27]. This means that vibration analysis will be used more reliably for fault detection than remaining useful lifetime predictions [28]. Vibration signals gathered from bearing operation are typically low amplitude and noisy; therefore, de-noising is almost always necessary to extract useful features from the data [1]. Because of these issues, direct spectral analysis of the vibration signal can often only detect relatively large faults [29]. Further, vibration analysis alone may be insufficient to detect and track bearing faults because of the effect that outside factors such as machine operating conditions and nearby machinery could have

on the measured vibration signal [30]. Even for an isolated bearing, vibration resulting from a fault may not always match up to the expected characteristic fault frequency due to a number of variables including aging, slipping, or changes in the contact angle [31].

2.3.2 Acoustics

A second common signal for bearing analysis is acoustic emission. Important parameters for acoustic emission monitoring include peak amplitude of the signal and ringdown counts, which measure how often the amplitude exceeds some threshold [32]. As a bearing approaches the end of its lifetime, an increase in ringdown counts will be seen. Using ringdown counts to monitor bearing acoustic emission requires expertise and engineering judgment to establish reasonable thresholds. Acoustic emission has the advantage of a high signal-to-noise ratio. However, acoustic data requires a high sampling frequency, and acoustic emission analysis can be expensive [26].

2.3.3 Temperature

Bearings have two important temperature ratings. The first is the rating of the bearing itself. This is the maximum temperature that the bearing steel can handle and perform as normal. The second is the temperature rating of the bearing lubrication. If the bearing lubrication fails, the bearing will likely degrade and eventually fail [33]. Thus temperature is an important process signal in analysis of bearings. Immediately before impending failure, bearing temperature tends to rise drastically [26]. Because the increase happens just before failure, temperature alone is not very valuable in terms of early fault detection.

2.3.4 Current

Current monitoring for bearings is particularly attractive because other machine monitoring and diagnostics already take advantage of current monitoring. Variations in torque resulting from a bearing fault have been shown to cause a significant change in stator current [18]. In fact, characteristic fault frequencies which be seen in the torque spectrum, which in turn results in changes in the

stator current spectrum. By comparing measured stator current signals to those from unfaulted bearings, faults can thus be detected.

2.4 Data analysis techniques for bearing monitoring

The data analysis techniques that are important for ball bearing monitoring can be split into three categories: time domain analysis, frequency analysis, and time-frequency analysis. Time domain techniques provide statistical information about the data as it changes with time, while frequency domain techniques provide a snapshot of signal frequencies at a given time and time-frequency domain techniques look at trends in signal frequencies over time.

2.4.1 Time domain analysis

Time domain analysis can be used to provide statistical feature information about the data. When a rolling element rolls over a defect, an impulse is generated [34]. This causes changes in process signals including vibration and acoustic emission. By monitoring the statistical features of these signals, changes can be seen as a defect occurs and propagates. Often, signal processing or filtering is used to increase the effectiveness of the statistical features for condition monitoring [34].

One of the most widely used features for bearing data analysis is the root mean square value of the vibration signal. It provides information about the general amplitude of the signal. This root mean square of the vibration can indicate an impending failure, as the overall vibration level tends to increase leading to failure. However, this is not an effective method for early detection of fault onset, as vibration tends to increase rapidly only just before failure. The following equation (2-5) describes the root mean square value for a waveform f(t) with period T.

$$RMS = \sqrt{\frac{1}{T}\int_{t_0}^{t_0+T} f(t)^2 dt} \tag{2-5}$$

Also useful is the crest factor of the vibration, which is the ratio of the peak value to the root mean square value [9], given in equation (2-6). The crest factor for the vibration signal stays constant during normal bearing operation. As a defect occurs, the peak value of the vibration, and thus the crest factor, will rise while the root mean square value remains relatively constant. Then, towards the end of the bearing lifetime, the crest factor will fall again as the RMS value increases. Thus crest factor is more valuable than RMS for early detection of faults.

$$CF = \frac{peak}{RMS} \tag{2-6}$$

Higher statistical moments such as variance, skewness, and kurtosis have also been used in bearing monitoring. The kurtosis of the vibration signal in particular has been found to be useful in fault detection. The kurtosis represents the peakedness of a distribution. A Gaussian distribution has a kurtosis of 3. Bearing vibration is about equal to 3 during normal operation and increases as the bearing reaches the end of its lifetime [35]. This increase in kurtosis corresponds to an increase in the peakedness of the vibration signal. Thus a vibration kurtosis value of greater than 3 is taken to signal impending failure. Care must be taken, however, as the kurtosis will fall back to "normal" levels right before failure [9]. The kurtosis is defined as

$$kurtosis = \frac{\int_{-\infty}^{\infty}(x-\bar{x})^4 P(x)dx}{\sigma^4}, \tag{2-7}$$

where P(x) is the probability density function, $\bar{x}$ is the mean, and σ is the standard deviation.

2.4.2 Frequency domain analysis

The time domain does not always tell us everything we need to know about a signal. Viewing and analyzing a data set in the frequency domain instead can give useful information that might not be apparent in the time domain signal. For bearings in particular, frequency domain analysis is useful to determine when a fault has occurred or to gather statistical data about bearing failure for use in

remaining useful life predictions because of the characteristic frequencies present at failure.

Likely the most common frequency domain method is the Fourier transform. The Fourier transform decomposes a signal into its harmonics, converting from the time to the frequency domain. This kind of transformation can give information about the sharpness and oscillations present in a signal. One disadvantage to this analysis method is that the Fourier transform requires a lot of computational power and still might not be useful for detecting bearing characteristic frequencies due to the large amount of noise present in a vibration signal. The common Fast Fourier transform makes significant improvements in processing speed. Fourier transforms of vibration signals can give warning of impending catastrophic failure, but are typically unable to predict failure early on.

The major downside to frequency domain analysis alone it that is only useful for stationary signals, meaning that it can't capture information about features that change over time [36]. Because of this, frequency domain analysis is not particularly useful on its own for bearing PHM except in the case of diagnostics where fault frequencies are known *a priori*.

2.4.3 Time-frequency analysis

A much more useful type of analysis for monitoring and prognostics of bearings is time-frequency analysis, where signals are viewed as a function of both time and frequency simultaneously. The vibration monitoring done in nuclear power plants is essentially a primitive time-frequency analysis, where frequency spectra are taken periodically and compared to previous spectra.

The short-time Fourier transform [37] is essentially an extension of this same process. The Fourier transform is applied over short time segments over the whole signal. Segments must be chosen small enough that they can be considered stationary. This segmentation can lead to lower resolution [38].

Joint time frequency analysis maps signal frequency components as they change with time by applying frequency transforms (traditionally the Fourier transform) to overlapping segments of the signal. This method allows for better analysis of how the signal frequencies change in time than traditional frequency spectra taken at various disjointed intervals [39]. A common method for joint time frequency analysis that is based on the Fourier transform is the Gabor transform [40], which decomposes a signal into a series of Fourier transforms taken over overlapping segments that are chosen using a kernel weighted window approach. As for the short-time Fourier transform, when the frequency transform used is designed for stationary signals, such as the Fourier transform is, time segments should be taken to be sufficiently small that the assumption of a stationary signal is reasonable, which can again result in decreased resolution [39].

The Wigner-Ville distribution, which is considered a bilinear transform, overcomes the resolution issues of the short-time Fourier transform and joint time frequency analysis by providing a distribution of signal energy in both the frequency and time domains simultaneously without the use of signal segmentation [41].

Similarly, the Hilbert-Huang transform is designed for analyzing non-stationary signals. With this method, a signal is decomposed into intrinsic mode functions using empirical mode decomposition. Unlike many other decompositions, like the Fourier transform, which decompose signals into functional forms of known parametric equations, empirical mode decomposition does not assume a specific functional form, making it much more flexible. The Hilbert transform is then applied to the intrinsic mode functions to determine the instantaneous frequency and signal amplitude [42]. The final result is a picture of the signal amplitude over both time and frequency domains simultaneously.

Wavelet analysis differs from the previous methods described as it is not strictly a time-frequency analysis, but rather offers a time-scale representation of a signal [38]. An advantage of the wavelet transform for bearing monitoring is that it has the ability to provide good low frequency resolution by using long time intervals where needed [39]. The wavelet transform can also reduce noise of raw signals. The difficulty in this method comes with choosing the parameters for the wavelet analysis.

2.5 Data analysis techniques for bearing prognostics

Because bearings are instrumental components in a wide variety of rotating machinery, developing an efficient bearing maintenance program can have a drastic effect on the overall system maintenance efficiency. In general, a good maintenance plan minimizes costs and downtime while ensuring safety. This can be achieved through condition-based maintenance. A key component of condition-based maintenance is the use of prognostic methods, which provide remaining useful lifetime (RUL) estimates [38]. Accurate bearing RUL estimates are key in planning efficient maintenance actions.

Prognostic methods can be divided into three categories: type I, type II, and type III. Type I prognostic methods use population data and statistics to estimate RUL for the average component operating at average conditions. Type II methods account for component-specific operating and load conditions. Finally, Type III methods use component-specific data to estimate component-specific RUL [43]. Because bearing failure is dependent on so many factors, even identical bearings under similar operating conditions can have vastly different lifetimes. In fact, it would not be uncommon that a defected bearing could be replaced with a new one that has a shorter RUL than the replaced faulted bearing [44]! Thus, Type III prognostics methods provide the most reliable and accurate RUL estimations for rolling ball bearings.

Type III prognostics methods that have been explored for bearings can be grouped into two major categories: methods based on feature trending and methods based on machine learning. The most common methods based on machine learning include artificial neural networks [45-48], fuzzy logic [49], genetic algorithms [50, 51], and hidden Markov modeling [52]. These methods all require significant computation, and, while they have been able provide reliable remaining useful life predictions for bearings, their development is much more in-depth than for models based on feature trending. The research presented here will focus on methods based on feature trending in order to motivate the continuous monitoring of bearing health in nuclear power plants using multiple process signals.

Some prognostics approaches have overcome the limitation of reliance on previous data by incorporating physics-based models [53]. Unfortunately, the development of accurate physics models becomes very difficult when the bearing is incorporated into a system rather than viewed alone. Such hybrid physics and data driven methods are thus not at all practical in the application of nuclear power plants, where many different types of bearings are present in many different systems.

Many bearing prognostics methods take advantage of the feature trending methods discussed in 2.4. The most common include Fast Fourier transform (FFT), wavelet transform, Hilbert-Huang transform, and statistical feature trending. As discussed, the major downside to these methods is that they typically do not signal defects very early, particularly in cases where a single process signal is used. It is thus difficult to predict RUL early in the bearing lifetime. They also typically rely on previous failure and degradation data to make future predictions [53]. This reliance can also affect the accuracy of the predictions because of the complicated nature of bearing failure. In the case of

nuclear power plants, model reliance on previous data is not a serious limitation because of the abundance of process data that is already collected and stored.

CHAPTER THREE: METHODOLOGY

With the techniques and signals of interest discussed in Chapter 2 in mind, a testbed was designed to perform accelerated degradation testing of bearings while collecting significant process signals. The following sections describe the testbed and its operation.

3.1 Design of the bearing testbed

In order to collect data that could be used to develop prognostics models an accelerated degradation bearing testbed was designed and built. The testbed was designed so that ¾" R12 open steel rolling ball bearings could be failed through up to 30% dynamic overload in the radial direction with the use of a large compression spring. Figure 3.1 shows a schematic diagram of the rig with specifications for commercial, off-the-shelf parts found in Table 3.1; the remaining testbed components were machined in the University of Tennessee Mechanical Engineering machine shop. The schematic shown in Figure 3.1 includes a torque sensor between the motor and test bearing shaft which has since been removed from the design due to operational issues with the sensor. None of the testing presented in this paper used the torque sensor.

The spring used to apply force on the bearing housing and thus radially load the bearing is a 6" long compression spring that measures 4.22" when fully compressed. It applies 1307 lbs./inch of compression. The linearity of the force applied by the spring was confirmed before testing.

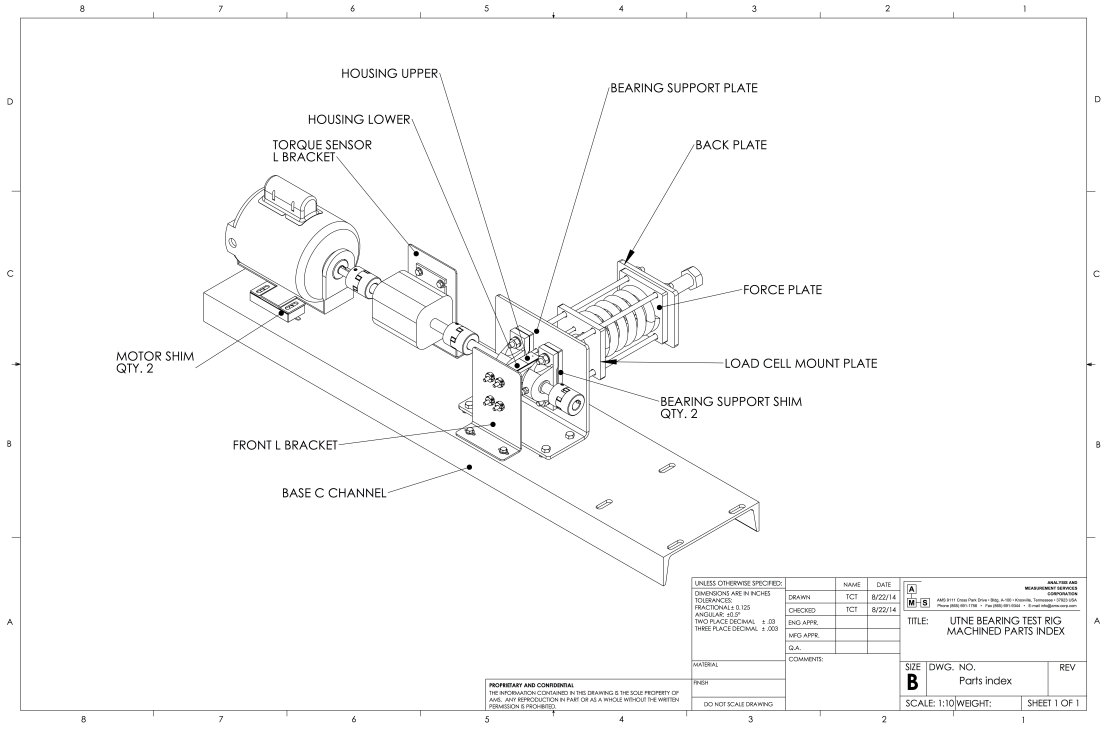

Figure 3.1. Testbed schematic.

Table 3.1. Bearing rig part specifications.

Part Function	**Supplier**	**Part #**	**Specifications**
Motor	McMaster-Carr	5990K79	1.5 hp, AC, 3450 rpm
Support bearings	McMaster-Carr	6494K13	Double sealed ball bearing, 2877 lb. dynamic load rating
Test bearing	McMaster-Carr	60355K507	Open ball bearing, 1785 lb. dynamic load rating
Spring	McMaster-Carr	96485K331	1307lb./in., 2328 lb. max
Titanium Shaft	McMaster Carr	89055K58	Grade 5 titanium, ¾” diameter

3.1.1 Data acquisition

The sensors used to measure process data include a thermocouple for measuring the temperature of the test bearing (marked 1 in Figure 3.1), two accelerometers for measuring the horizontal and vertical vibrations of the test bearing (marked 2 in Figure 3.1), a microphone for measuring the sound pressure from the direction of the test bearing (marked 3 in Figure 3.1), a microphone pointing away from the bearing for noise cancellation, a load cell for measuring the force applied to the test bearing housing via the spring, a current clamp for measuring the current to the single phase motor, and a tachometer for measuring the shaft rotation (marked 4 in Figure 3.1). All of these sensors are hooked to a data acquisition system using a National Instruments NI cDAQ-9178 DAQ chassis and various NI modules, listed in Table 3.2. The data are collected using National Instruments LabVIEW software.

Time series data from all of the sensors are collected at 1024 Hz to ensure sampling rate greater than twice that of the characteristic failure frequencies of the bearings, given in Table 4.2. Later, these data are analyzed using MATLAB, as described in Chapter 4.

Table 3.2. Sensor specifications.

Part Function	**DAQ Module**
Microphone	NI 9234
Horizontal accelerometer	NI 9234
Vertical accelerometer	NI 9234
Thermocouple	NI 9211
Rod end load cell	NI 9239
Current clamp	NI 9239
Tachymeter	NI 9234

3.1.2 Safety Shutoff System

A safety system is put in place to shut off the power to the motor in the event that the bearing fails, allowing continuous, unattended running of the testbed. It relies on a relay (Digi Key PB321-ND) that is powered by the data acquisition system through a National Instruments module, model NI-9481. When the external power to the relay is cut, through loss of power or system design, the relay opens and power to the motor is lost.

The safety shutoff is triggered on either temperature or motor current. Bearing temperature is a good indicator of the integrity of the grease in the bearing, while motor current in a good indicator or whether the shaft has seized. By triggering on either of these values, testing is automatically stopped if either the grease has failed, which could cause the bearing to fail subsequently, or if the bearing has failed and caused the shaft to seize. The safety shutoff system will also shut the motor off if the data acquisition stops for any reason including loss of power or computer malfunction.

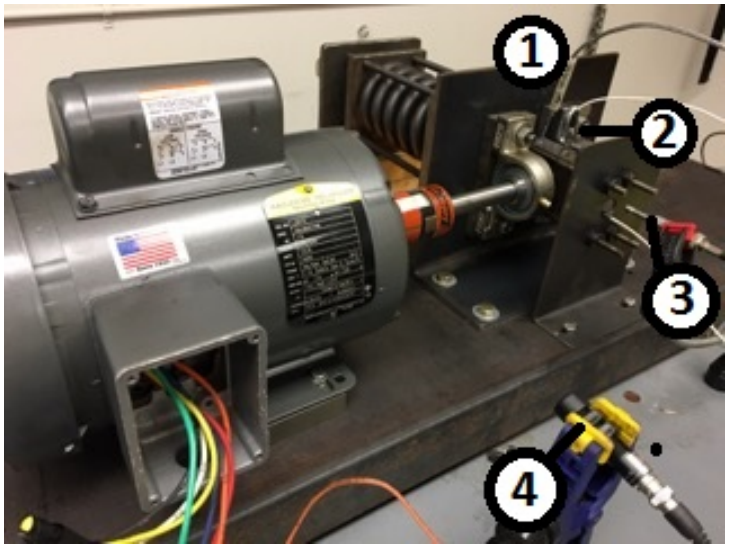

Figure 3.2. Side view of the experiment.

3.1.3 Bearing and grease specifications

The bearings tested are ¾" R12 open steel rolling ball bearings (Table 3.3). They have a dynamic load rating of 1785 lbs. and a static load rating of 1000 lbs. The maximum speed is 17,200 rpm. The temperature operating range of the bearings is -28°C to 115°C. Because the bearings do not come pre-greased, a high temperature synthetic grease with an operating range of 0°C to 260°C is added [54].

Table 3.3. Bearing dimensions.

Fault Type	**Characteristic Frequency**
Ball diameter, D_B	0.2"
Pitch diameter, D_P	1.1875"
Number of balls, N_B	10
Contact angle, θ	0°

The single-phase, 1.5 horsepower motor of the testbed, operating at 3450 rpm, never exceeds the rotational speed design limit of the bearings. Steady state temperatures with no load are observed around 50°C and it is not until imminent bearing failure that temperatures reach beyond the operating range. Thus the only design parameter of the bearings that the testbed is designed to exceed is the radial load. The testbed can supply up to 2300 lbs. of constant radial force to the bearing housing. This allows a load of up to 130% of the dynamic load capacity of the bearing.

3.2 Bearing testing process

The process used to perform accelerated testing on a bearing in order to fail it is as follows. First, an unused open ball bearing to be used for testing is packed with high temperature grease. Then the bearing is press fit onto the shaft, with the bearing housing secured around it. Loctite is used to ensure no slipping

occurs between the test bearing inner race and the shaft. Two support bearings used to hold the shaft in place are hand fit on either side of the test bearing, again using Loctite to secure. These support bearings are then bolted to the shaft L-bracket mount and the test bearing shaft is coupled to the motor shaft. The thermocouple is coated with thermal grease and inserted into a hole in the bearing housing. The magnetic mounts are used to secure the accelerometers to the test bearing housing in both the horizontal and vertical directions. One of the microphones is positioned to read the sound pressure from the test bearing in the same direction of the horizontal accelerometer, parallel to the ground and perpendicular to the test bearing shaft. The other microphone is positioned 180° away in an effort to measure background noise not due to the bearing. Retroreflective tape is secured to the shaft coupling, and the tachometer is aligned with the tape using a magnetically mounted clip to hold it in place. The current clamp is attached around the wiring from the wall to the motor. Figure 3.2 shows the assembled set-up, including: 1) the spring that provides a load to the bearing housing, 2) the hole in the bearing housing for insertion of the thermocouple, 3) the test bearing housing, 4) the steel rods that prevent movement of the test bearing along the shaft, and 5) the support bearings. With all of the sensors in place, the motor is turned on to spin the test shaft.

The system then runs unloaded for approximately 24 hours in order to bring the system to steady state conditions and collect sufficient data from the unfaulted bearing condition. In order to apply load to the test bearing, a bolt is tightened to compress the spring and apply force to the bearing housing. The bearing is loaded dynamically according to the scheme laid out in Table 4.1.

If the test bearing seizes or the bearing grease reaches temperature above its operational limit, the motor automatically shuts off via the built-in safety shutoff system.

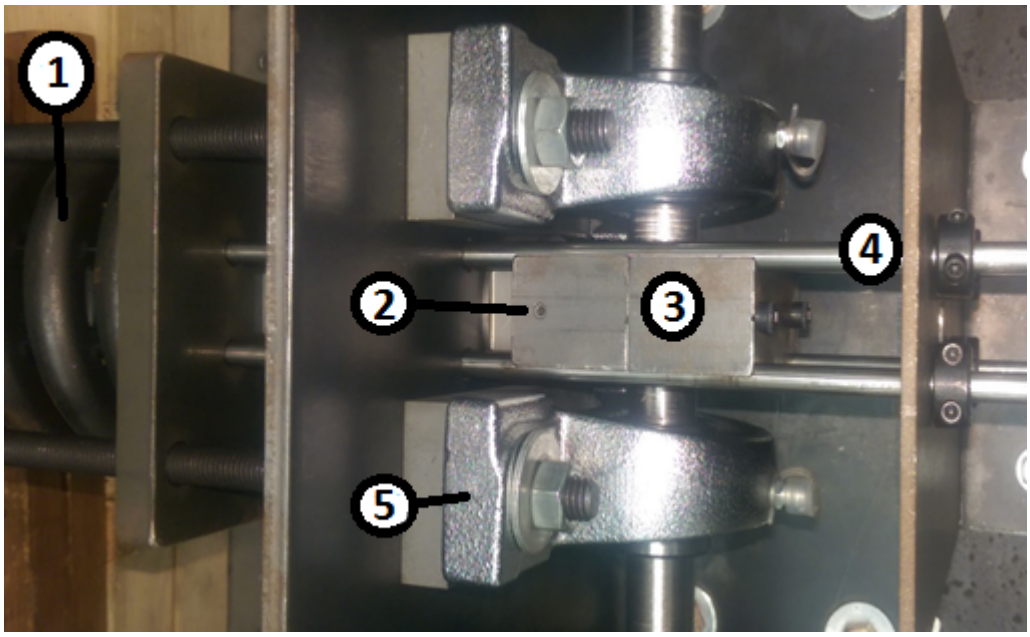

Figure 3.3. Aerial view of the test bearing housing.

CHAPTER FOUR: RESULTS AND DISCUSSION

The first step in evaluating the value of the bearing degradation testbed was to confirm that the data collected are useful degradation and failure data through some comparison with known characteristics of faulted bearing data. The next step involved initial statistical analysis to determine which signals could be useful for future bearing monitoring and diagnostics and to evaluate the data collection frequency needs throughout bearing life.

4.1 Data substantiation

Six data sets were evaluated. The data collected includes the following bearing loadings, with all bearings initially run with no load for approximately 24 hours, as described in Chapter 3. Approximate loading times and failure times are given in Table 4.1. Deviations from the desired 24 hours are due only to logistics and likely have no large impact on overall bearing testing after loading occurs.

Table 4.1. Bearing loading scheme.

Bearing	Loading scheme	Failure time
1	Unloaded (22 hours), 500 lbs. until failure	30 hours
2	Unloaded (20 hours), 500 lbs. until failure	70 hours
3	Unloaded (70 hours), 500 lbs. (~24 hours), increased to 700 lbs. until failure	115 hours
4	Unloaded (18 hours), 500 lbs. (~48 hours), increase to 700 lbs. until failure	70 hours
5	Unloaded (22 hours), 1000 lbs. until failure	28 hours
6	Unloaded (26 hours) 1500 lbs. until failure	27 hours

As the table shows, all of the bearings failed without exceeding their dynamic load rating. Potential causes will be explored in Chapter 5.

4.1.1 Frequency domain analysis

The characteristic bearing fault frequencies were calculated, as shown in Table 4.2, according to equations 2-1 through 2-4. Bearing dimensions are given in Table 3.2, and shaft rotational speed, F_R is equal to 57.7 Hz.

Table 4.2. Bearing characteristic frequencies.

Fault Type	Characteristic Frequency
Cage fault	23.9 Hz
Outer race fault	239.1 Hz
Inner race fault	335.9 Hz
Ball fault	165.9 Hz

The horizontal vibration signal, vertical vibration signal, and acoustic signal were processed using a Fast Fourier transform over 1 second of data every hour. This allows for an initial analysis of how the frequencies are changing over time and whether the fault type can be determined from the frequency spectra alone. The acoustic data was taken from the microphone pointed directly at the bearing alone. Upon evaluation it was determined that the second microphone intended for noise cancelling was not necessary, especially as the majority of the testing took place in an otherwise quiet environment. The Fast Fourier transform plots for each of the data sets are given in Appendix A.

The following figures show the frequency spectra analysis for bearing 2 as an illustrative example because of its relatively long runtime and constant load at 500 lbs.

Figures 4.1 and 4.2 show the frequency spectra of the horizontal and vertical vibrations, respectively. Multiples of the shaft rotational frequency are apparent in

both, as is expected. The horizontal vibrations have lower amplitude than the vertical vibrations, likely due to the force of the spring on the bearing housing lessening vibrations in the horizontal directions. In both plots, the amplitude increases significantly at the end of the life.

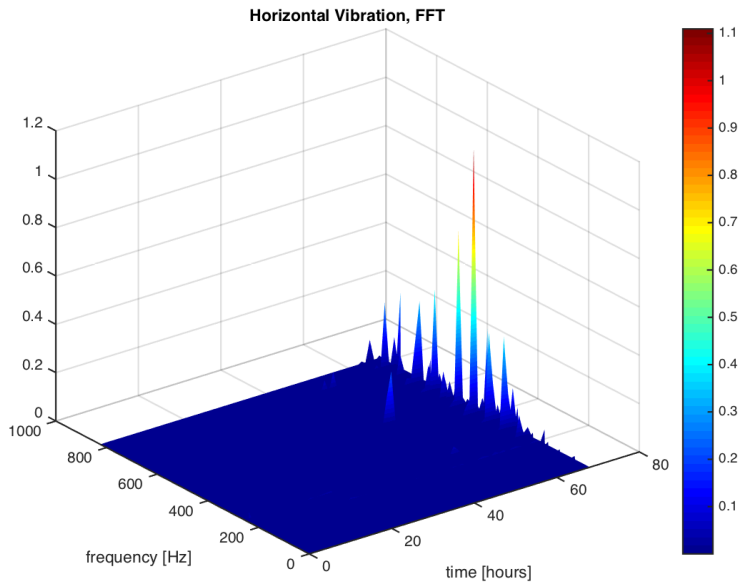

Figure 4.1. Bearing 2 horizontal vibration.

Figure 4.3 shows similar trends for the acoustic emission as in Figures 4.1 and 4.2. The main difference is that many high amplitude peaks show up in the high frequencies late in the bearing lifetime, which skews the plot and dwarfs many of the other peaks.

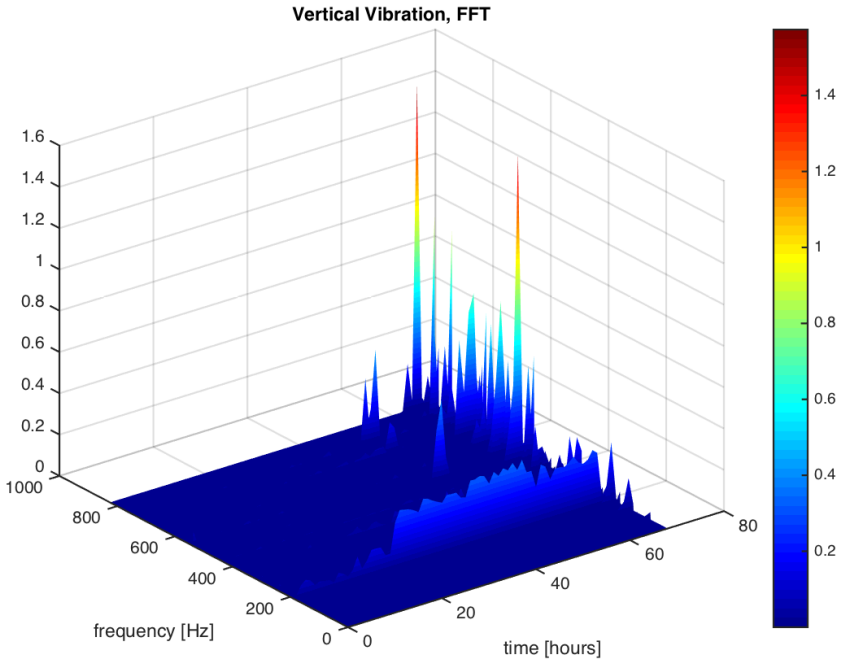

Figure 4.2. Bearing 2 vertical vibration.

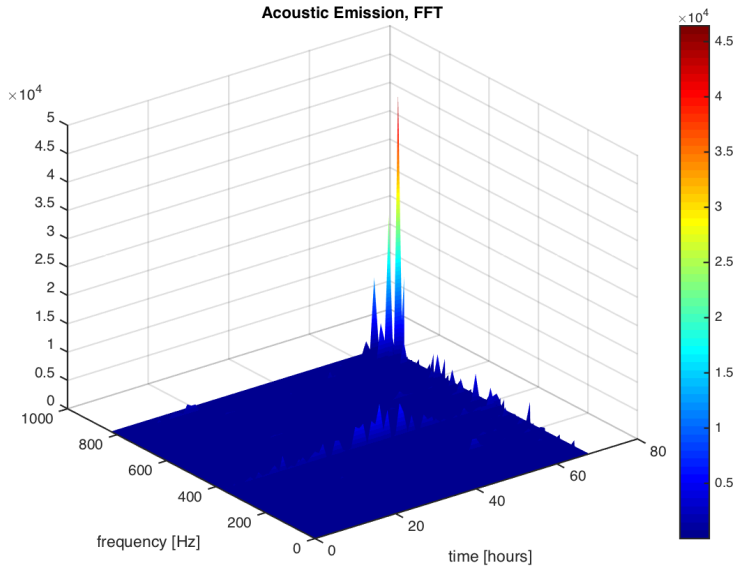

Figure 4.3. Bearing 2 acoustic emission.

In general, there are not any obvious characteristic frequencies present. The shaft rotational frequency of 60 Hz, as well as its multiples, can be seen quite definitively. These possibly dwarf any present characteristic fault frequencies. In some instances the outer race fault frequency of 239 Hz may be present in the frequency spectra, but the certainty of its presence is clouded by the shaft rotational frequency multiple of 240 Hz. The absence of characteristic fault frequencies does not necessarily mean that the data collected is not good or that the faults are not there. As discussed in Chapter 2, many things can contribute to both the values of the fault frequencies and their ability to be detected in frequency spectra.

In all of the data sets, though some more than others, there is an increase in vibration and sound amplitude as expected. Additionally, there are numerous frequencies that show up much later in the bearing life, which is another known phenomenon of bearing failure. Looking at vibration signals alone, the vertical vibration is a much better indicator of overall bearing vibration than the horizontal vibration in frequency domain and time domain analysis because as a significant load is applied in the horizontal direction the horizontal vibrations are suppressed.

4.1.2 Time domain statistical trending

As discussed in Chapter 2, we expect to see a rise in the temperature, acoustic emission, and vibration amplitudes just before failure. In order to show that the vibration and acoustic emission levels increase, we look at the RMS and crest factor. In each of the data sets examined, these values rise at the end of the bearing life as expected. Additionally, we see very clear and rapid increases in temperature just at the end of each bearing life. These features are illustrated with bearing 2, below, as in the previous section. The rest of the data set time domain plots are given in Appendix B.

Figure 4.4, below, shows the 500 lb. radial load applied to the bearing at approximately 20 hours. In each figure, the red dashed line indicates when the loading occurred.

When the load is applied, there is a sharp rise in temperature that then slowly decreases until leveling off at a slightly higher temperature than it was before the loading occurred, illustrated by Figure 4.5. This phenomenon occurs with every bearing.

Vertical vibration is illustrated through the signal crest factor (Figure 4.6), RMS (Figure 4.7), peak-to-peak amplitude (Figure 4.8), and kurtosis (Figure 4.9). The crest factor, peak-to-peak amplitude, and kurtosis generally remain constant until about 60 hours where they each increase significantly. The RMS, on the other hand, increases very slightly for the entire run up until about 60 hours, where it also increases significantly. The crest factor does not seem to provide an earlier warning than the RMS as it is purported to do. The kurtosis follows the expected behavior, remaining right around 3 until the end of the bearing life, when the value increases.

The horizontal vibration RMS is given in Figure 4.10 to illustrate the difference in amplitude between the horizontal and vertical vibrations. Specifically, the horizontal vibration RMS has a lower overall value than that of the vertical vibration for the entirety of the run. The horizontal vibration also decreases after the introduction of the load, as expected. For these reasons, the vibration signal is sufficient in providing information to assess the bearing condition without the use of the horizontal vibration signal.

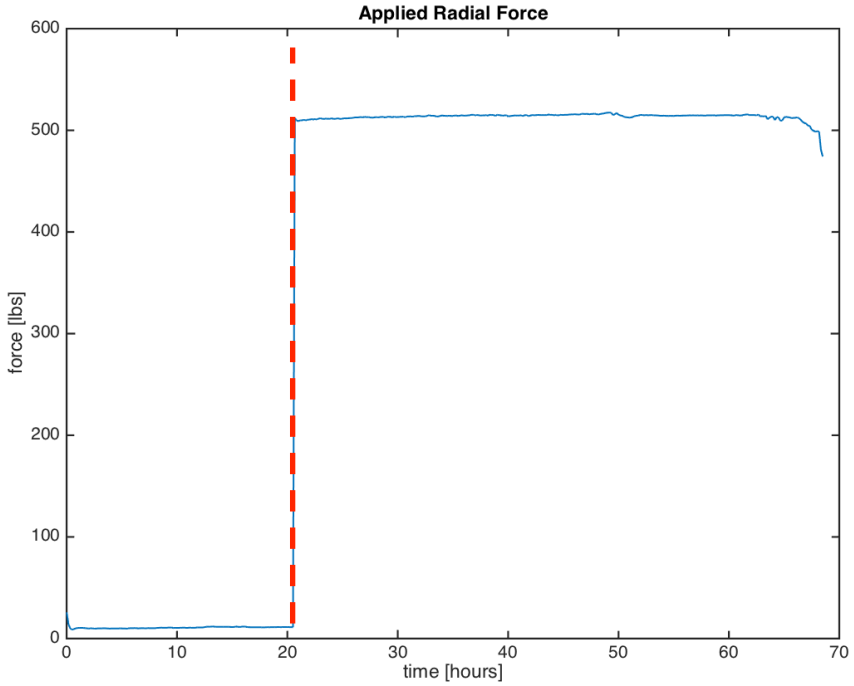

Figure 4.4. Bearing 2 applied radial load of 500 lbs.

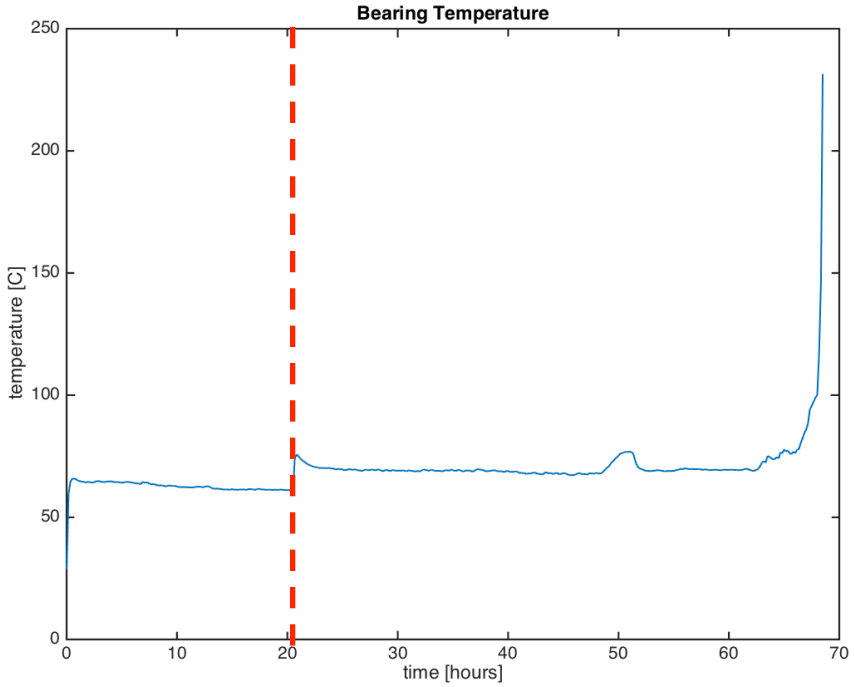

Figure 4.5. Bearing 2 temperature signal.

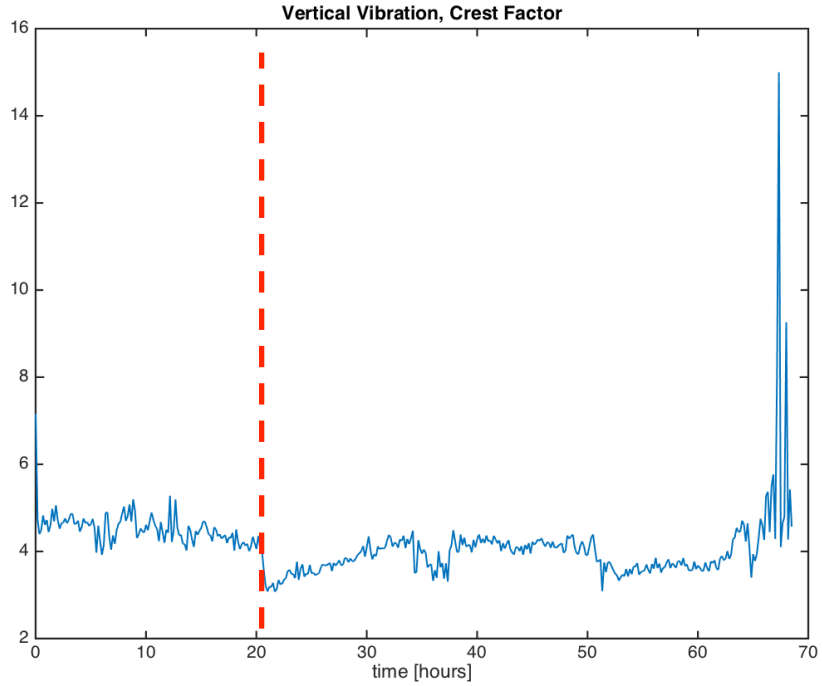

Figure 4.6. Bearing 2 vertical vibration signal crest factor.

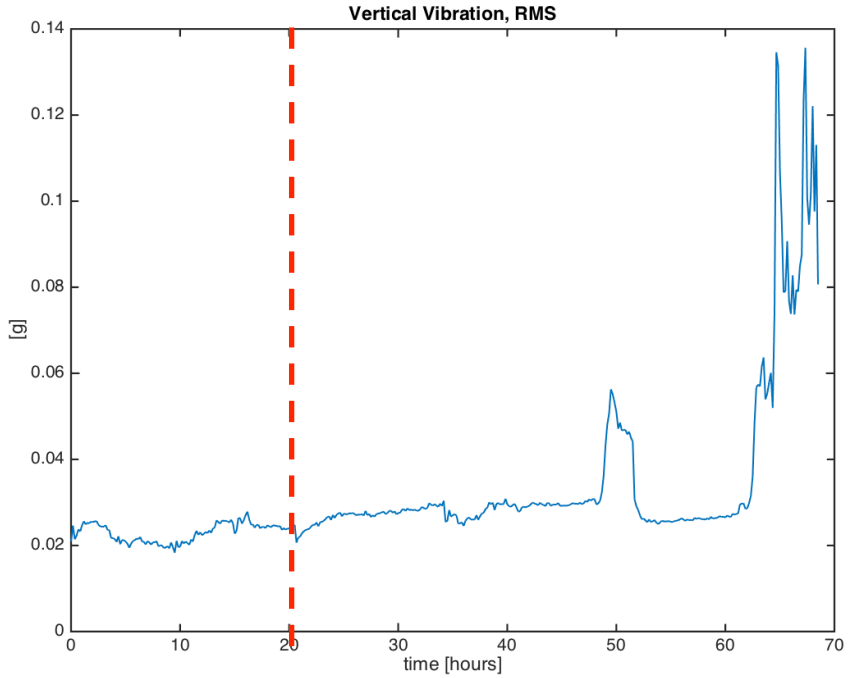

Figure 4.7. Bearing 2 vertical vibration signal RMS.

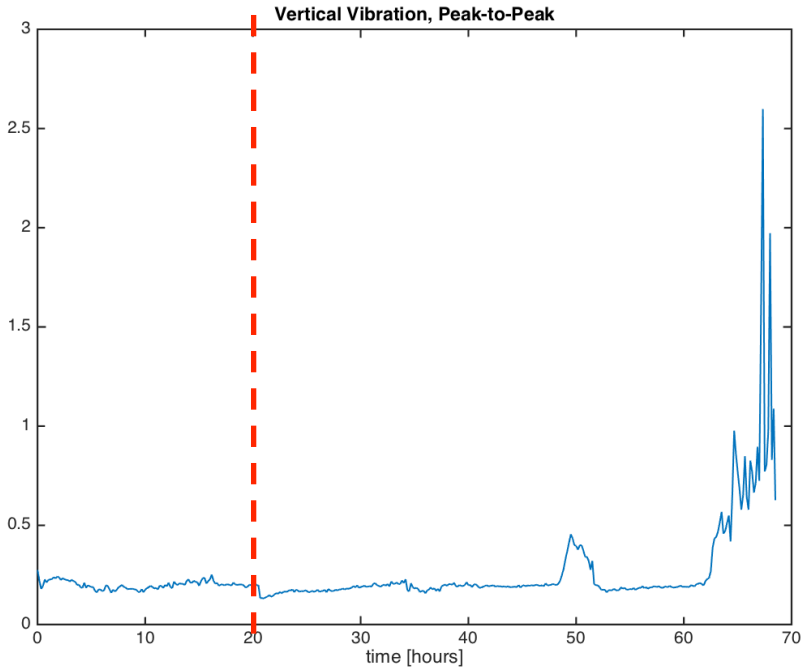

Figure 4.8. Bearing 2 vertical vibration signal peak-to-peak.

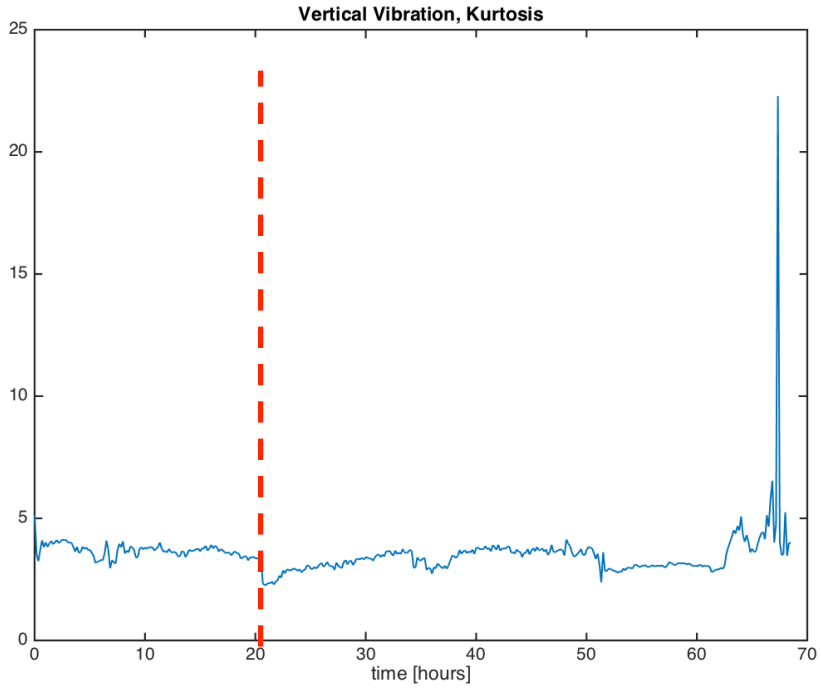

Figure 4.9. Bearing 2 vertical vibration signal kurtosis.

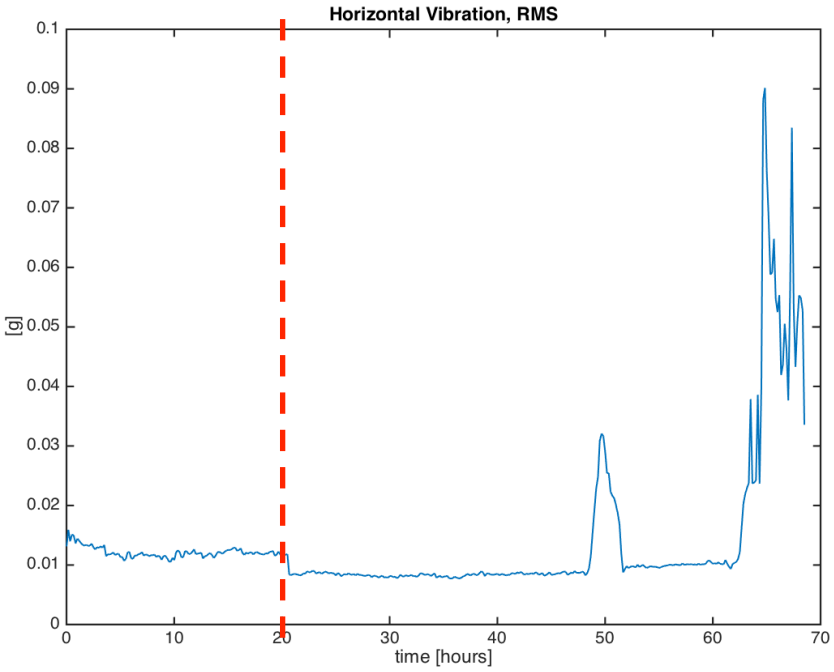

Figure 4.10. Bearing 2 horizontal vibration signal RMS.

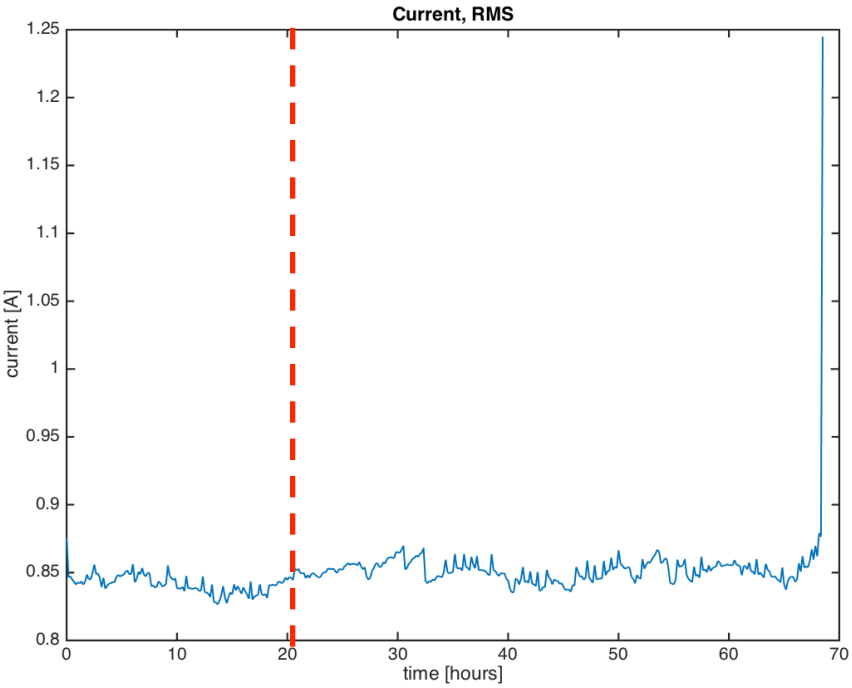

Figure 4.11. Bearing 2 current signal RMS.

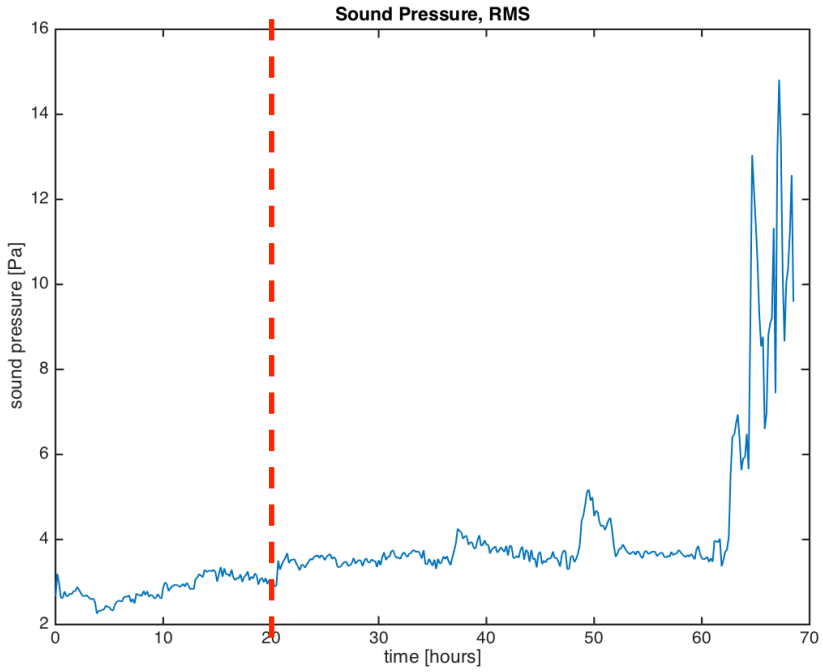

Figure 4.12. Bearing 2 acoustic emission signal RMS.

Finally, the RMS values for the current and acoustic emission are given in Figures 4.11 and 4.12, respectively. Both of these show similar quick increases at 60 hours. The acoustic emission RMS more closely resembles the vertical vibration RMS as it is increasing slowly for the entire bearing life.

The signals of all of the bearings behave generally as expected. When the load increases we see a slight drop in vibration and increase in temperature. There is an increase in sound, current, vibration, and temperature right before failure. The vibration signal kurtosis stays fairly steady at a value of about 3 until just before failure where it peaks and then falls back down.

The inflection around 50 hours in some of the plots could be an early sign of impending failure. It is around this same time that we see some large frequency peaks show up around 500 Hz, 700 Hz, and 750 Hz (Figure 4.1).

4.2 Signal evaluation

The following signal statistics were calculated for the horizontal and vertical vibration, the current, and the acoustic emission: RMS, peak-to-peak ratio, crest factor, and kurtosis. These were calculated over 1 minute lengths of data every 10 minutes. For each data set, correlation coefficients were then calculated among these as well as the radial load and bearing temperature in order to determine whether there are strong relationships among the signals.

Correlations of statistical features that are related by their calculation are omitted from the results shown in Tables 4.3, 4.4, and 4.5.

In this particular data set, there are few correlations. Temperature is relatively highly correlated with motor current and somewhat correlated with vertical vibration, horizontal vibration, and acoustic emission. It makes sense that the horizontal vibration signal has the weakest correlation with temperature because when load goes up and temperature similarly goes up, the horizontal vibrations tend to decrease, or at least not increase as much as the vertical vibrations. Acoustic emission shows correlation to vibration, as could be expected. A model could potentially be built to take advantage of the correlation between temperature and the rest of the signals. The other data sets show similar trends.

Table 4.3. Bearing 2 statistical features correlation coefficients (1/3).

		Temperature	**Load**
Motor Current	**RMS**	0.804	0.236
	Peak-to-Peak	0.749	0.143
	Crest Factor	0.491	0.051
	Kurtosis	0.757	0.058

4.3 Postmortem visual inspection

Following testing, the bearings were examined visually for any definitive signs of failure and cause of failure. Because of the severity of failure that most of the bearings experienced, there are no telltale signs of initial faults. Instead, the bearings show signs of severe damage in multiple areas with the most common being bearing steel discoloration and grease failure, most likely due to high temperatures, and cage and ball damage to the point where the bearing clearly no longer functions as intended, including completely loose balls and broken cages. Figures 4.13, 4.14, and 4.15 show examples of how the bearings looked after failure. Appendix C contains additional photographs.

Figure 4.13. Bearing 1, postmortem.

Figure 4.14. Bearing 2, postmortem.

Figure 4.15. Bearing 3, postmortem.

Table 4.4. Bearing 2 statistical features correlation coefficients (2/3).

		Acoustic Emission			
		RMS	**Peak-to-Peak**	**Crest Factor**	**Kurtosis**
Vertical Vibration	**RMS**	0.966	0.950	-0.104	-0.048
	Peak-to-Peak	0.860	0.863	-0.112	-0.108
	Crest Factor	0.339	0.374	0.029	-0.022
	Kurtosis	0.386	0.417	0.054	0.046
Horizontal Vibration	**RMS**	0.885	0.842	-0.246	-0.180
	Peak-to-Peak	0.864	0.818	-0.270	-0.222
	Crest Factor	-0.036	-0.112	-0.383	-0.441
	Kurtosis	0.506	0.405	-0.457	-0.423

Table 4.5. Bearing 2 statistical features correlation coefficients (3/3).

		Temperature	Load	Motor Current			
				RMS	Peak-to-Peak	Crest Factor	Kurtosis
Vertical Vibration	**RMS**	0.582	0.312	0.208	0.184	0.125	0.167
	Peak-to-Peak	0.493	0.147	0.150	0.121	0.069	0.115
	Crest Factor	0.097	-0.310	-0.017	0.013	0.031	0.043
	Kurtosis	0.130	-0.103	-0.002	0.034	0.059	0.043
Horizontal Vibration	**RMS**	0.439	0.080	0.112	0.109	0.083	0.107
	Peak-to-Peak	0.412	-0.002	0.091	0.094	0.076	0.099
	Crest Factor	-0.138	-0.585	-0.115	-0.102	-0.086	-0.057
	Kurtosis	0.163	-0.276	-0.004	-0.017	-0.042	0.026
Acoustic Emission	**RMS**	0.610	0.375	0.245	0.207	0.130	0.188
	Peak-to-Peak	0.630	0.453	0.279	0.239	0.153	0.217
	Crest Factor	0.000	0.358	0.046	0.042	0.039	0.022
	Kurtosis	0.122	0.434	0.168	0.186	0.164	0.168

CHAPTER FIVE: RECOMMENDATIONS

Many issues in the design of the testbed were worked out through the course of the research done, until the point where the testbed would reliably fail the test bearings with the application of a radial load. While further major changes to the design of the testbed itself are unnecessary, modifications to the data acquisition and analysis could improve the design for further data analysis and prognostics modeling.

5.1 Potential testbed modifications

Ensuring that failure occurs due to only to load and not other outside factors, like misalignment or contaminants in the bearing grease would make the testbed a source of more reliable failure data for industry applications where these factors are controlled for very rigorously. A laser alignment system would be useful for ensuring proper alignment. The use of sealed and pre-greased bearings would be beneficial to remove the possibility of outside contaminants that could cause failure. Changing the test bearing will likely require some additional modifications to the testbed including the redesign of the bearing housing. It may be possible to find bearings that otherwise fit all of the necessary criteria so that no changes past the bearing housing redesign are necessary.

5.2 Data acquisition recommendations

Future work should focus on collecting more data at various loading schemes to ensure the model can be used under different loading conditions. Applying the same modeling techniques to failure data of completely different bearings could further generalize the results.

Adding onto and improving the current sensors would be useful for expanding the capabilities of the testbed. A torque meter added between the motor and the test bearing shaft could give an accurate measurement of the torque forces on the bearing shaft, which may increase as a bearing fault occurs and eventually

causes failure. Proper alignment would be particularly important in this case, as this would add another shaft coupling to the rig. The acoustic emission sensors would likely be more useful mounted on the bearing housing, rather than just pointing in the direction of the bearing.

In order to verify the mode of failure, the failed bearings could be viewed under a microscope. The difficulty in doing this is that sometimes the original cause of failure will not always be obvious. Still, using visual inspection after failure would provide another source of data.

In order to increase post-processing efficiency and reduce the amount of storage necessary, adjustments should be made to the LabView program that collects and saves the process data. All of the data collected for the purposes of this research was collected continuously at 1024 Hz, creating a large amount of data – more than is necessary to perform analysis. Frequency spectra of the vibration and sound signals can be saved over one or two seconds at specified intervals, no longer than one hour apart. All other signals can be saved for one minute bursts every 10 minutes. It might also prove useful to save continuously at 1024 Hz for the very last part of the bearing life. The current and temperature readings would likely be the most reliable and easy source of information for creating an automatic system to change the rate at which data is saved because they both reliably increase significantly at end of life. Increasing the amount of data collected towards the end of the bearing life would allow for more detailed analysis to be done during this major transient period.

5.3 Data analysis recommendations

Because bearing temperature is dependent on the operating load, it might be interesting to normalize the temperature signal with respect to the typical steady state operating temperature at the given load. This could increase the usefulness of the temperature signal and perhaps allow for earlier recognition of a fault.

As it was measured, the acoustic emission signal is not particularly useful. It can essentially be replaced by the horizontal vibration signal, which provides a stronger signal of the bearing vibration in that direction. Changes suggested in the previous section could make the signal more valuable.

CHAPTER SIX: CONCLUSIONS

The constructed accelerated degradation testbed successfully and reliably fails bearings through radial loading. The signals collected show promise in their usefulness for use in online bearing monitoring and prognostics modeling.

Frequency domain analysis alone does not yield definitive information about the type of fault that occurs, but there is an overall increase in vibration as well as some frequency peaks that show up later in life, possibly indicating a fault.

Time domain analysis shows that the data collected follows the expected trends for bearing failure. While correlations among the data statistical features looked at are not very strong, further analysis should be done before determining which combinations of signals might be useful for prognostics modeling.

Changes in the testbed design will likely yield even more reliable and repeatable results. The most pressing is perhaps the use of sealed and pre-greased bearings to eliminate the possibility of grease contamination. Significant changes in the data collection are not needed; however, the amount of data saved should be adjusted to decrease storage needs and increase efficiency of post processing.

REFERENCES

[1] H. Qiu, J. Lee, J. Lin, and G. Yu, "Robust performance degradation assessment methods for enhanced rolling element bearing prognostics," *Advanced Engineering Informatics,* vol. 17, pp. 127-140, 7// 2003.
[2] S. Nandi, H. A. Toliyat, and X. Li, "Condition monitoring and fault diagnosis of electrical motors-a review," *Energy Conversion, IEEE Transactions on,* vol. 20, pp. 719-729, 2005.
[3] J. Ma and J. Jiang, "Applications of fault detection and diagnosis methods in nuclear power plants: A review," *Progress in Nuclear Energy,* vol. 53, pp. 255-266, 4// 2011.
[4] G. R. Overbeck, "Manual reactor trip due to vibration and bearing temperature increases in reactor coolant pump," Palo Verde Nuclear Generating Station, Licensee Event Report 97-006-00, November 12, 1997.
[5] H. M. Hashemian, "On-line monitoring applications in nuclear power plants," *Progress in Nuclear Energy,* vol. 53, pp. 167-181, 3// 2011.
[6] B. Mevel and J. Guyader, "Routes to chaos in ball bearings," *Journal of Sound and Vibration,* vol. 162, pp. 471-487, 1993.
[7] C. S. Sunnersjö, "Varying compliance vibrations of rolling bearings," *Journal of Sound and Vibration,* vol. 58, pp. 363-373, 1978/06/08 1978.
[8] A. Rafsanjani, S. Abbasion, A. Farshidianfar, and H. Moeenfard, "Nonlinear dynamic modeling of surface defects in rolling element bearing systems," *Journal of Sound and Vibration,* vol. 319, pp. 1150-1174, 2009.
[9] N. Tandon and A. Choudhury, "A review of vibration and acoustic measurement methods for the detection of defects in rolling element bearings," *Tribology International,* vol. 32, pp. 469-480, 8// 1999.
[10] J. Miettinen and P. Andersson, "Acoustic emission of rolling bearings lubricated with contaminated grease," *Tribology International,* vol. 33, pp. 777-787, 2000.
[11] P. D. McFadden and J. D. Smith, "Model for the vibration produced by a single point defect in a rolling element bearing," *Journal of Sound and Vibration,* vol. 96, pp. 69-82, 1984/09/08 1984.
[12] H. Schreiber, "The contact angle of various rolling bearings and its effect on bearing selection," *Tribology,* vol. 1, pp. 214-218, 1968.
[13] R. R. Schoen, T. G. Habetler, F. Kamran, and R. Bartfield, "Motor bearing damage detection using stator current monitoring," *Industry Applications, IEEE Transactions on,* vol. 31, pp. 1274-1279, 1995.
[14] "Bearing Failure: Causes and Cures," W. Research, Ed., ed.
[15] T. T. Company, "Bearing Failure Prevention Guide," ed.
[16] R. D. Evans, "Classic Bearing Damage Modes," in *Wind Turbine Tribology Seminar*, Broomfield, CO, USA, 2011.
[17] A. M. Al-Ghamd and D. Mba, "A comparative experimental study on the use of acoustic emission and vibration analysis for bearing defect identification and estimation of defect size," *Mechanical systems and signal processing,* vol. 20, pp. 1537-1571, 2006.

[18] M. Blödt, P. Granjon, B. Raison, and G. Rostaing, "Models for bearing damage detection in induction motors using stator current monitoring," *Industrial Electronics, IEEE Transactions on,* vol. 55, pp. 1813-1822, 2008.
[19] J. R. Stack, T. G. Habetler, and R. G. Harley, "Experimentally generating faults in rolling element bearings via shaft current," *Industry Applications, IEEE Transactions on,* vol. 41, pp. 25-29, 2005.
[20] C. Anger, C. Preusche, and U. Klingauf, "Asynchronous Motor Test Bench for the Generation and Current Signal Diagnostics of Accelerated Bearing Damage."
[21] H. E. Boyanton and G. Hodges, "Bearing fluting [motors]," *Industry Applications Magazine, IEEE,* vol. 8, pp. 53-57, 2002.
[22] Y.-T. Su and S.-J. Lin, "On initial fault detection of a tapered roller bearing: frequency domain analysis," *Journal of Sound and Vibration,* vol. 155, pp. 75-84, 1992.
[23] W. Oh, "Preventing VFD/AC Drive Induced Electrical Damage to AC Motor Bearings," Electro Static Technology, An ITW Company, A Technial White Paper2006.
[24] T. Williams, X. Ribadeneira, S. Billington, and T. Kurfess, "ROLLING ELEMENT BEARING DIAGNOSTICS IN RUN-TO-FAILURE LIFETIME TESTING," *Mechanical Systems and Signal Processing,* vol. 15, pp. 979-993, 9// 2001.
[25] S. Janjarasjitt, H. Ocak, and K. Loparo, "Bearing condition diagnosis and prognosis using applied nonlinear dynamical analysis of machine vibration signal," *Journal of Sound and Vibration,* vol. 317, pp. 112-126, 2008.
[26] N. Jammu and P. Kankar, "A review on prognosis of rolling element bearings," *International Journal of Engineering Science and Technology,* vol. 3, pp. 7497-7503, 2011.
[27] C. S. Sunnersjö, "Rolling bearing vibrations—The effects of geometrical imperfections and wear," *Journal of Sound and Vibration,* vol. 98, pp. 455-474, 2/22/ 1985.
[28] R. J. Hansen, D. L. Hall, and S. K. Kurtz, "A new approach to the challenge of machinery prognostics," in *ASME 1994 International Gas Turbine and Aeroengine Congress and Exposition*, 1994, pp. V005T15A001-V005T15A001.
[29] N. Tandon and B. Nakra, "Detection of defects in rolling element bearings by vibration monitoring," *Indian Journal of Mechanical Engineering Division,* vol. 73, pp. 271-282, 1993.
[30] C. J. Li and H. Shin, "Tracking bearing spall severity through inverse modeling," in *Proceedings of the ASME International Mechanical Engineering Congress*, 2004, pp. 1-6.
[31] J. Harmouche, C. Delpha, and D. Diallo, "A global approach for the classification of bearing faults conditions using spectral features," in *Industrial Electronics Society, IECON 2013-39th Annual Conference of the IEEE*, 2013, pp. 7352-7357.

[32] A. Choudhury and N. Tandon, "Application of acoustic emission technique for the detection of defects in rolling element bearings," *Tribology International,* vol. 33, pp. 39-45, 1// 2000.
[33] P. Cann, J. Doner, M. Webster, and V. Wikstrom, "Grease degradation in rolling element bearings," *Tribology Transactions,* vol. 44, pp. 399-404, 2001.
[34] W. Yan, H. Qiu, and N. Iyer, "Feature extraction for bearing prognostics and health management (phm)-a survey," in *62nd Meeting of the Society for Machinery, Virginia Beach, VA*, 2008.
[35] D. Dyer and R. Stewart, "Detection of rolling element bearing damage by statistical vibration analysis," *Journal of mechanical design,* vol. 100, pp. 229-235, 1978.
[36] S. Qian and D. Chen, "Joint time-frequency analysis," *Signal Processing Magazine, IEEE,* vol. 16, pp. 52-67, 1999.
[37] P. D. Welch, "The use of fast Fourier transform for the estimation of power spectra: A method based on time averaging over short, modified periodograms," *IEEE Transactions on audio and electroacoustics,* vol. 15, pp. 70-73, 1967.
[38] A. K. S. Jardine, D. Lin, and D. Banjevic, "A review on machinery diagnostics and prognostics implementing condition-based maintenance," *Mechanical Systems and Signal Processing,* vol. 20, pp. 1483-1510, 10// 2006.
[39] M. E. Sharp, "Prognostic Approaches Using Transient Monitoring Methods," 2012.
[40] D. Gabor, "Theory of communication. Part 1: The analysis of information," *Electrical Engineers-Part III: Radio and Communication Engineering, Journal of the Institution of,* vol. 93, pp. 429-441, 1946.
[41] Q. Meng and L. Qu, "Rotating machinery fault diagnosis using Wigner distribution," *Mechanical Systems and Signal Processing,* vol. 5, pp. 155-166, 1991.
[42] N. E. Huang and Z. Wu, "A review on Hilbert-Huang transform: Method and its applications to geophysical studies," *Reviews of Geophysics,* vol. 46, 2008.
[43] J. B. Coble and J. Hines, "Prognostic algorithm categorization with PHM challenge application," in *Prognostics and Health Management, 2008. PHM 2008. International Conference on*, 2008, pp. 1-11.
[44] F. Camci, K. Medjaher, N. Zerhouni, and P. Nectoux, "Feature evaluation for effective bearing prognostics," *Quality and reliability engineering international,* vol. 29, pp. 477-486, 2013.
[45] P. Wang and G. Vachtsevanos, "Fault prognostics using dynamic wavelet neural networks," *AI EDAM,* vol. 15, pp. 349-365, 2001.
[46] Y. Shao and K. Nezu, "Prognosis of remaining bearing life using neural networks," *Proceedings of the Institution of Mechanical Engineers, Part I: Journal of Systems and Control Engineering,* vol. 214, pp. 217-230, 2000.

[47] R. Huang, L. Xi, X. Li, C. R. Liu, H. Qiu, and J. Lee, "Residual life predictions for ball bearings based on self-organizing map and back propagation neural network methods," *Mechanical Systems and Signal Processing,* vol. 21, pp. 193-207, 2007.

[48] I. E. Alguindigue, A. Loskiewicz-Buczak, and R. E. Uhrig, "Monitoring and diagnosis of rolling element bearings using artificial neural networks," *Industrial Electronics, IEEE Transactions on,* vol. 40, pp. 209-217, 1993.

[49] B. Satish and N. Sarma, "A fuzzy BP approach for diagnosis and prognosis of bearing faults in induction motors," in *Power Engineering Society General Meeting, 2005. IEEE*, 2005, pp. 2291-2294.

[50] F. Z. Feng, D. D. Zhu, P. C. Jiang, and H. Jiang, "GA-SVR based bearing condition degradation prediction," in *Key Engineering Materials*, 2009, pp. 431-437.

[51] Z. Li, Z. He, Y. Zi, and H. Jiang, "Rotating machinery fault diagnosis using signal-adapted lifting scheme," *Mechanical Systems and Signal Processing,* vol. 22, pp. 542-556, 2008.

[52] X. Zhang, R. Xu, C. Kwan, S. Y. Liang, Q. Xie, and L. Haynes, "An integrated approach to bearing fault diagnostics and prognostics," in *American Control Conference, 2005. Proceedings of the 2005*, 2005, pp. 2750-2755.

[53] A. Heng, S. Zhang, A. C. Tan, and J. Mathew, "Rotating machinery prognostics: State of the art, challenges and opportunities," *Mechanical Systems and Signal Processing,* vol. 23, pp. 724-739, 2009.

[54] McMaster-Carr, "Ball Bearing, Trade No. R12, for 3/4" Shaft Diameter, 1-5/8" OD," ed.

APPENDICES

APPENDIX A: FREQUENCY DOMAIN ANALYSIS

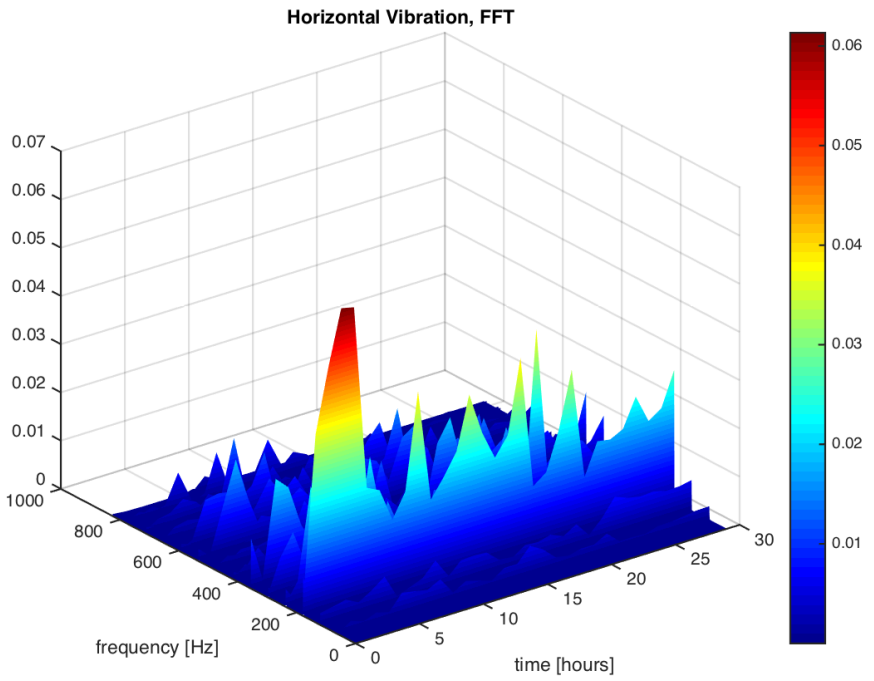

Figure A.1. Bearing 1 horizontal vibration.

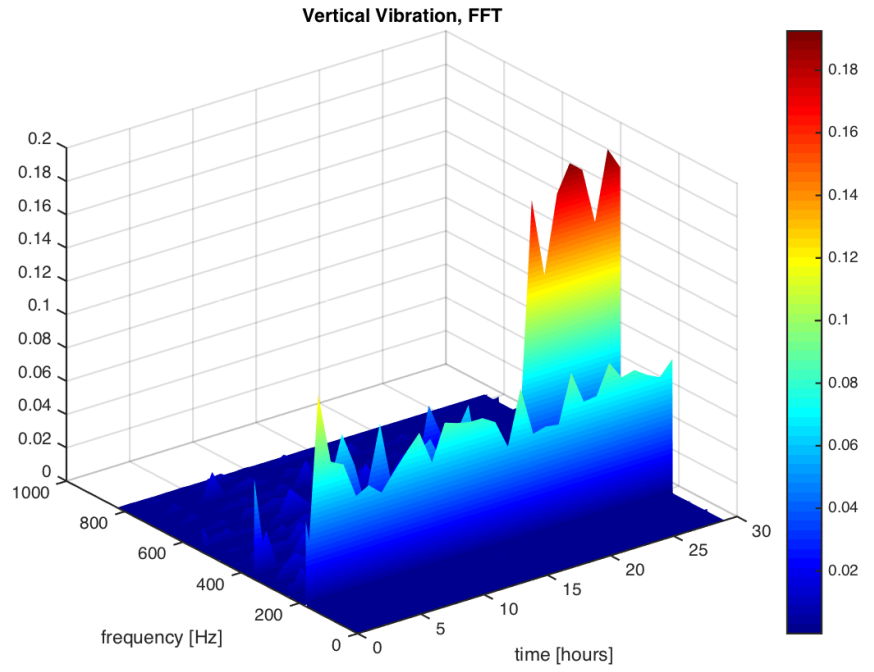

Figure A.2. Bearing 1 vertical vibration.

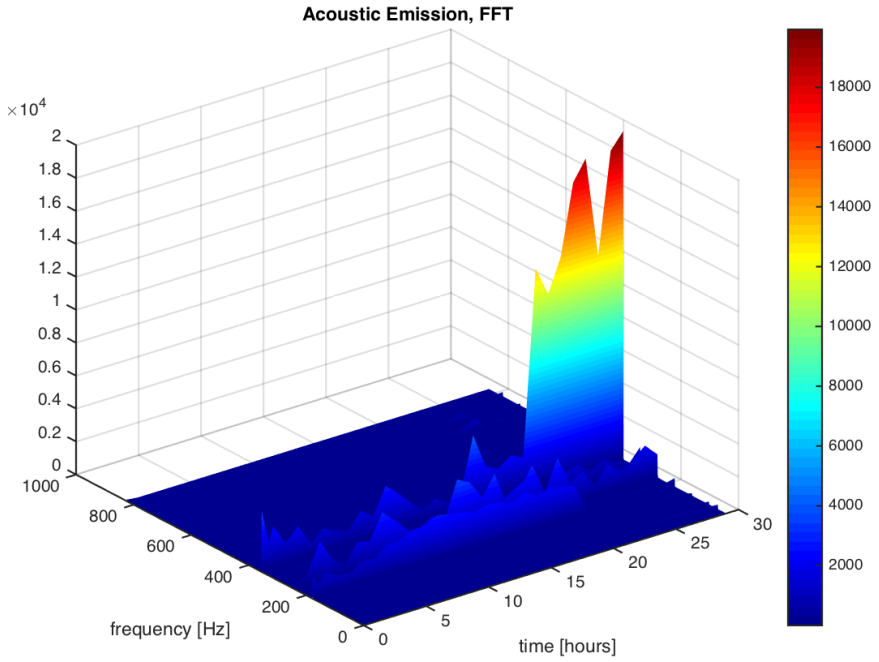

Figure A.3. Bearing 1 acoustic emission.

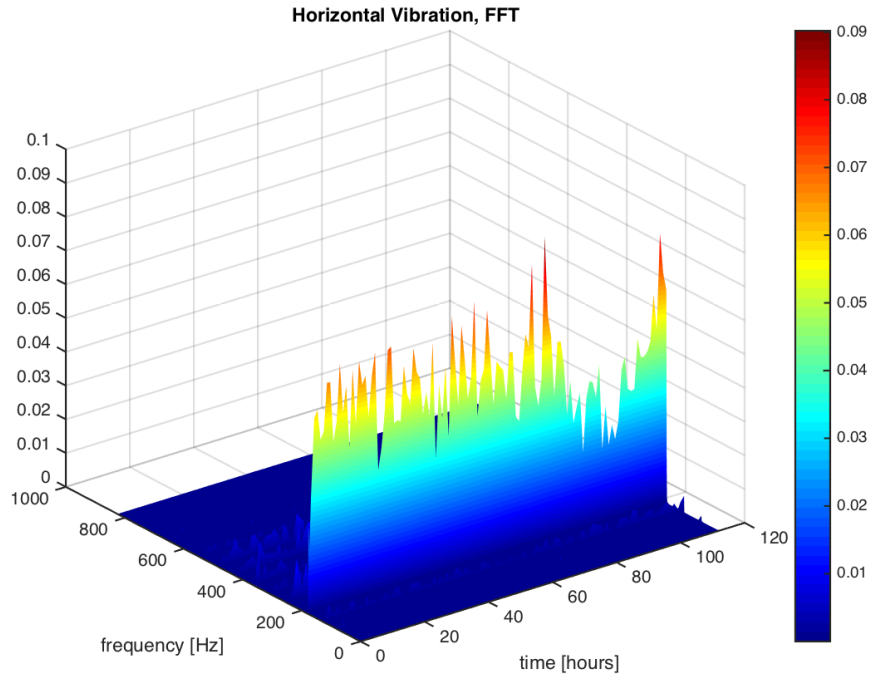

Figure A.4. Bearing 3 horizontal vibration.

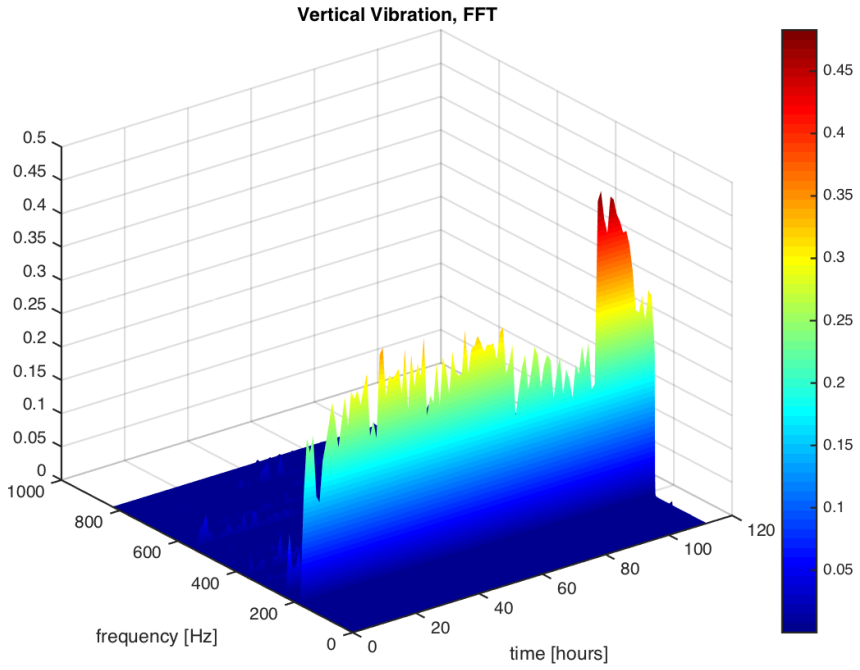

Figure A.5. Bearing 3 vertical vibration.

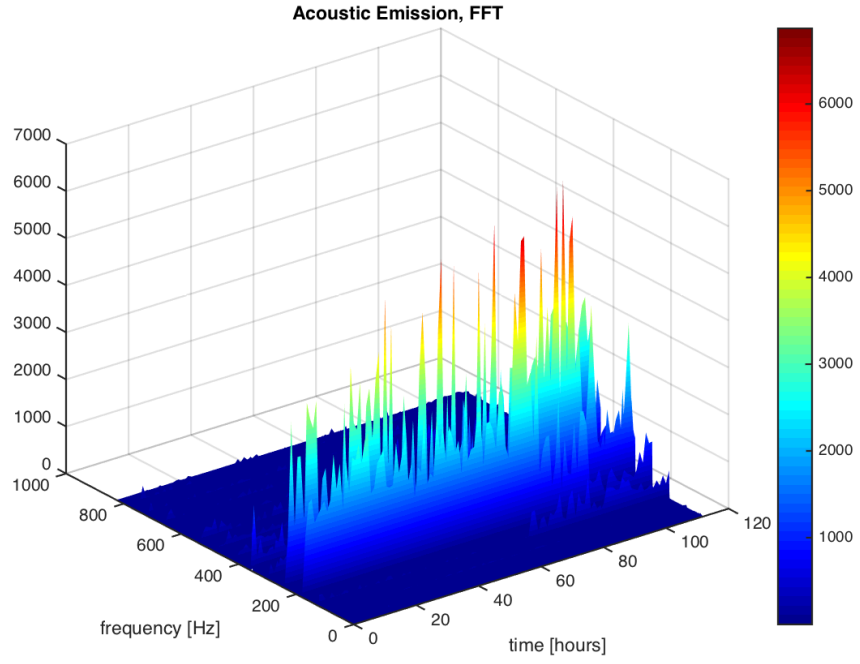

Figure A.6. Bearing 3 acoustic emission.

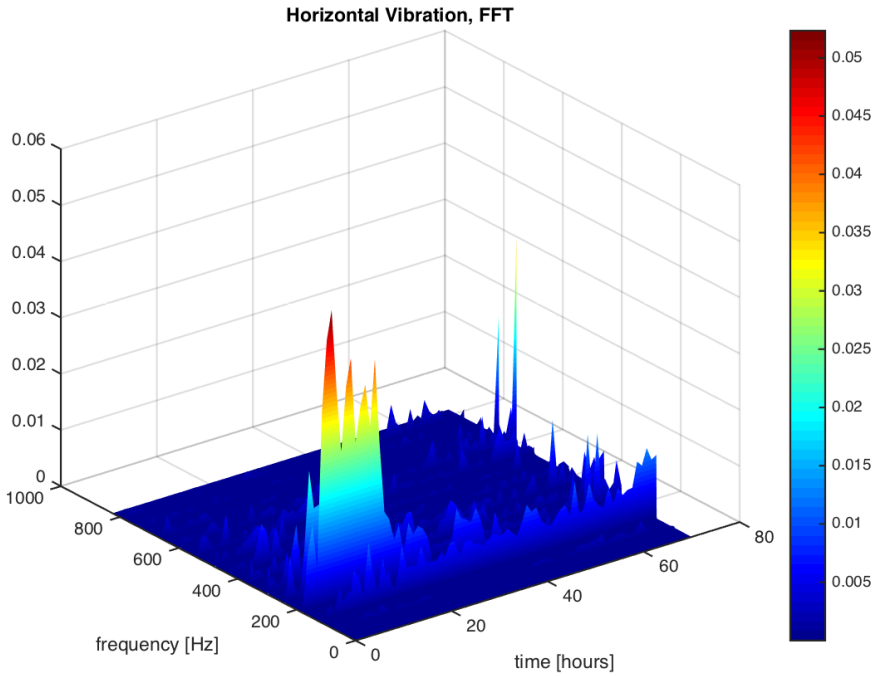

Figure A.7. Bearing 4 horizontal vibration.

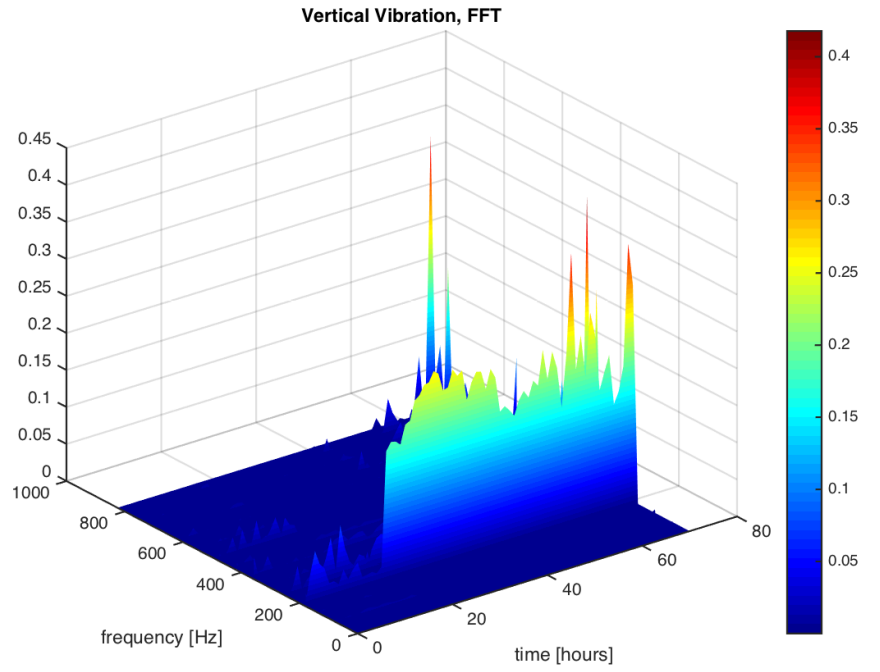

Figure A.8. Bearing 4 vertical vibration.

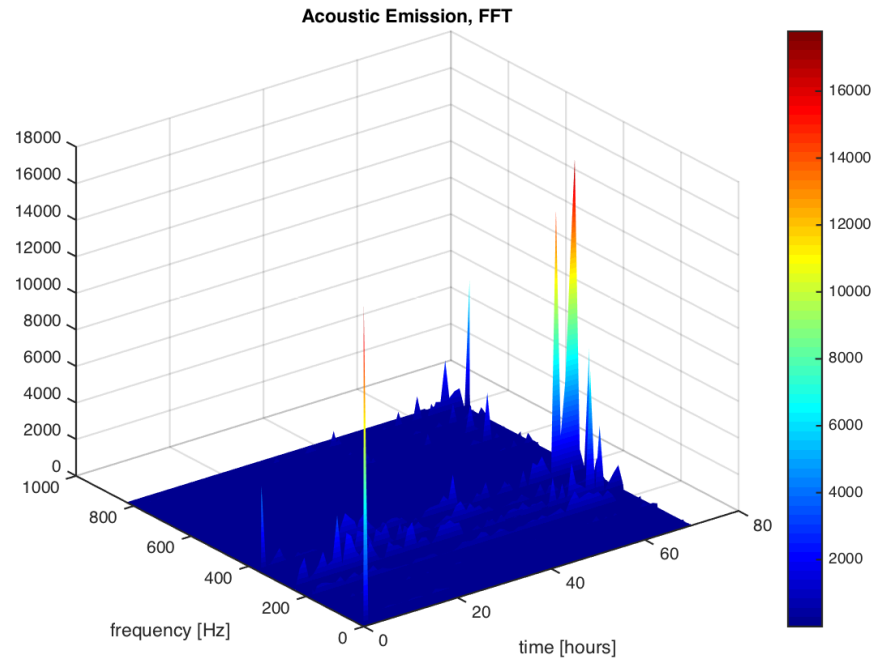

Figure A.9. Bearing 4 acoustic emission.

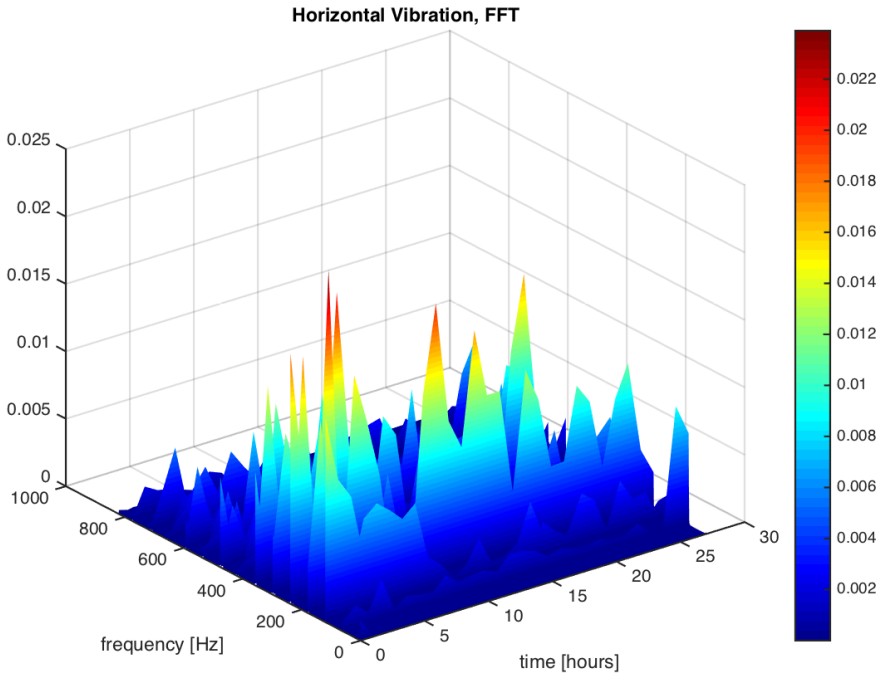

Figure A.10. Bearing 5 horizontal vibration.

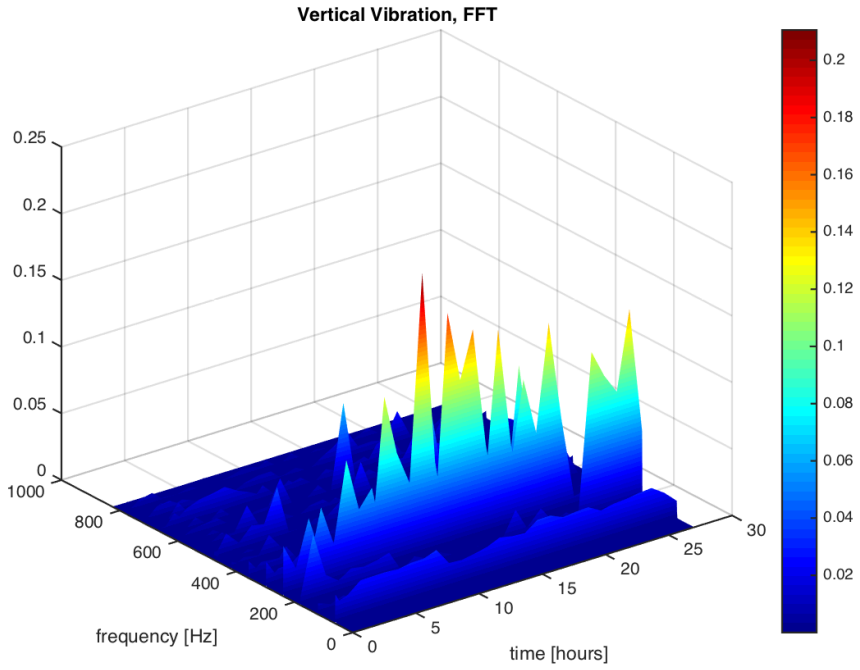

Figure A.11. Bearing 5 vertical vibration.

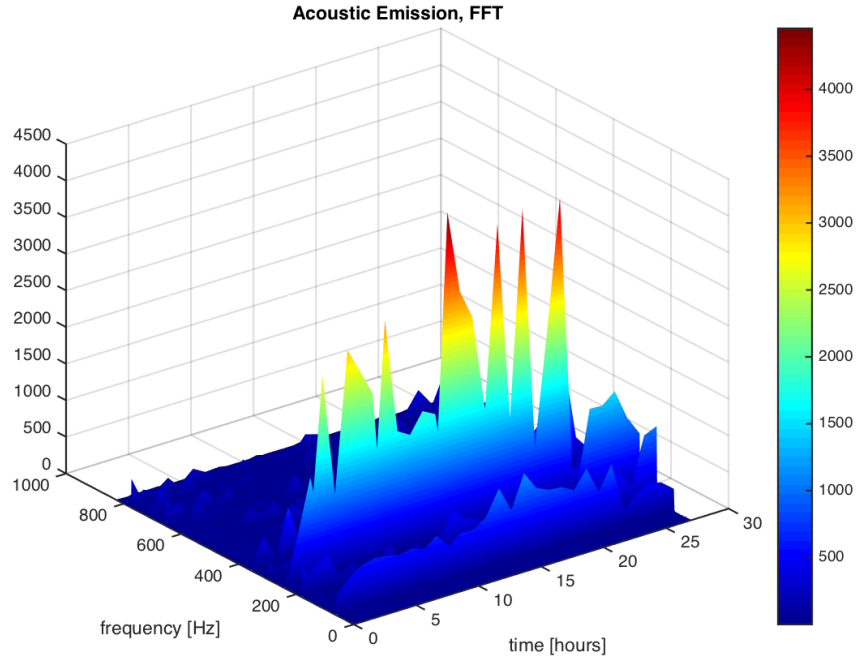

Figure A.12. Bearing 5 acoustic emission.

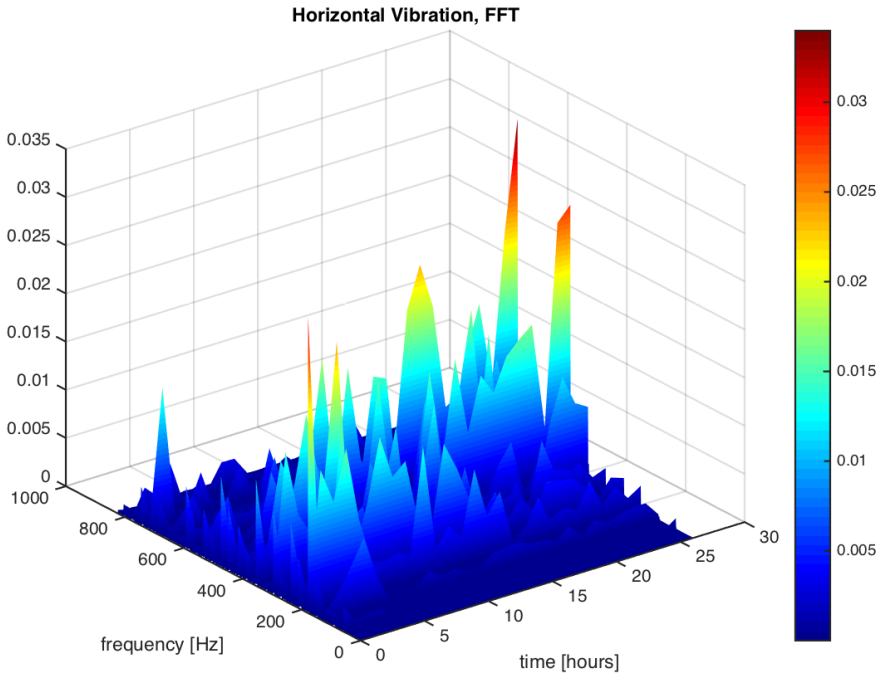

Figure A.13. Bearing 6 horizontal vibration.

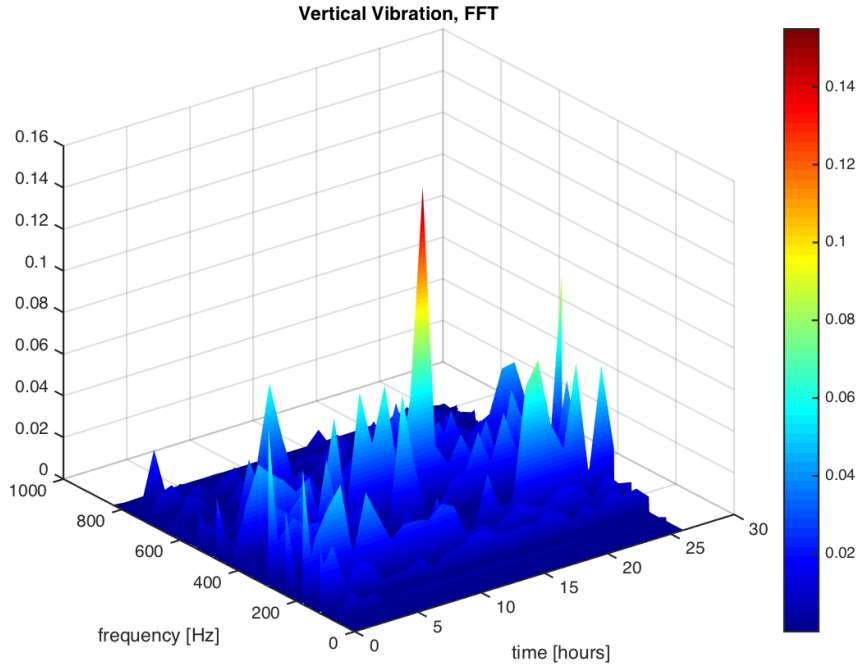

Figure A.14. Bearing 6 vertical vibration.

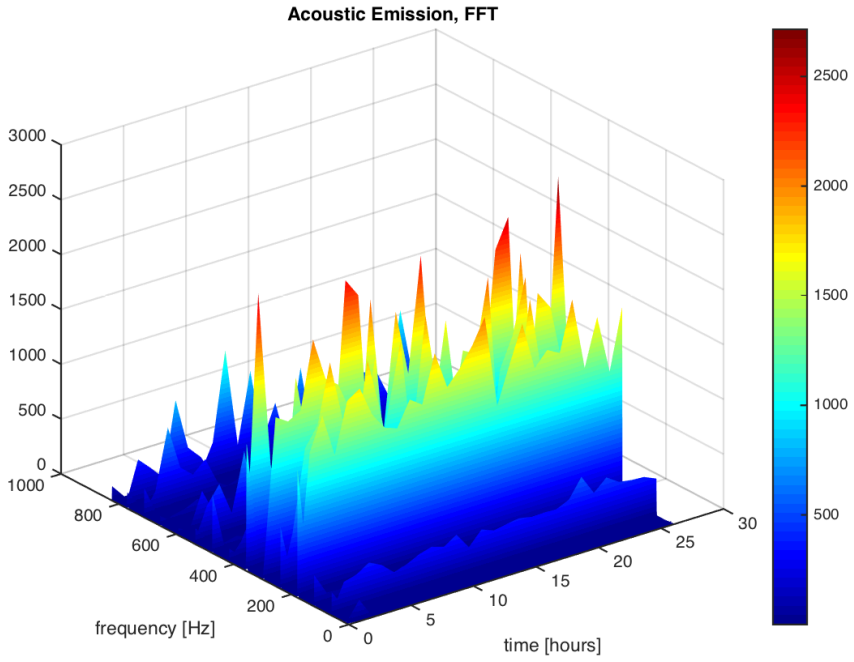

Figure A.15. Bearing 6 acoustic emission.

APPENDIX B: TIME DOMAIN ANALYSIS

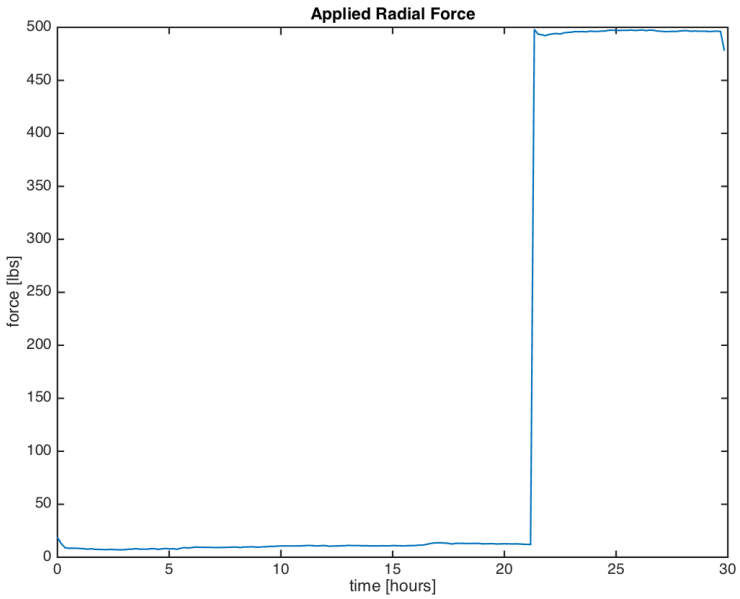

Figure B.16. Bearing 1 applied radial load.

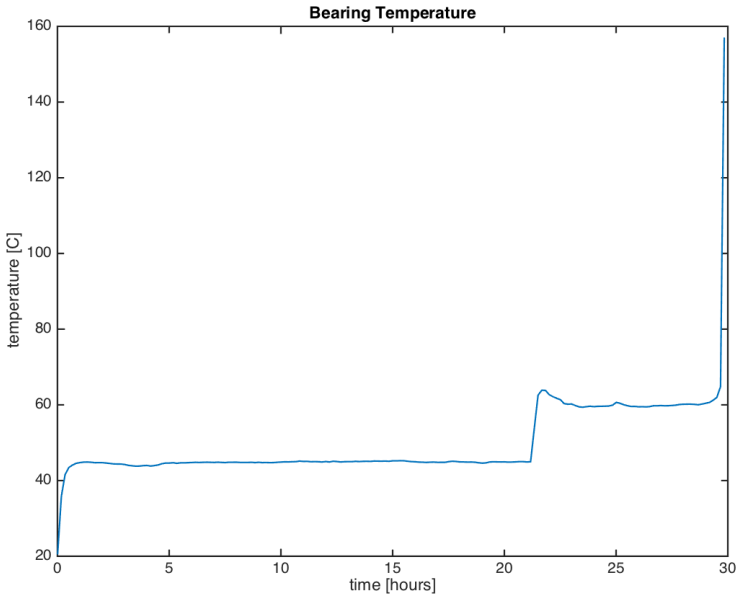

Figure B.17. Bearing 1 temperature.

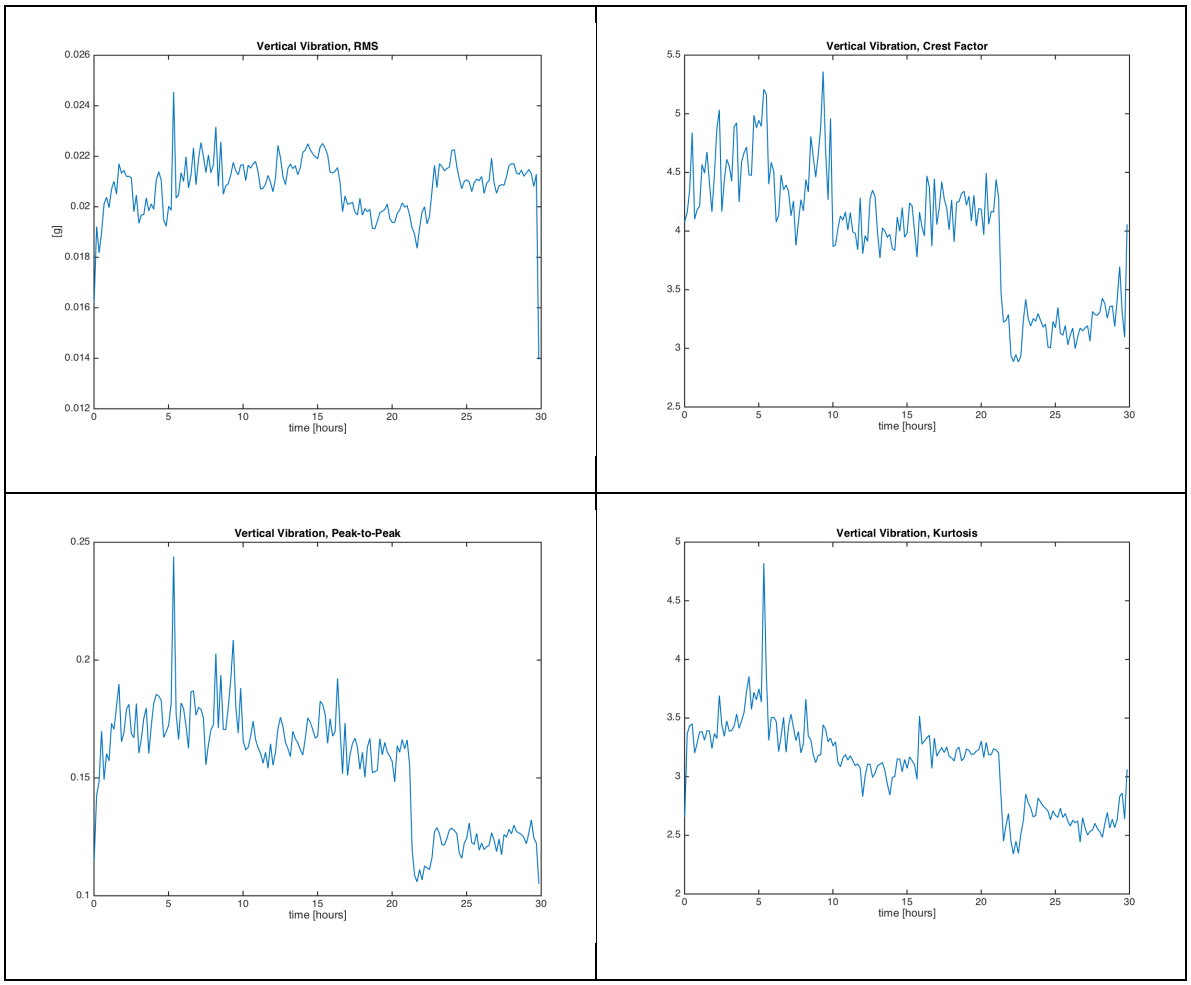

Figure B.18. Bearing 1 vertical vibration, from top left: a) RMS, b) crest factor, c) peak-to-peak ratio, and d) kurtosis.

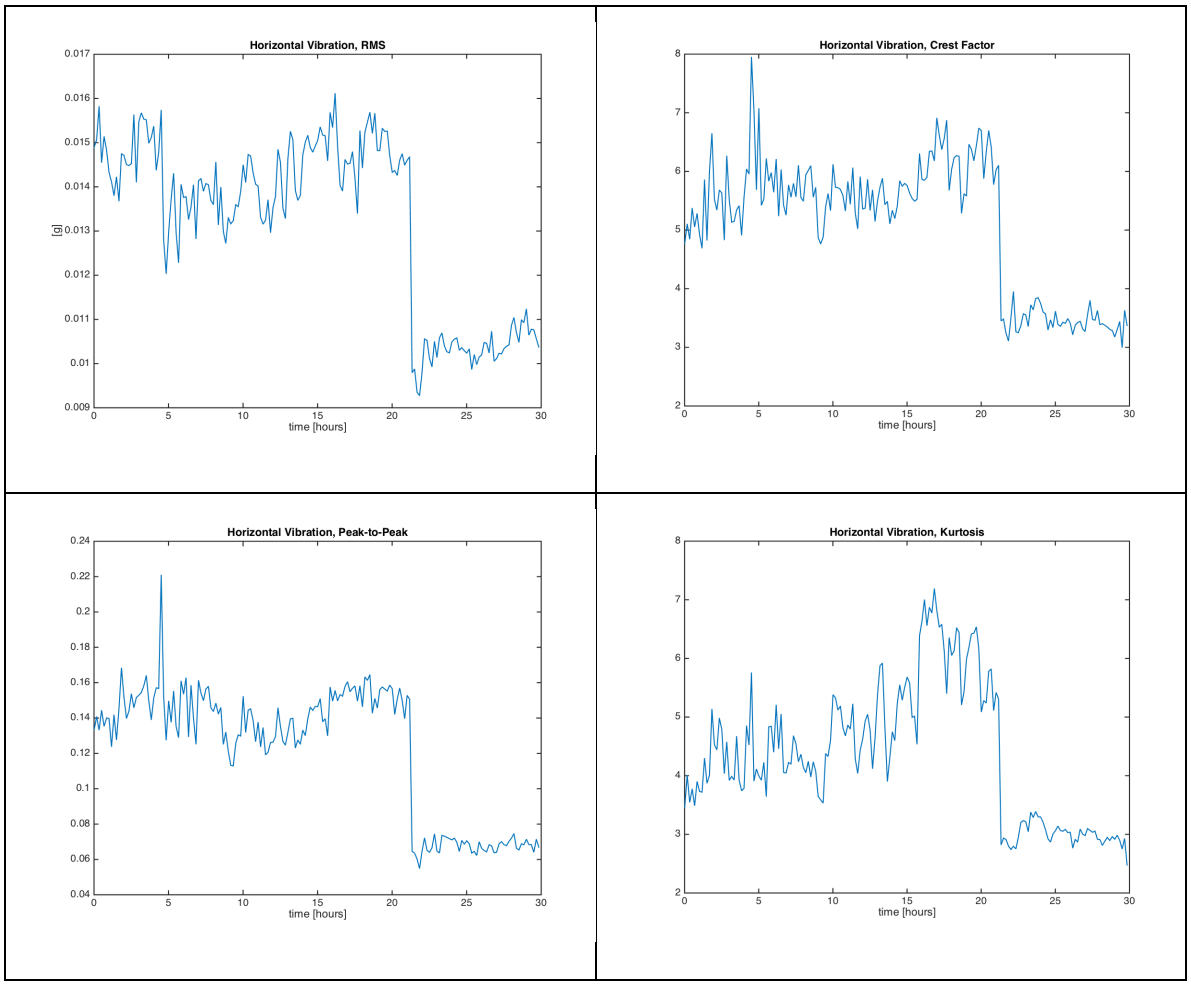

Figure B.19. Bearing 1 horizontal vibration, from top left: a) RMS, b) crest factor, c) peak-to-peak ratio, and d) kurtosis.

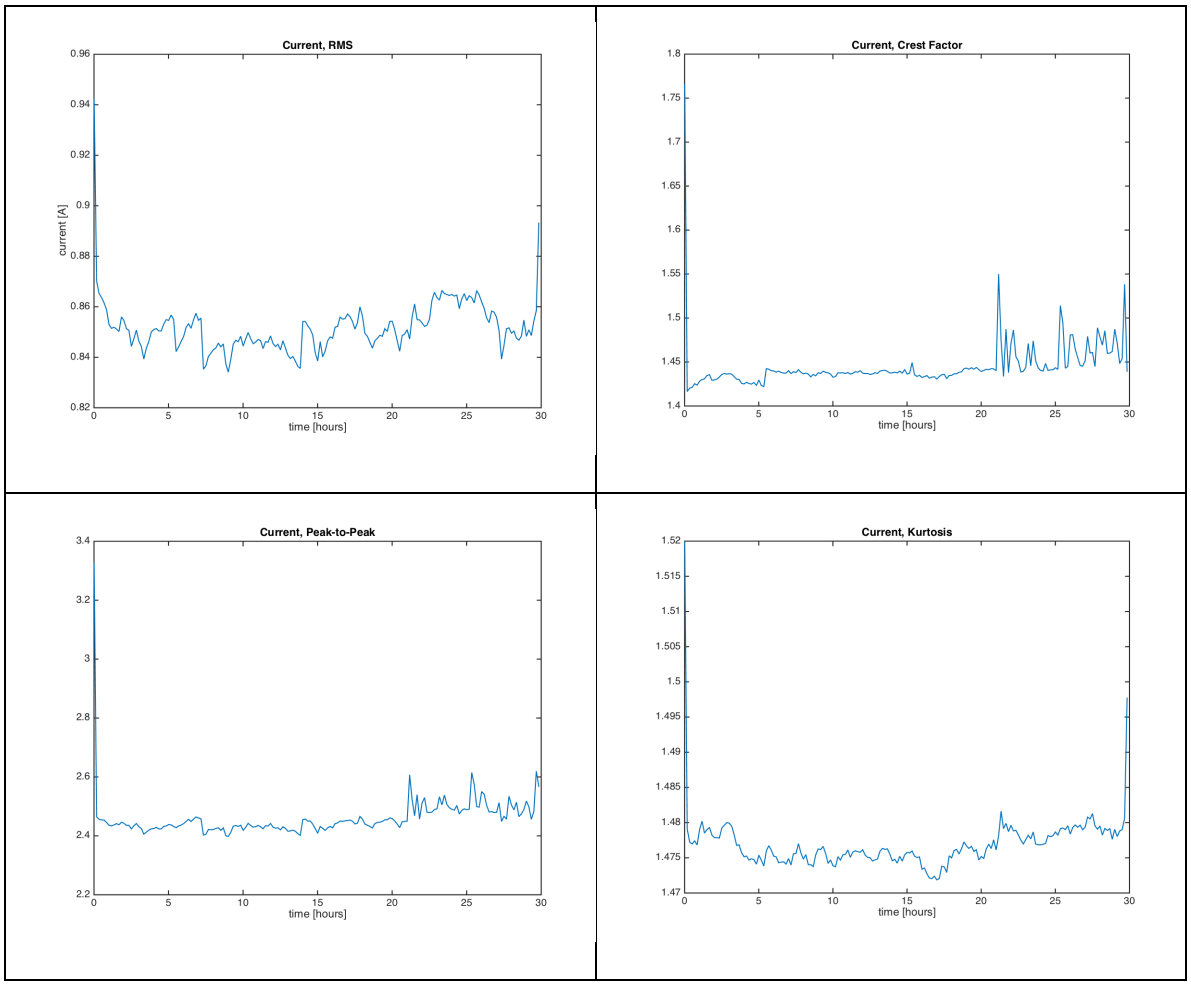

Figure B.20. Bearing 1 current signal, from top left: a) RMS, b) crest factor, c) peak-to-peak ratio, and d) kurtosis.

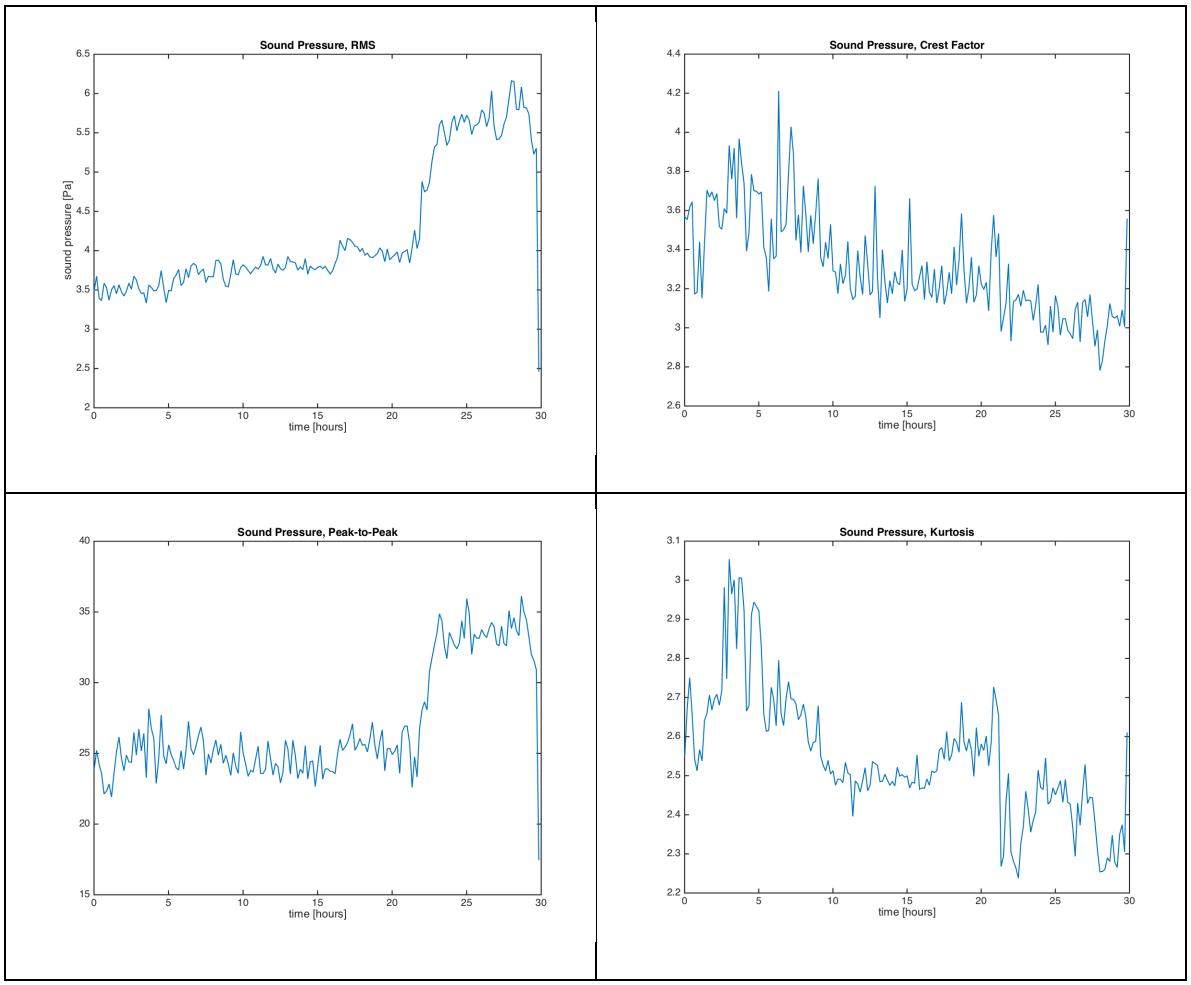

Figure B.21. Bearing 1 acoustic emission, from top left: a) RMS, b) crest factor, c) peak-to-peak ratio, and d) kurtosis.

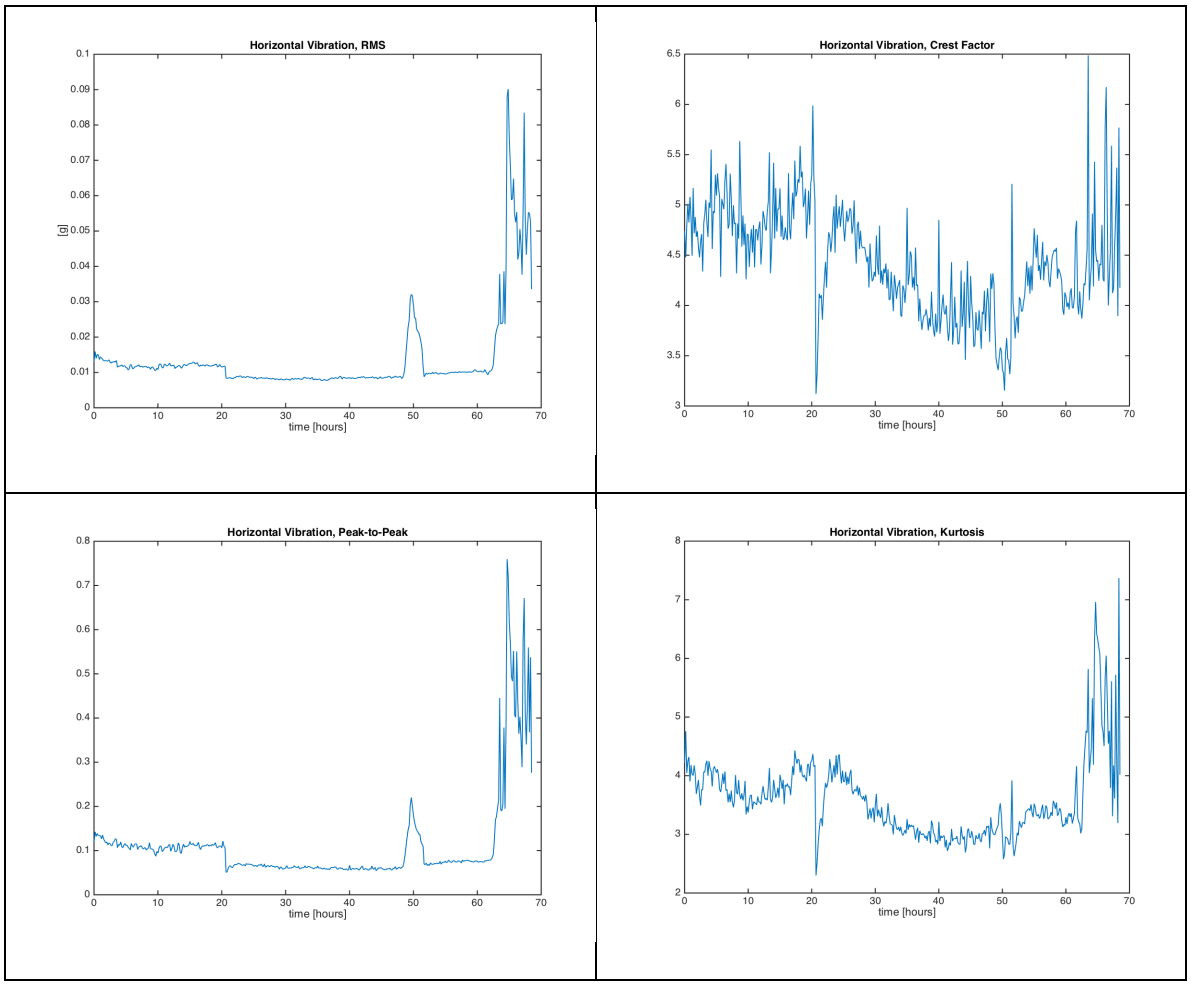

Figure B.22. Bearing 2 horizontal vibration, from top left: a) RMS, b) crest factor, c) peak-to-peak ratio, and d) kurtosis.

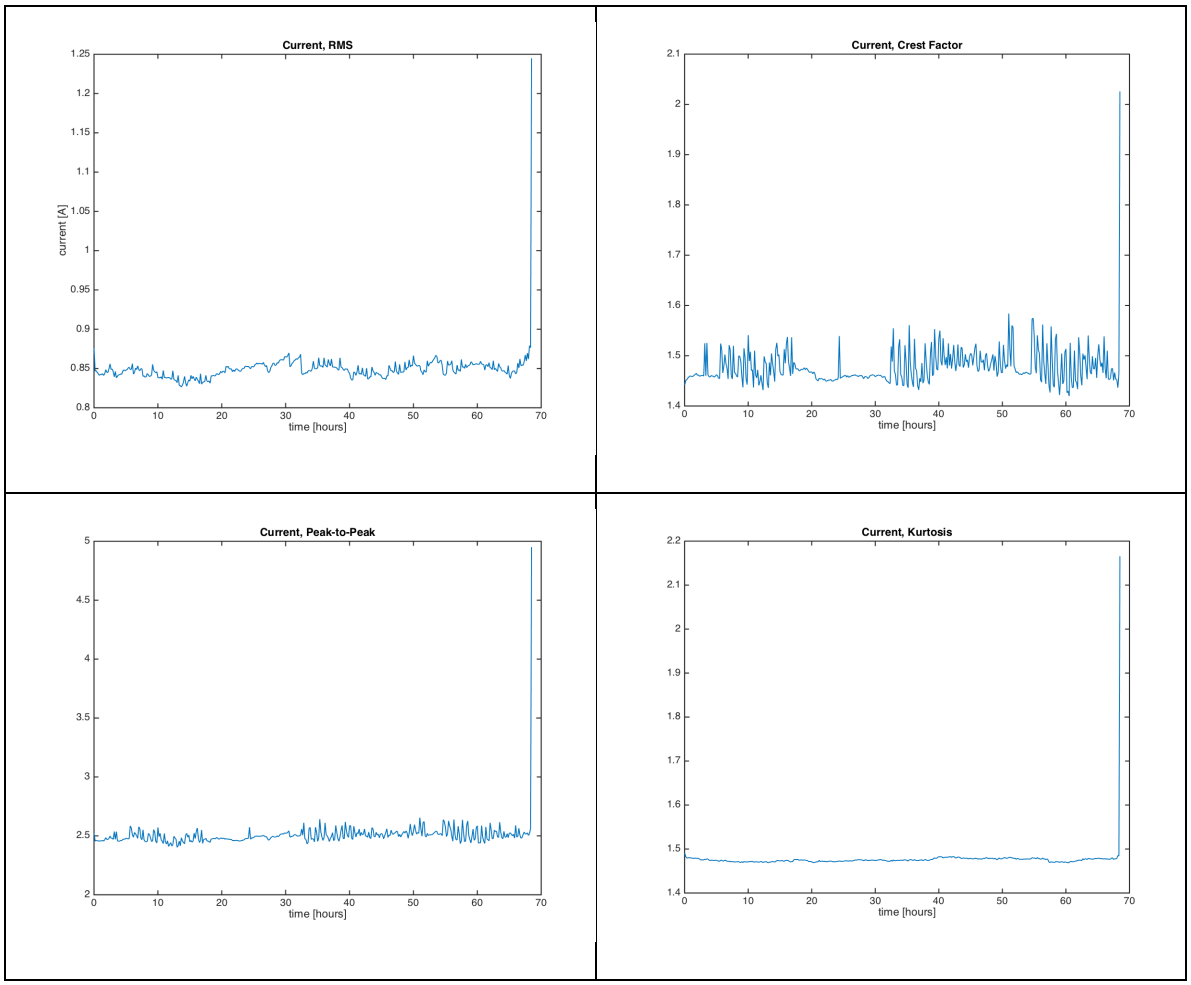

Figure B.23. Bearing 2 current signal, from top left: a) RMS, b) crest factor, c) peak-to-peak ratio, and d) kurtosis.

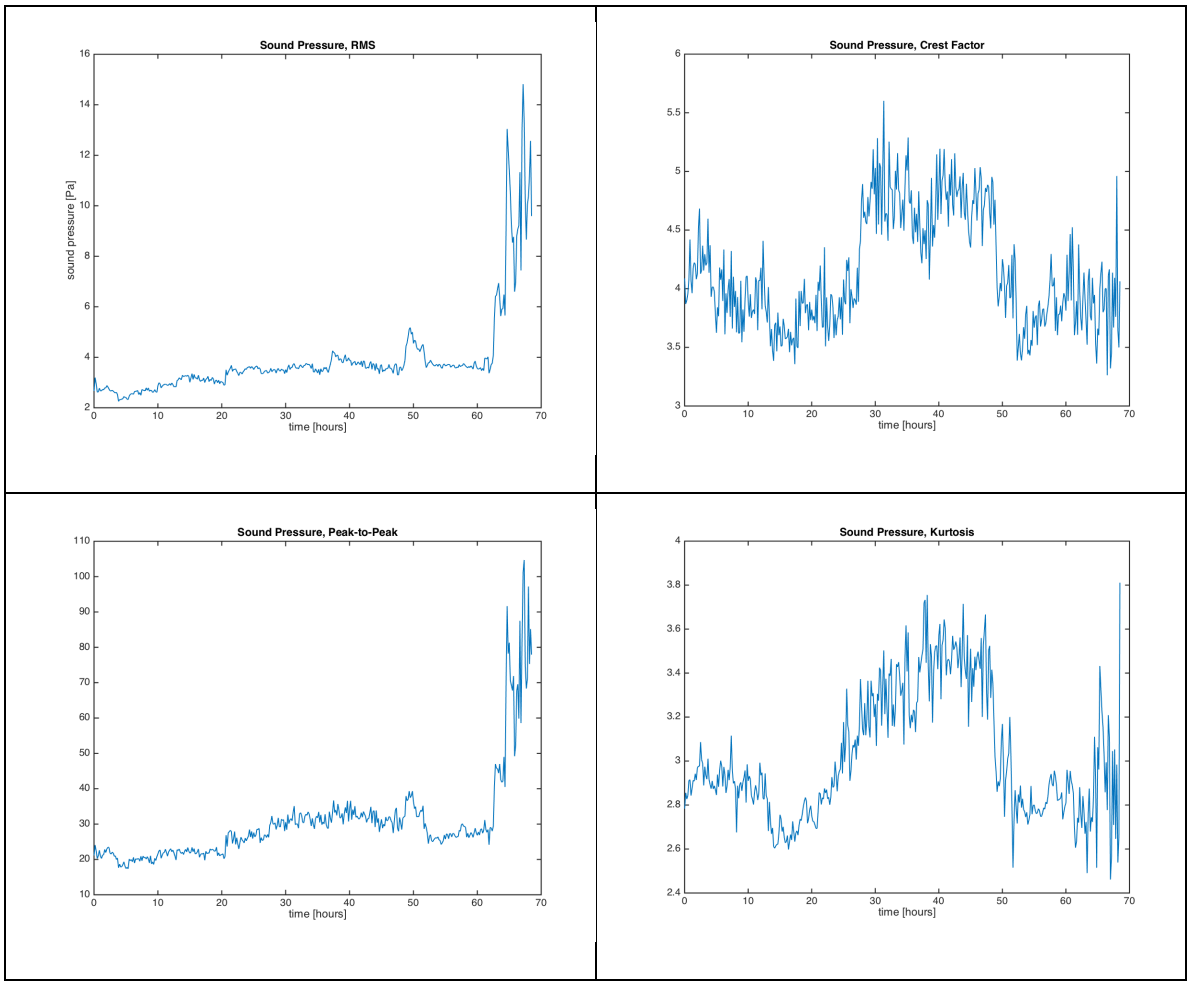

Figure B.24. Bearing 2 acoustic emission, from top left: a) RMS, b) crest factor, c) peak-to-peak ratio, and d) kurtosis.

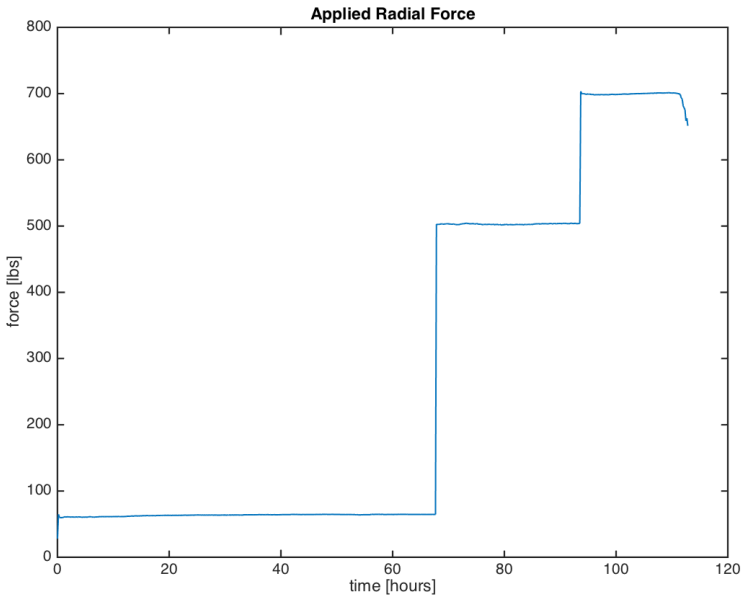

Figure B.25. Bearing 3 applied radial load.

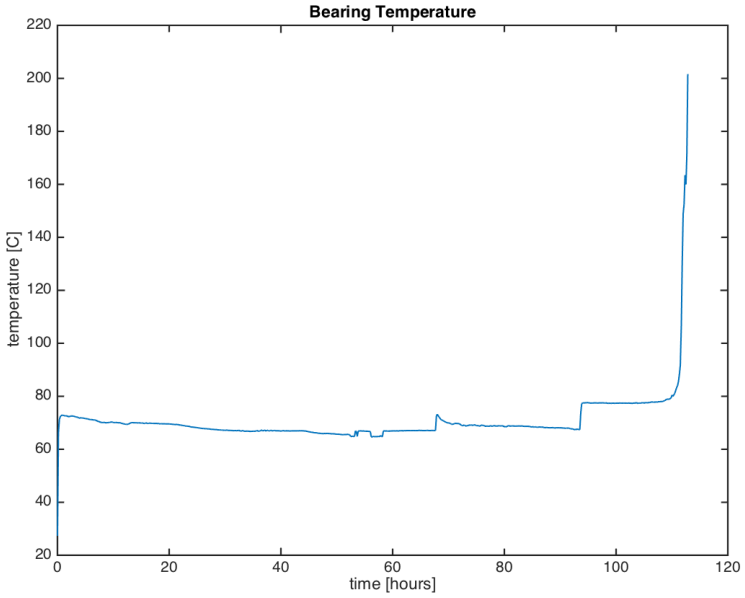

Figure B.26. Bearing 3 temperature.

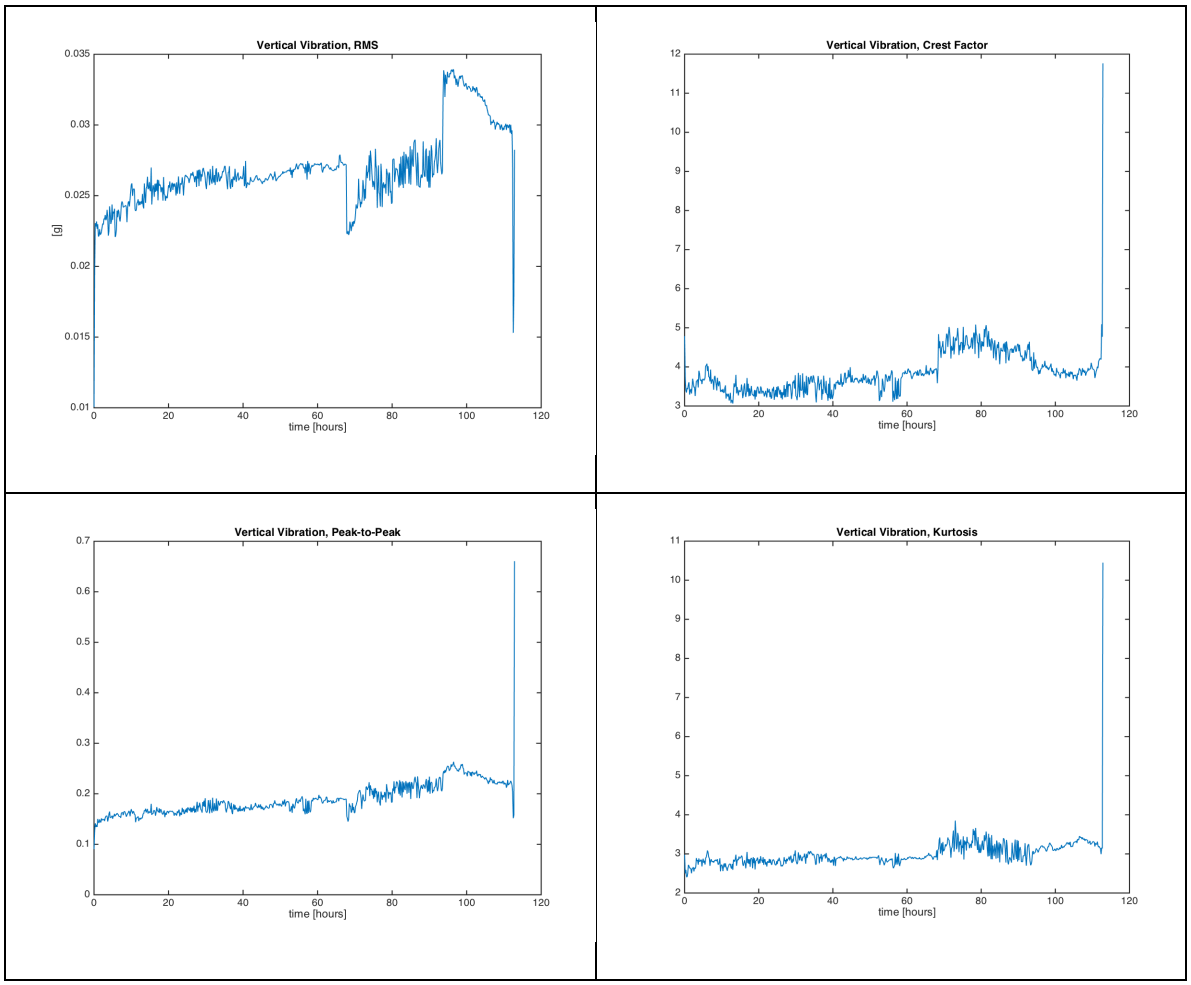

Figure B.27. Bearing 3 vertical vibration, from top left: a) RMS, b) crest factor, c) peak-to-peak ratio, and d) kurtosis.

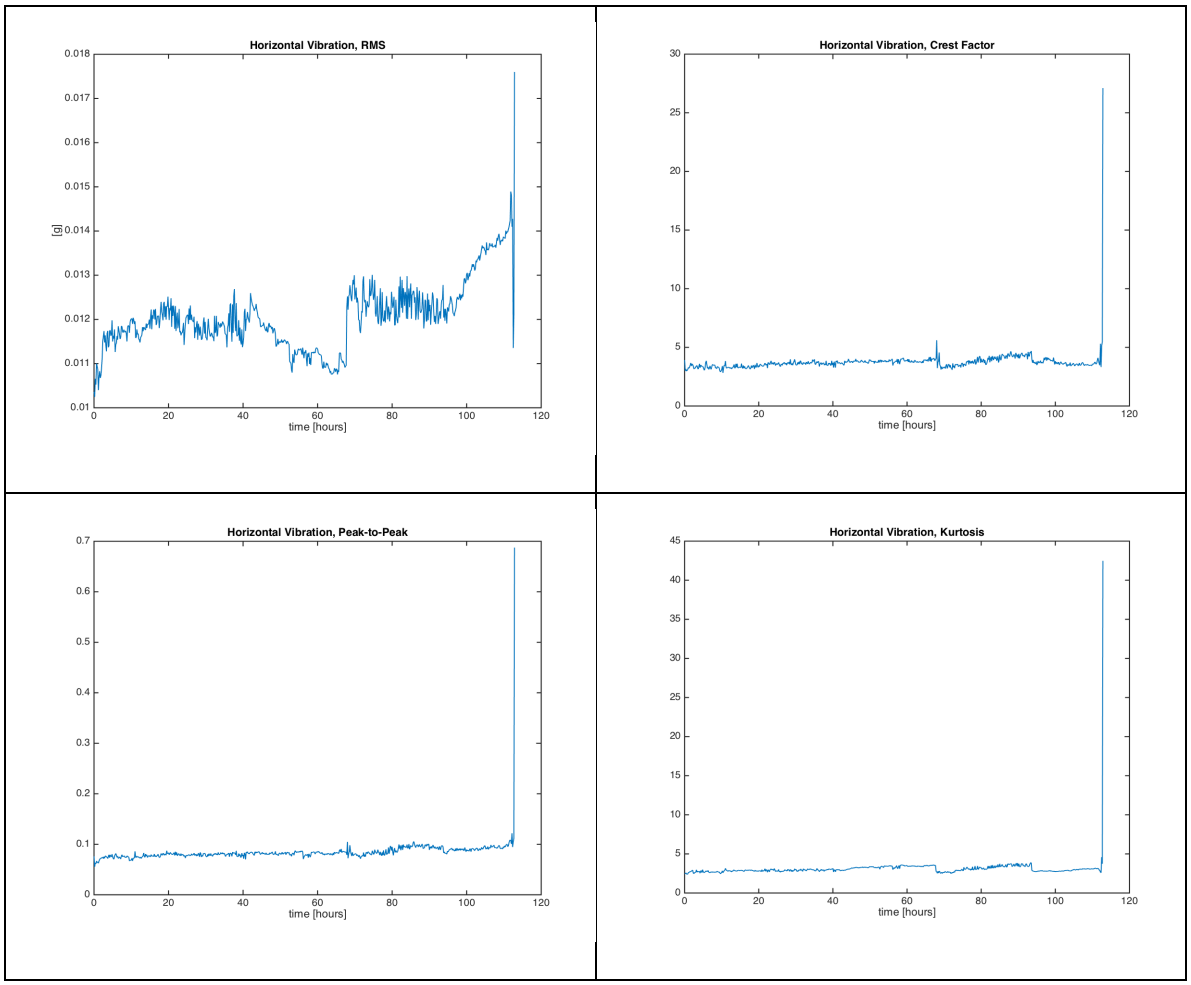

Figure B.28. Bearing 3 horizontal vibration, from top left: a) RMS, b) crest factor, c) peak-to-peak ratio, and d) kurtosis.

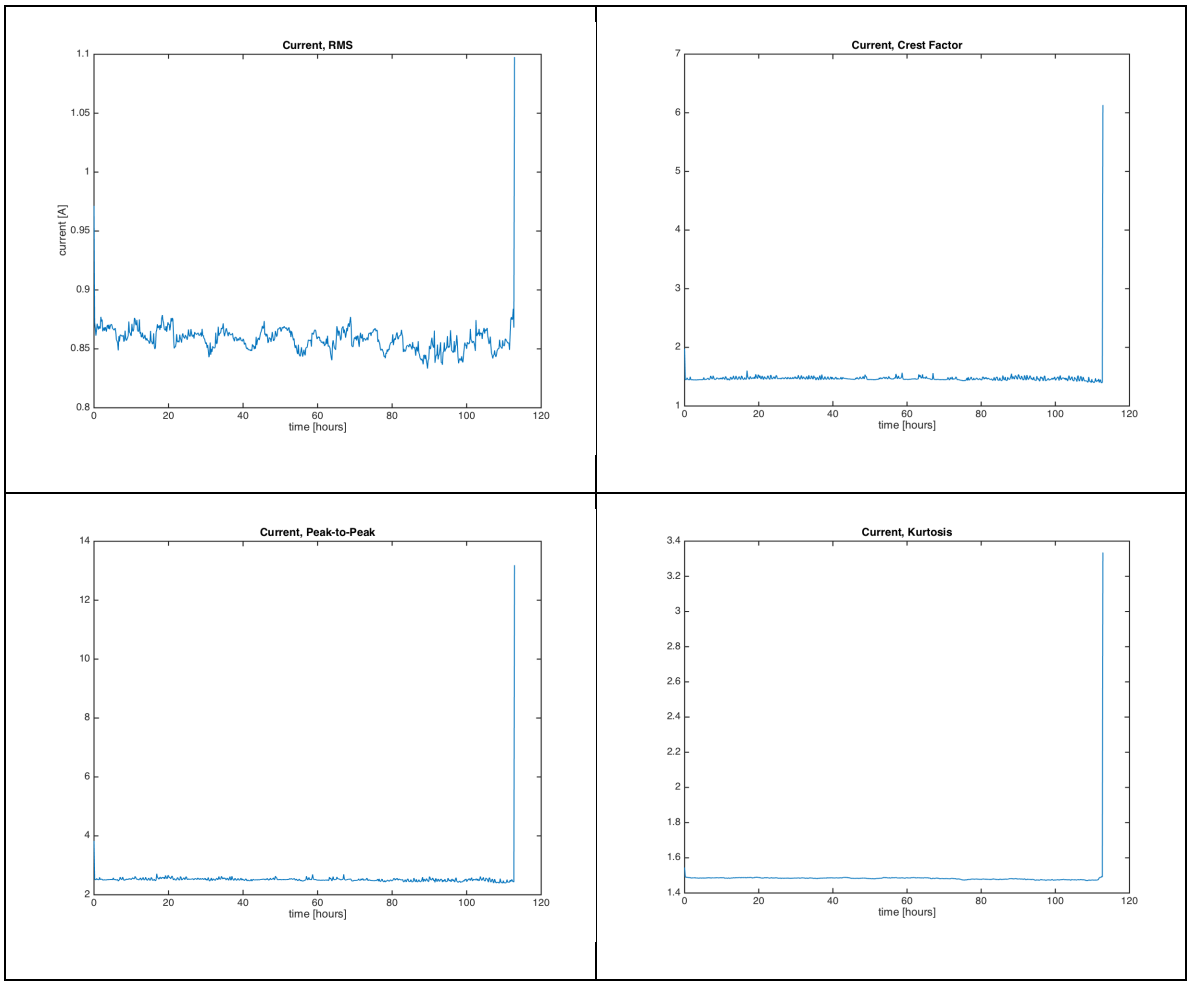

Figure B.29. Bearing 3 current signal, from top left: a) RMS, b) crest factor, c) peak-to-peak ratio, and d) kurtosis.

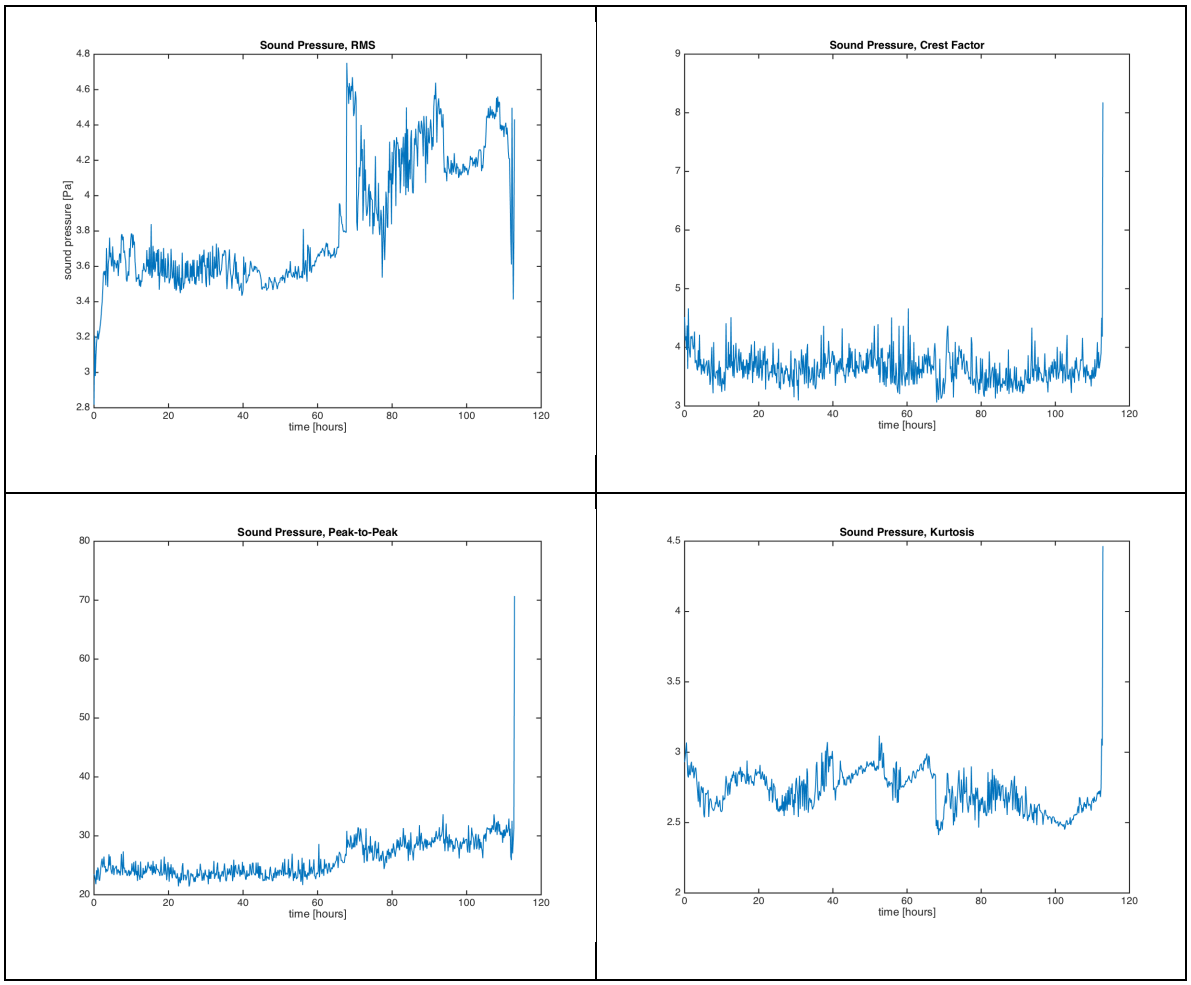

Figure B.30. Bearing 3 acoustic emission, from top left: a) RMS, b) crest factor, c) peak-to-peak ratio, and d) kurtosis.

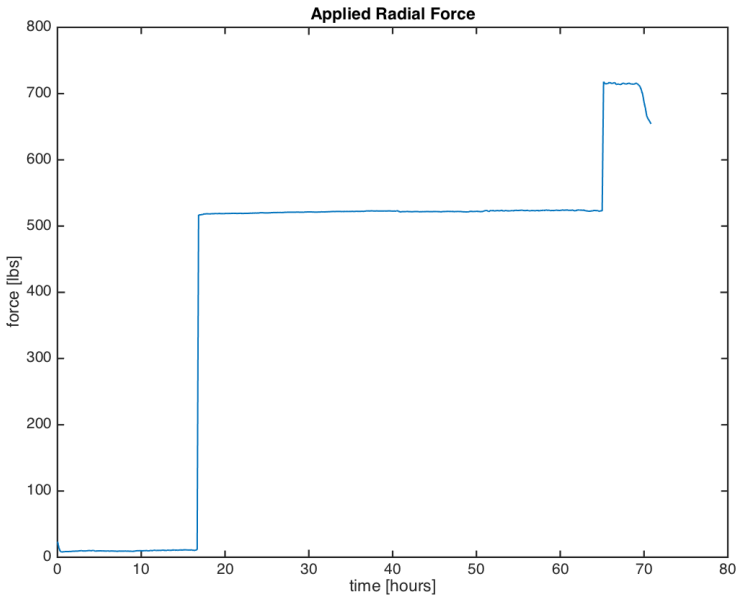

Figure B.31. Bearing 4 applied radial load.

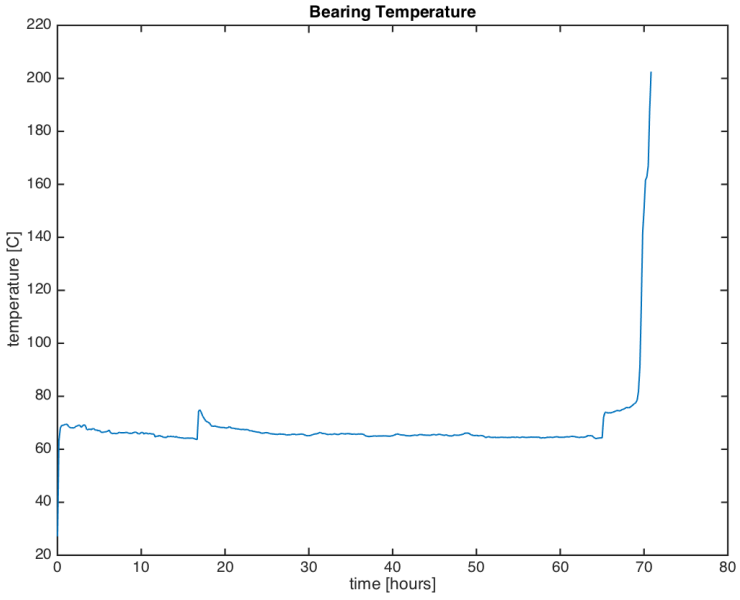

Figure B.32. Bearing 4 temperature.

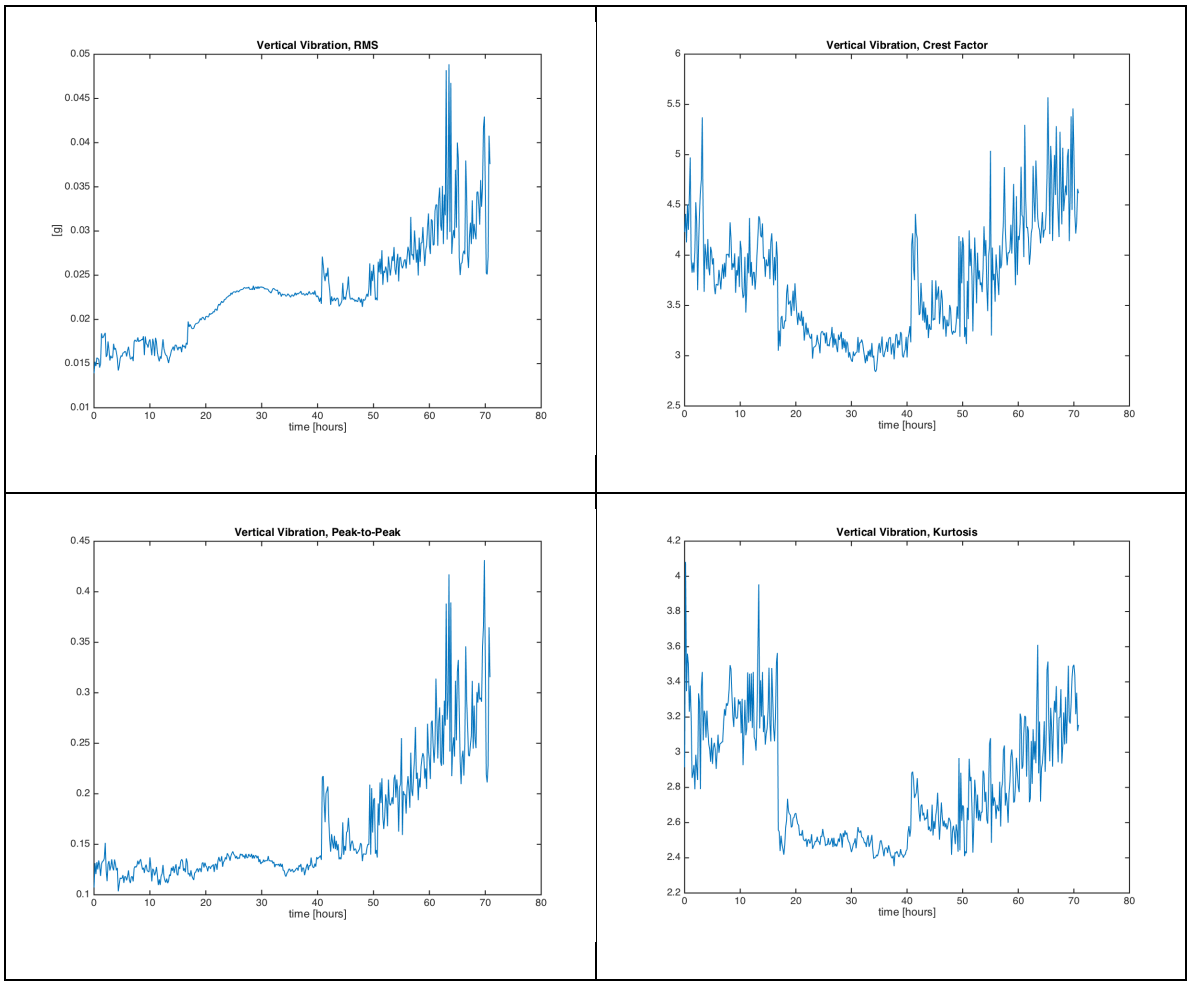

Figure B.33. Bearing 4 vertical vibration, from top left: a) RMS, b) crest factor, c) peak-to-peak ratio, and d) kurtosis.

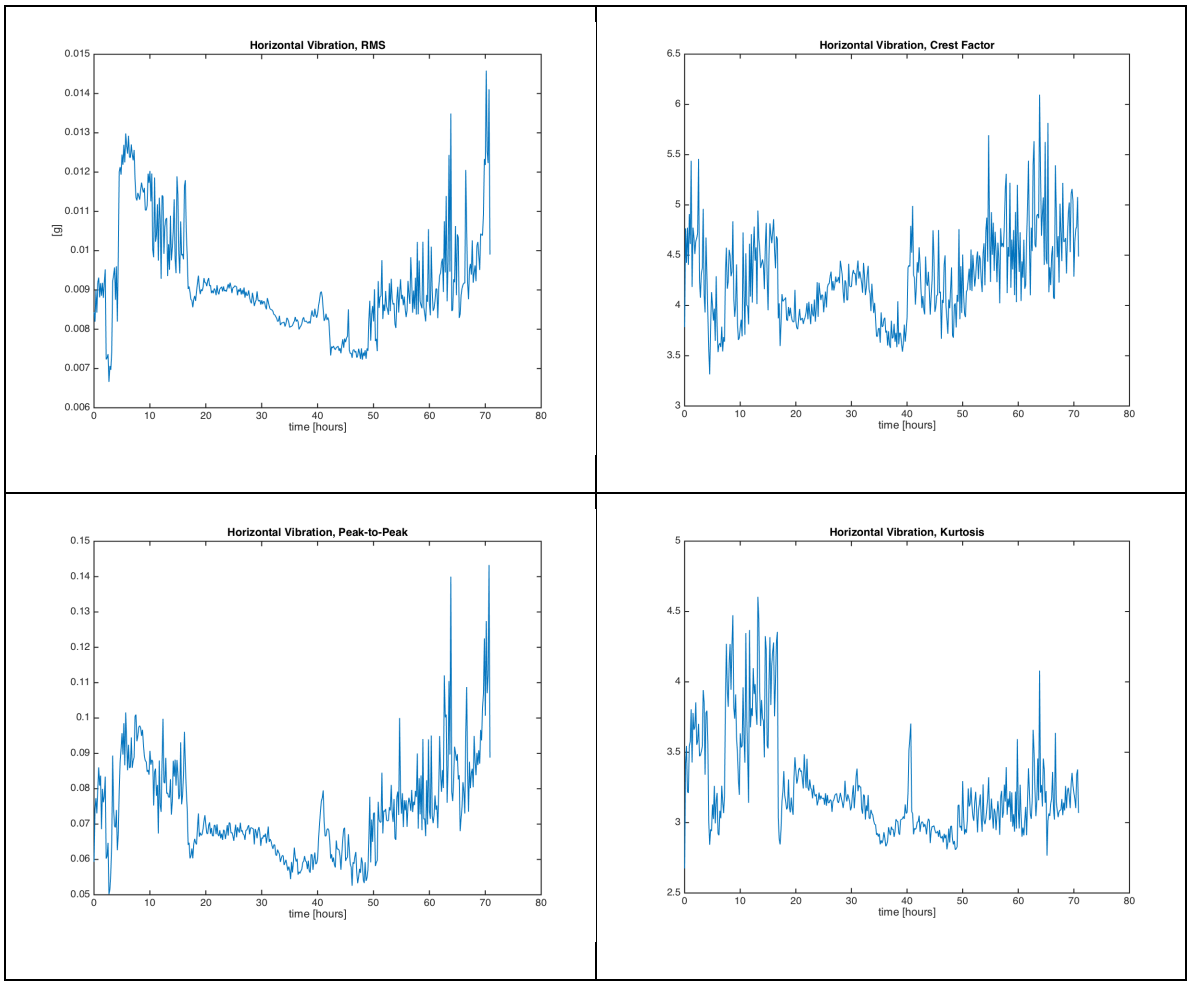

Figure B.34. Bearing 4 horizontal vibration, from top left: a) RMS, b) crest factor, c) peak-to-peak ratio, and d) kurtosis.

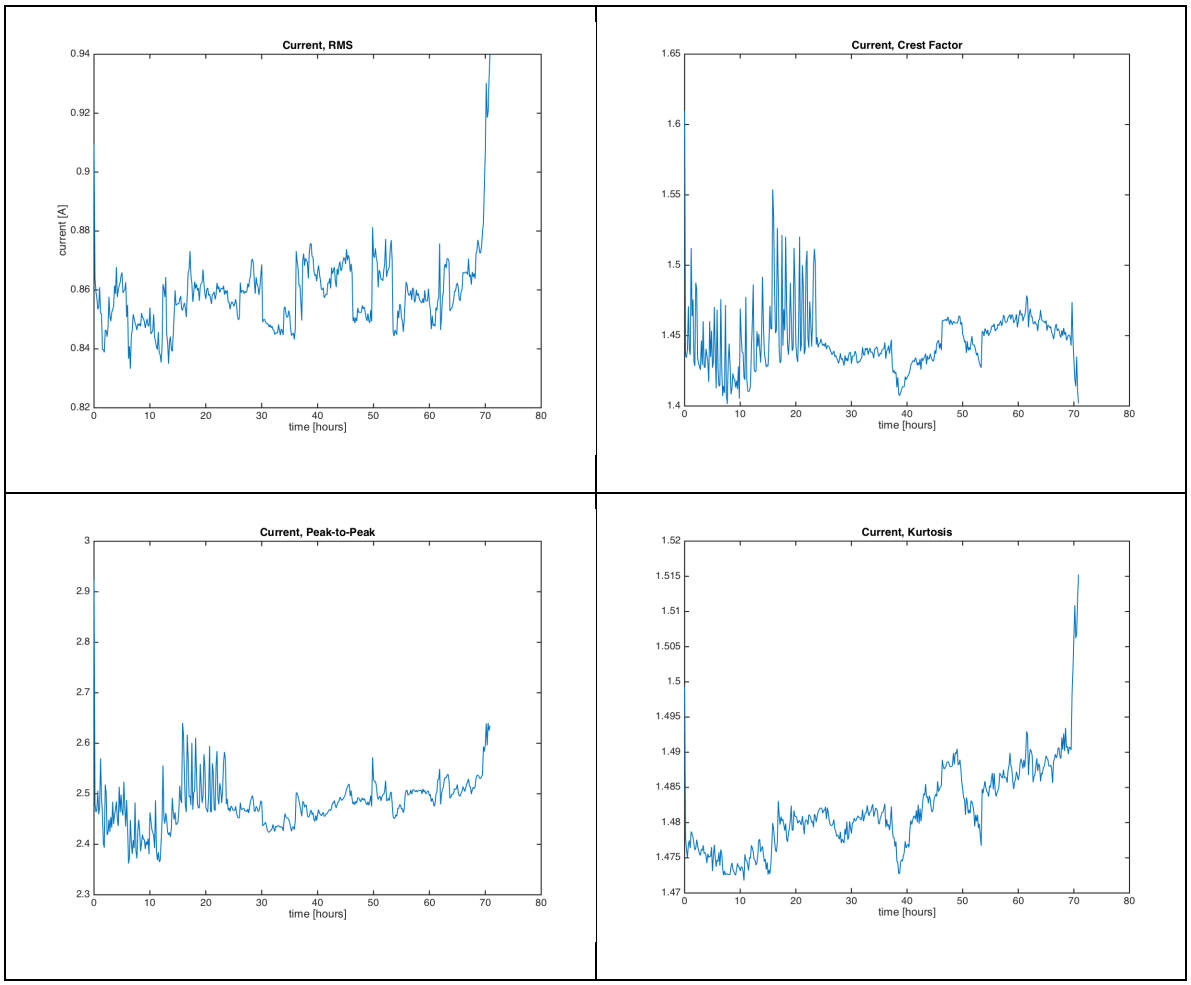

Figure B.35. Bearing 4 current signal, from top left: a) RMS, b) crest factor, c) peak-to-peak ratio, and d) kurtosis.

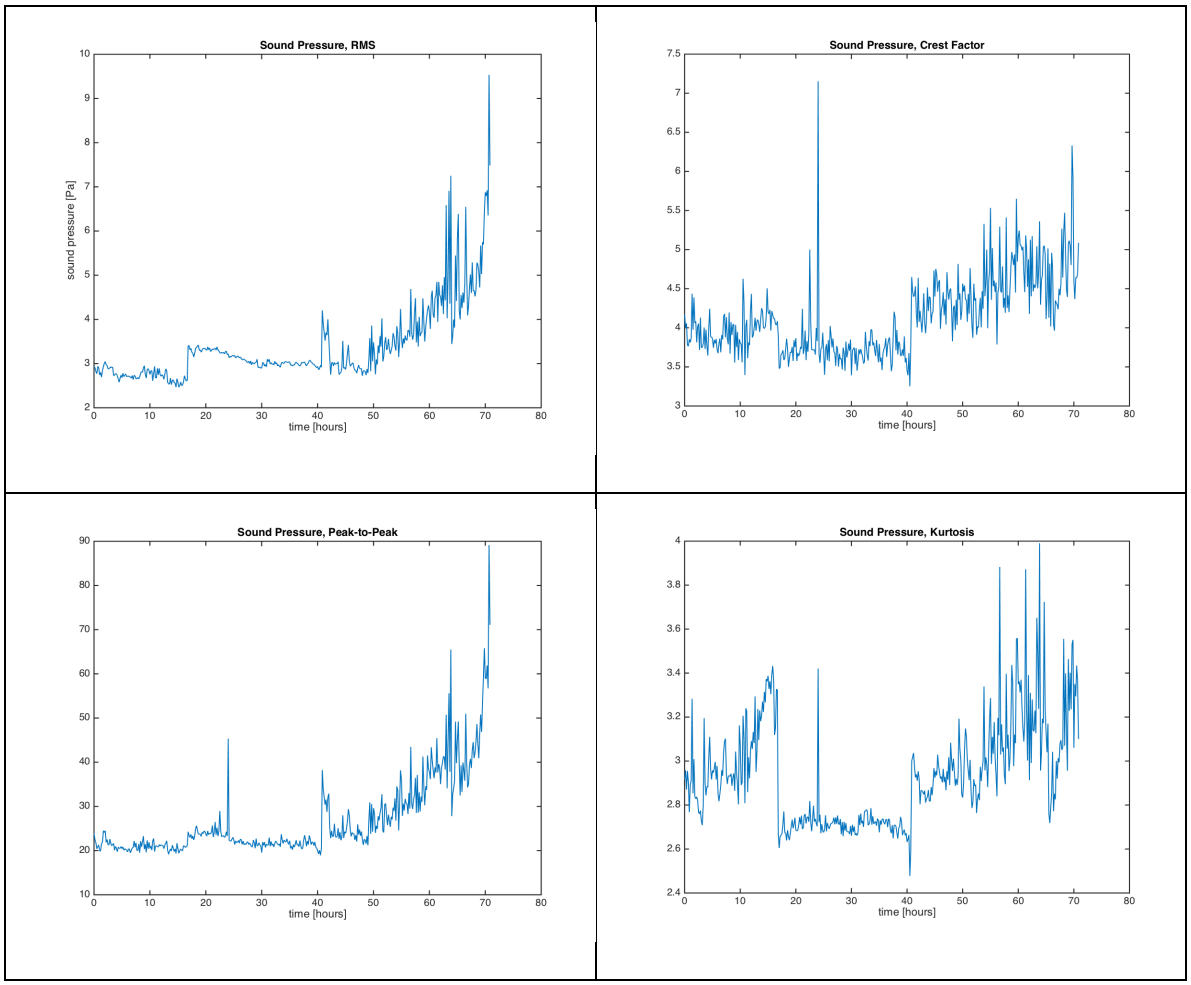

Figure B.36. Bearing 4 acoustic emission, from top left: a) RMS, b) crest factor, c) peak-to-peak ratio, and d) kurtosis.

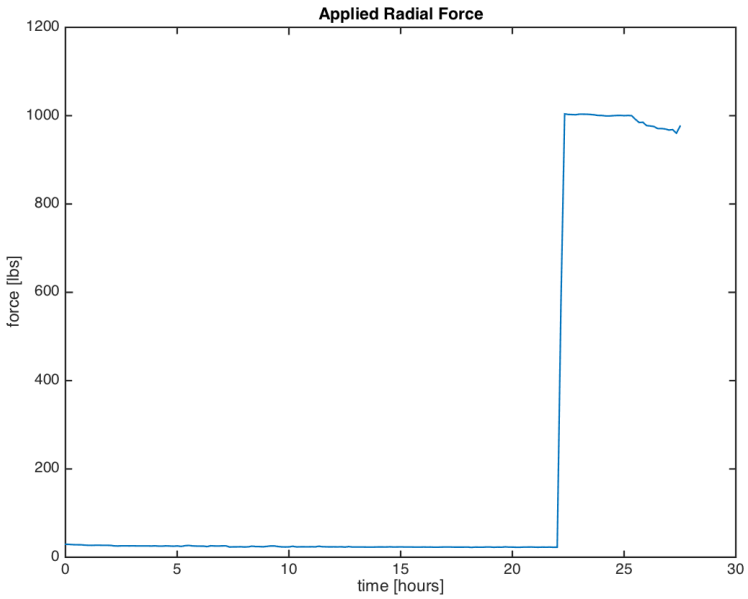

Figure B.37. Bearing 5 applied radial load.

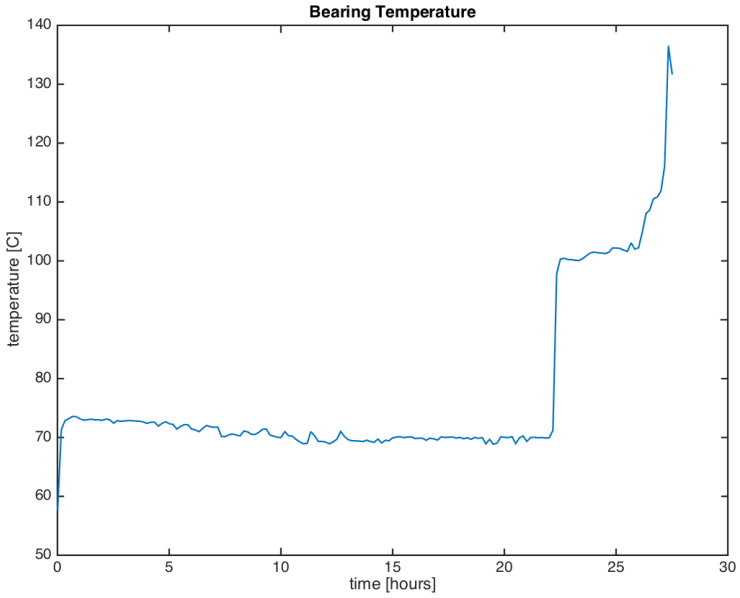

Figure B.38. Bearing 5 temperature.

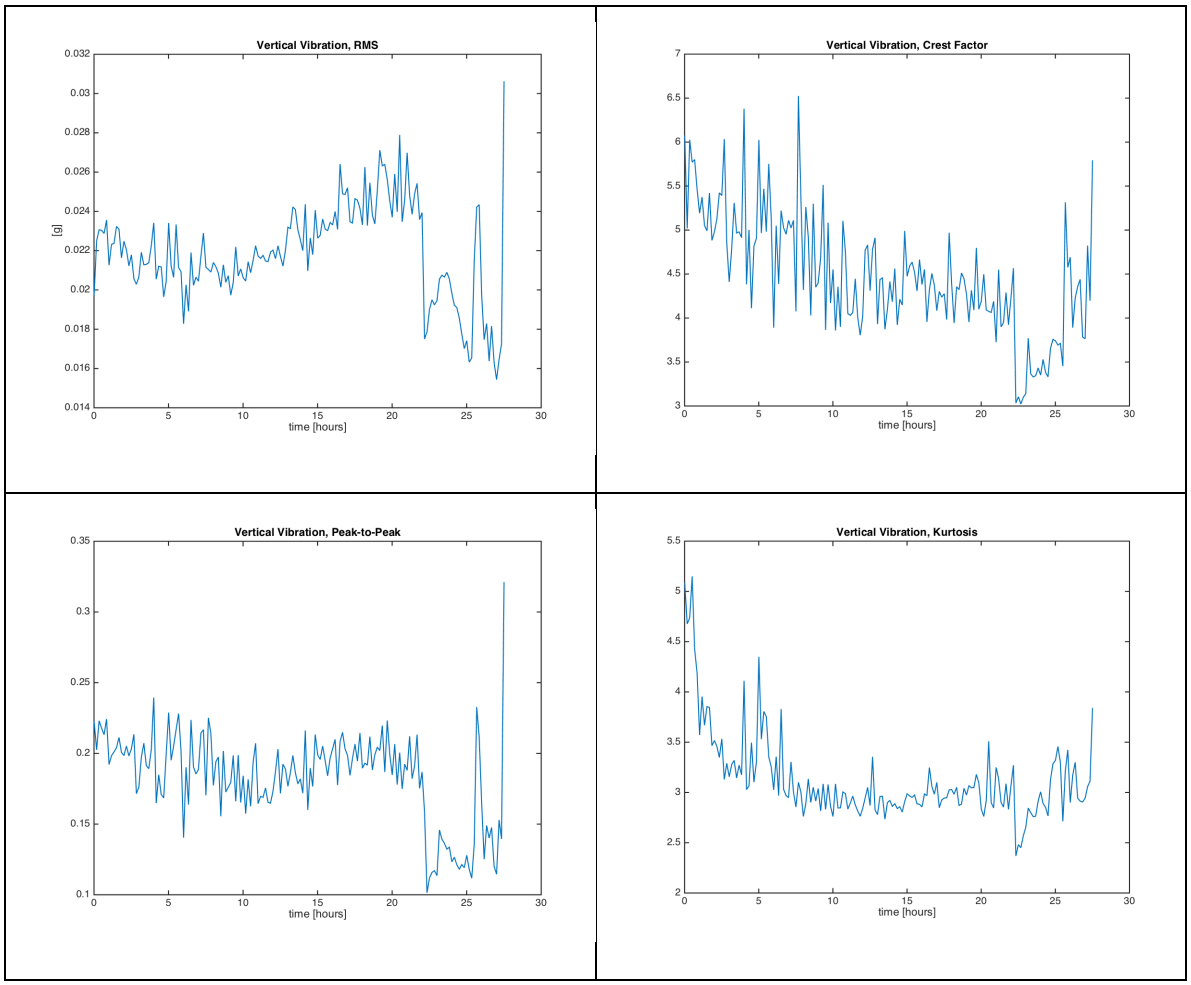

Figure B.39. Bearing 5 vertical vibration, from top left: a) RMS, b) crest factor, c) peak-to-peak ratio, and d) kurtosis.

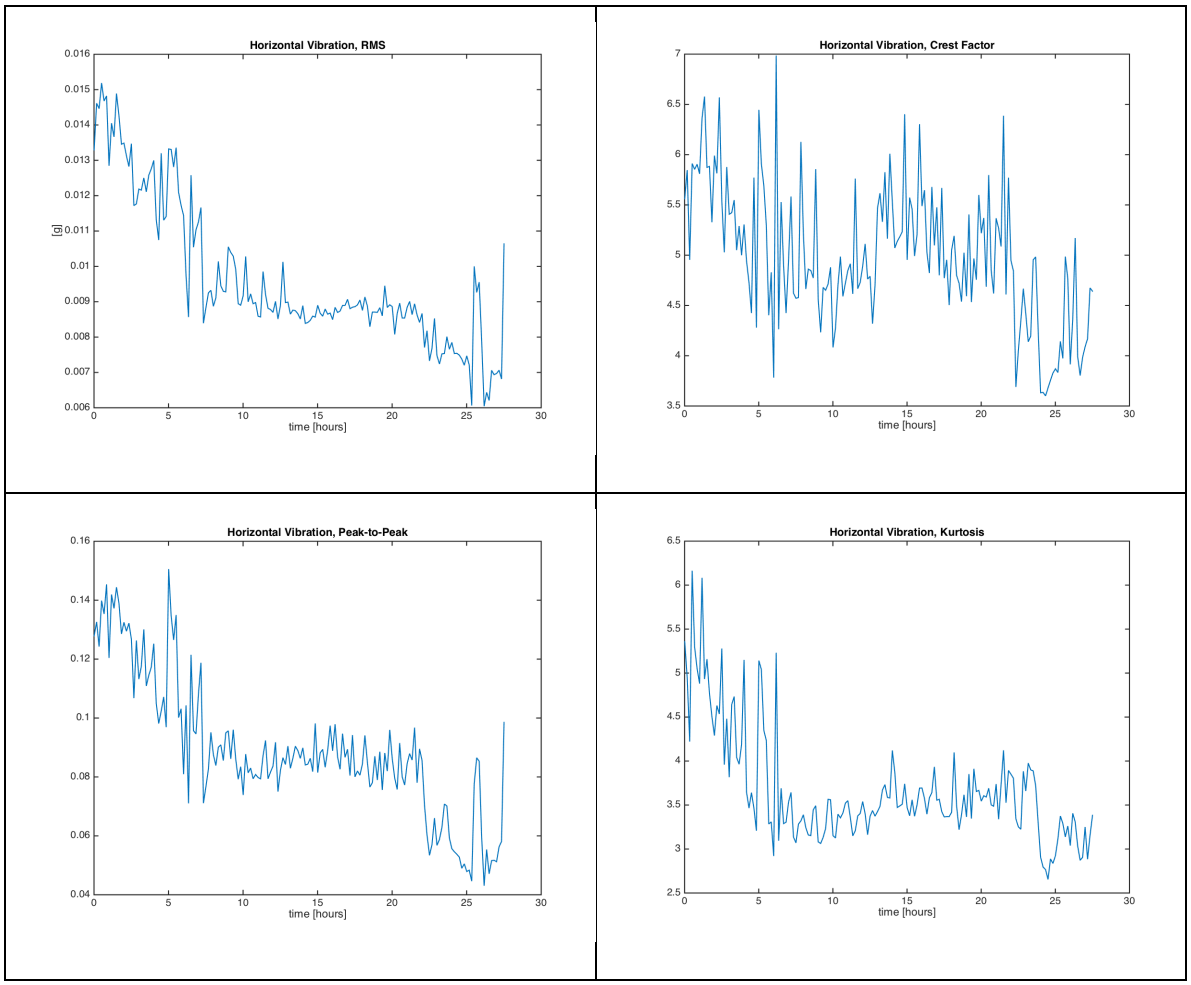

Figure B.40. Bearing 5 horizontal vibration, from top left: a) RMS, b) crest factor, c) peak-to-peak ratio, and d) kurtosis.

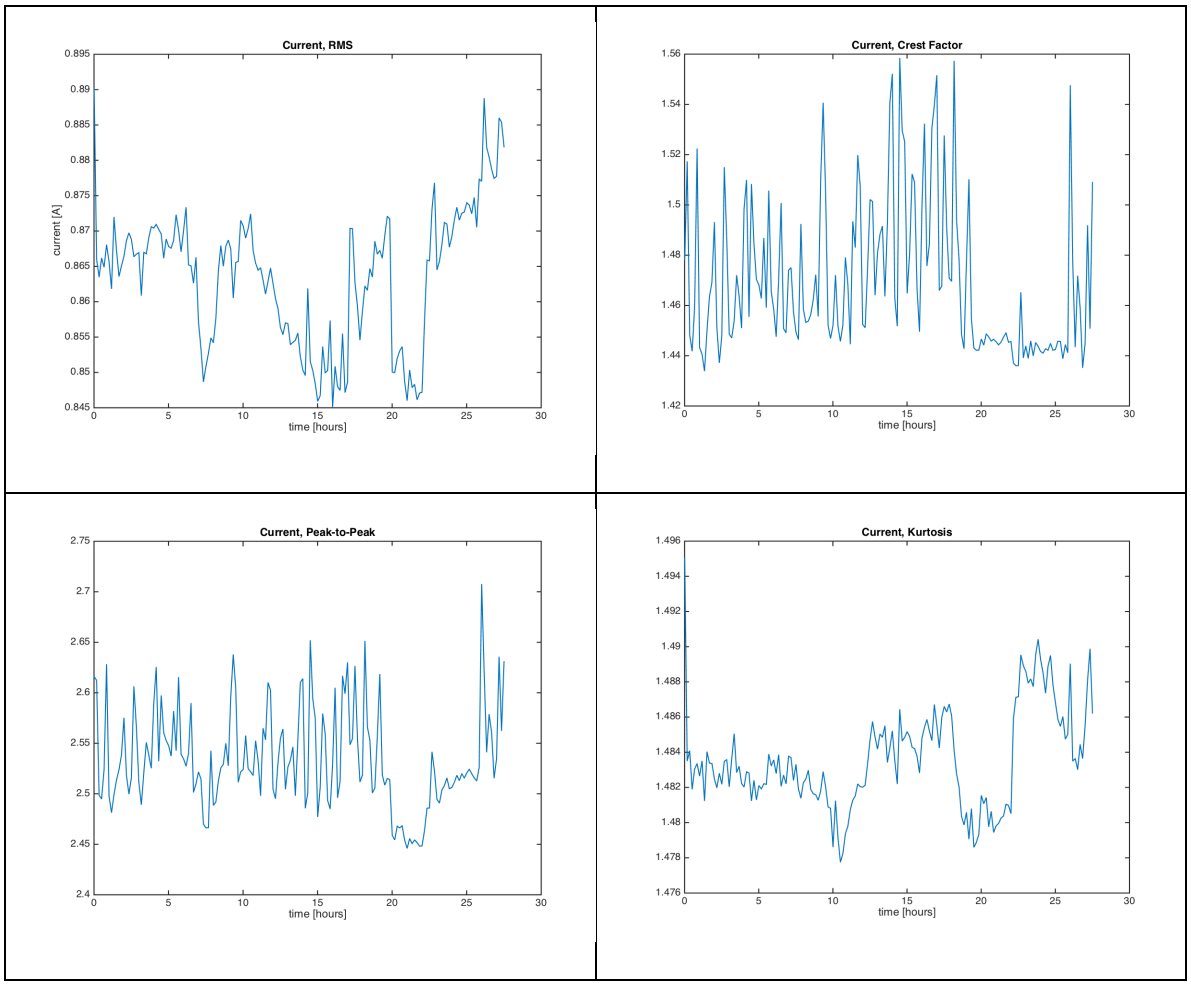

Figure B.41. Bearing 5 current signal, from top left: a) RMS, b) crest factor, c) peak-to-peak ratio, and d) kurtosis.

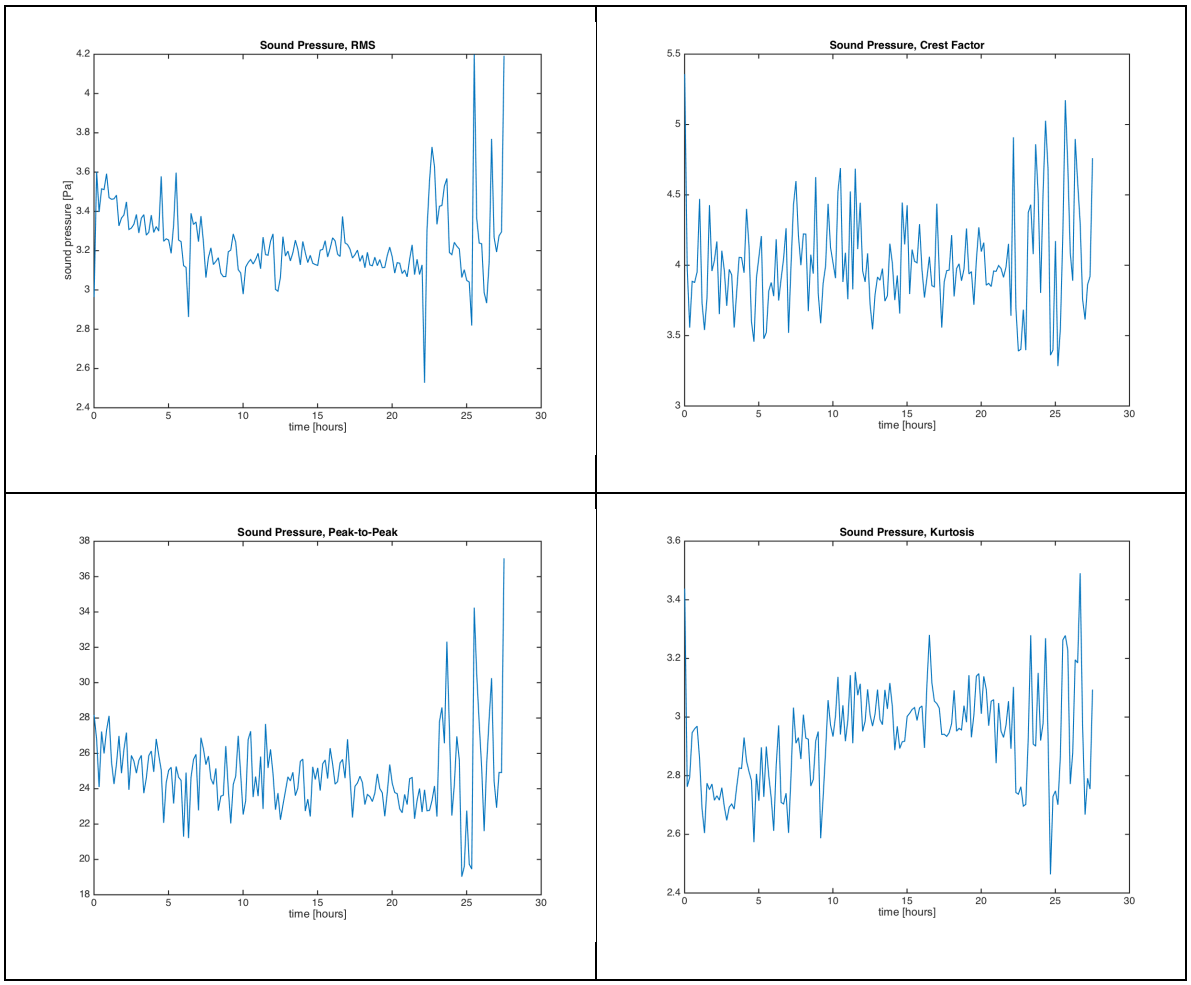

Figure B.42. Bearing 5 acoustic emission, from top left: a) RMS, b) crest factor, c) peak-to-peak ratio, and d) kurtosis.

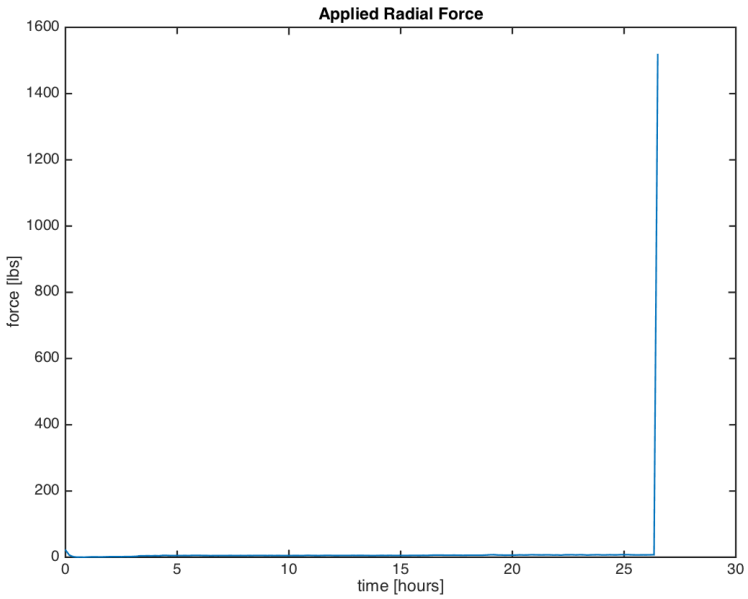

Figure B.43. Bearing 6 applied radial load.

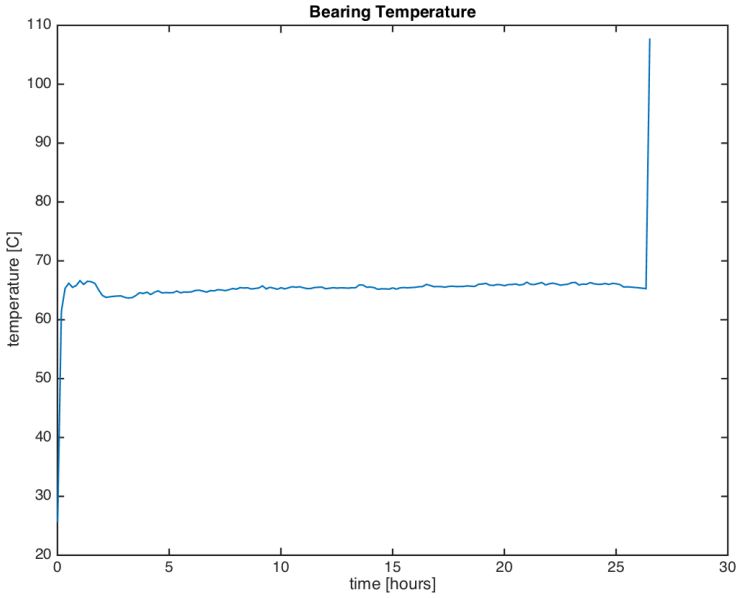

Figure B.44. Bearing 6 temperature.

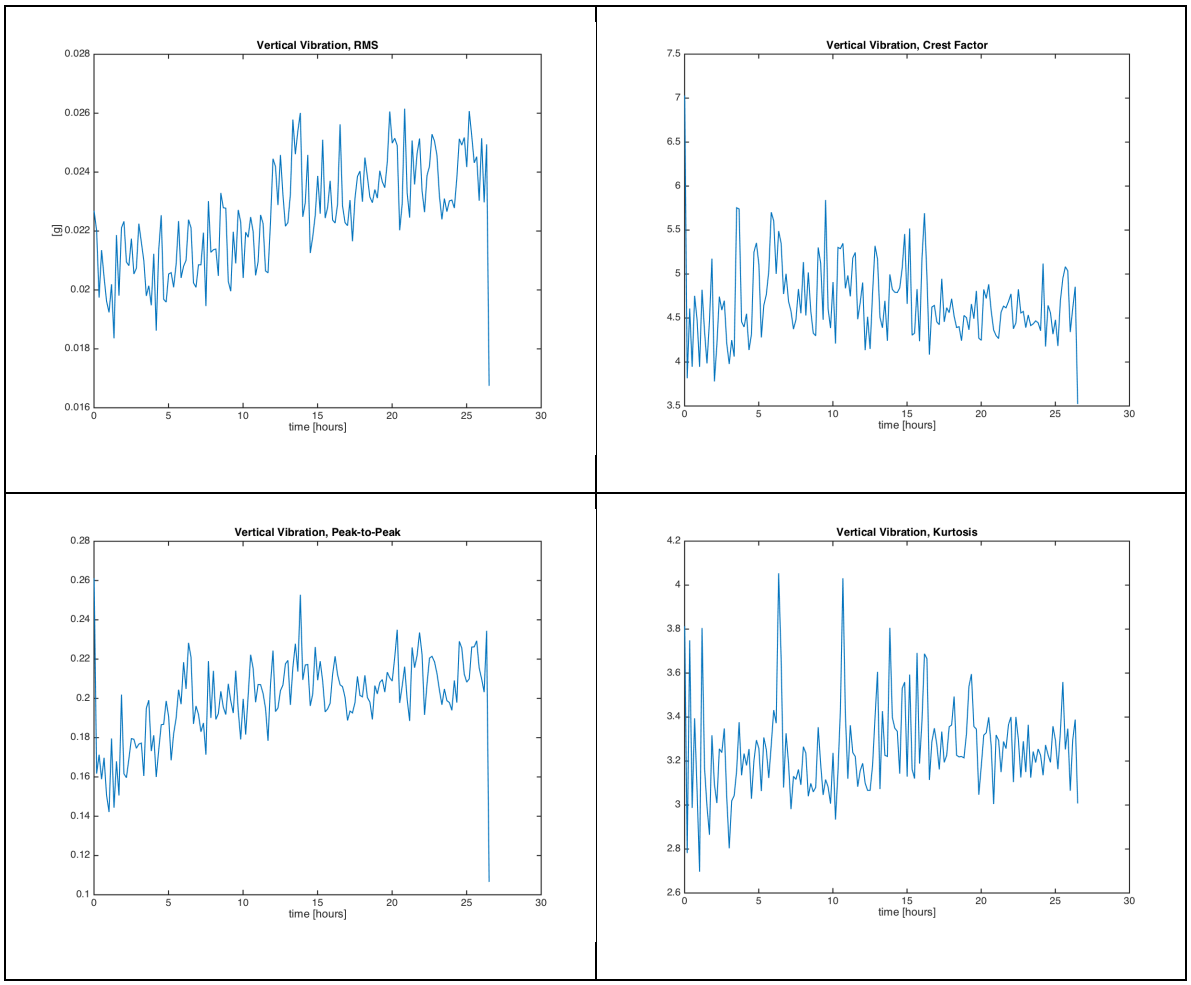

Figure B.45. Bearing 6 vertical vibration, from top left: a) RMS, b) crest factor, c) peak-to-peak ratio, and d) kurtosis.

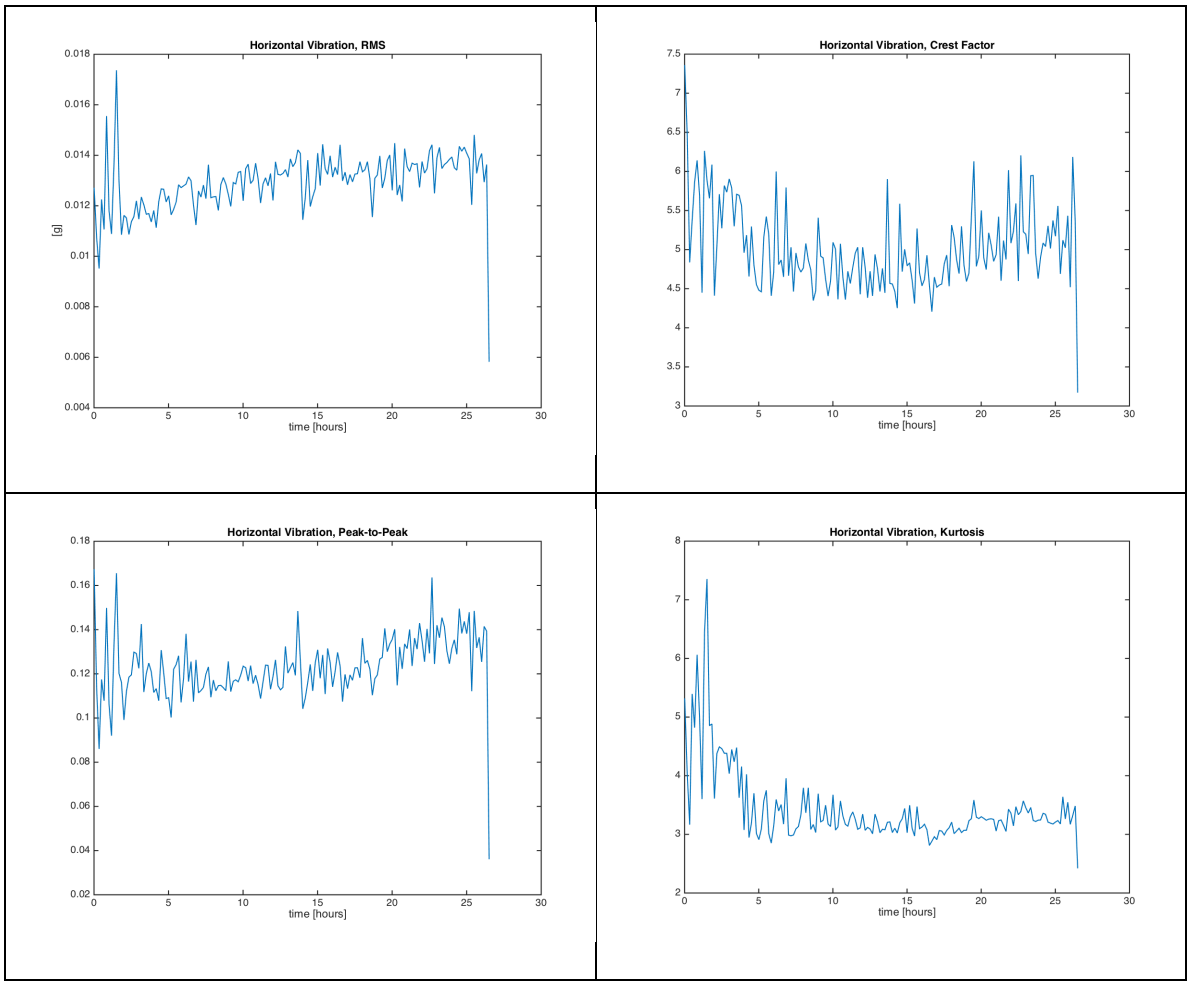

Figure B.46. Bearing 6 horizontal vibration, from top left: a) RMS, b) crest factor, c) peak-to-peak ratio, and d) kurtosis.

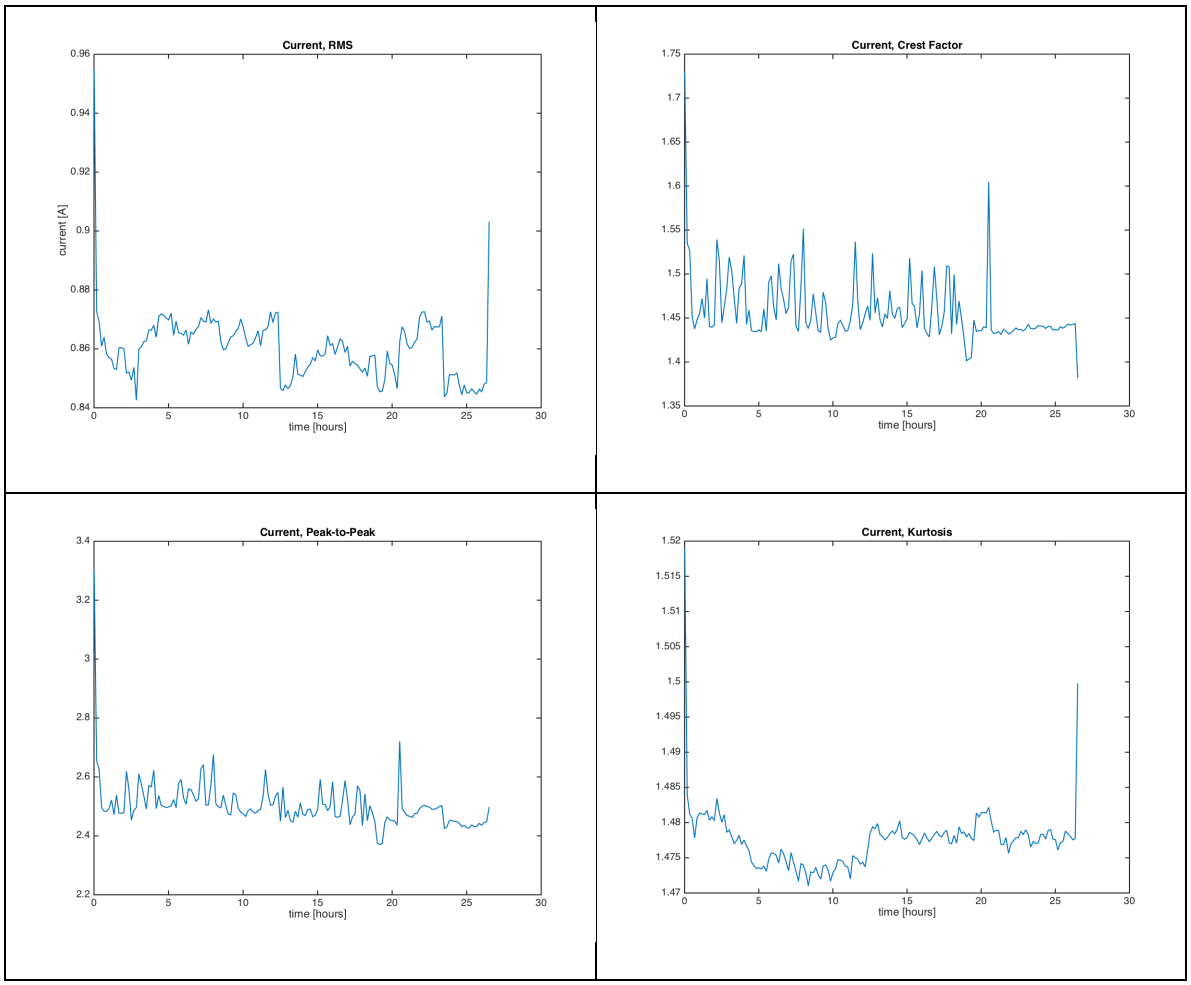

Figure B.47. Bearing 6 current signal, from top left: a) RMS, b) crest factor, c) peak-to-peak ratio, and d) kurtosis.

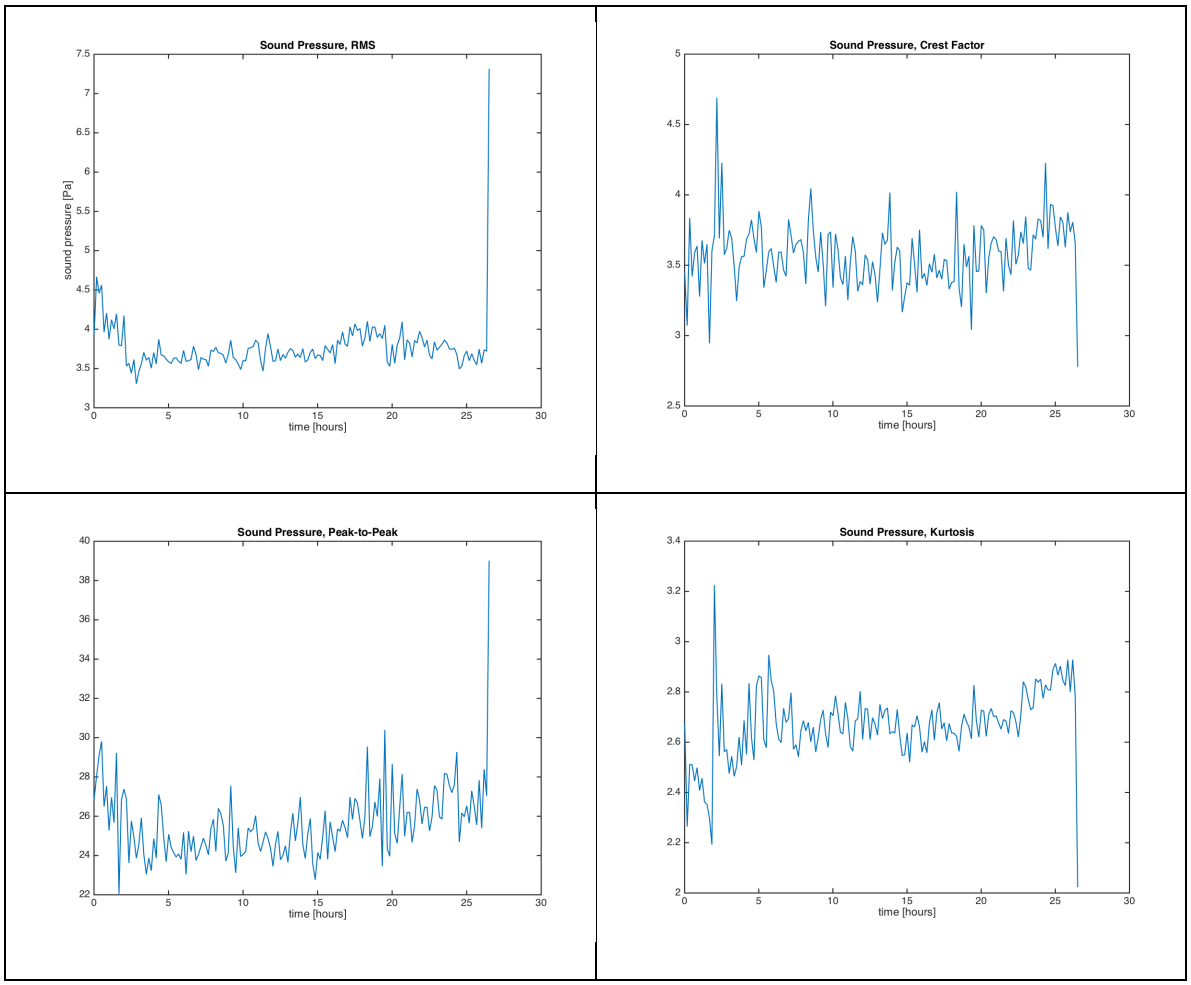

Figure B.48. Bearing 6 acoustic emission, from top left: a) RMS, b) crest factor, c) peak-to-peak ratio, and d) kurtosis.

APPENDIX C: POST-MORTEM ANALYSIS

Figure C.49. Bearing 4, postmortem.

Figure C.50. Bearing 5, postmortem.

Figure C.51. Bearing 6, postmortem.

VITA

Anna Mazzolini received a Bachelor of Science in Nuclear and Radiological Engineering from the Georgia Institute of Technology in 2014. She began studies at the University of Tennessee that same year to pursue a master's degree in Nuclear Engineering. There, she concentrated on Reliability and Maintainability Engineering. She hopes to pursue a career supporting safe, clean energy through nuclear power.